THE ROLE OF COMETS IN PANSPERMIA

By

Janaki Tara Wickramasinghe
BSc

Thesis submitted in candidature for the degree of Doctor of Philosophy at Cardiff University

ProQuest LLC
789 East Eisenhower Parkway
P.O. Box 1346
Ann Arbor, MI 48106-1346

Declaration

This work has not previously been accepted in substance for any degree and is not concurrently submitted in candidature for any degree.

Signed..J.Wickramasinghe.....(candidate) Date.25/5/07

STATEMENT 1

This thesis is being submitted in partial fulfillment of the requirements for the degree of PhD.

Signed..J.Wickramasinghe.....(candidate) Date.25/5/07

STATEMENT 2

This thesis is the result of my own independent work/investigation, except where otherwise stated.
Other sources are acknowledged by explicit references.

Signed ..J.Wickramasinghe.....(candidate) Date.25/5/07

STATEMENT 3

I hereby give consent for my thesis, if accepted, to be available for photocopying and for inter-library loan, and for the title and summary to be made available to outside organisations.

Signed ..J.Wickramasinghe.....(candidate) Date.25/5/07

STATEMENT 4 - BAR ON ACCESS APPROVED

I hereby give consent for my thesis, if accepted, to be available for photocopying and for inter-library loans **after expiry of a bar on access** approved by the Graduate Development Committee.

Signed ..J.Wickramasinghe.....(candidate) Date.25/5/07

Contents

Acknowledgements

I am very grateful to my supervisor Professor W.M. Napier for his careful guidance throughout the course of this work. His critical comments and suggestions have helped to develop the structure of the present thesis. I also wish to thank Max Wallis for all his help and advice.

A special thank you goes to Brig Klyce and the Astrobiology Research Trust of the USA for generously sponsoring and supporting this work.

And finally, thank you to my parents for their support and especially to my father, Chandra Wickramasinghe, who endlessly encouraged me throughout my academic pursuits and continues to inspire me.

Janaki Tara Wickramasinghe
Cardiff
25 May 2007

Summary

The thesis presents a re-evaluation of the theory of panspermia. I show that collisions of comets with Earth and Earth-like planets play a role in transferring microbial life across the galaxy.

After a brief overview of panspermia in Chapter 1, Chapter 2 develops the theory of cosmic dust. The extinction curve for the galaxy SBS0909+532 at red shift z=0.83, confirms the organic composition of dust upto distances that are a substantial fraction of the Hubble radius.

In Chapter 3 a brief overview of comets is presented. Chapter 4 examines dynamical interactions of the Oort cloud of comets with molecular clouds in the galaxy. Using a numerical integration procedure, including the effect of the galactic tide, we show that such interactions lead to sporadic and recurrent injections of comets into the inner solar system. Chapter 5 examines the fate of comets deflected at the present epoch into the inner regions of the solar system. Estimates of the flux of such comets show that there should be ~100 times more comets in Halley-type orbits than are actually observed. This discrepancy can be resolved if comets develop porous, organic crusts of very low albedos.

Chapter 6 discusses the expulsion of microorganisms from the solar system and their survival prospects, leading to the conclusion that an adequate fraction survives for re-incorporation into exosolar planetary systems. The final chapter considers the problem of liquid water in comets. Arguments for radiogenic melting of primordial comets are re-examined. It is shown that comets with radii $\geq$ 8km can retain liquid water cores for timescales ~ 1My after their formation, thus providing sites for amplification of small initial compliments of bacteria. By modelling solar heat flow near perihelion onto a crusted, rotating comet it is shown that transient sub-surface pools can be generated, providing habitats for microbes. Data from *Deep Impact* for comet Tempel 1 is modelled to show evidence for clays, organics and liquid water, and potential microbial habitats.

Chapter One: Introduction

1.1 General introduction

In this thesis I propose to re-investigate the theory of panspermia in light of recent developments, focussing particularly on the role of comets in originating and distributing microbial life. Evidence pointing to the feasibility that terrestrial life may have come from elsewhere in the solar system has accumulated over the past decade. Complex organic molecules in interstellar dust and comets appear to be biologically derived, or at least closely related spectroscopically and structurally to such material or their degradation products. Developments in microbiology have led to the discovery of various extremophiles, bacteria that can survive in harsh conditions previously thought to be unfavourable to life. Such bacteria with properties ideally suited to space travel gives further credence to panspermia. An ever-increasing number of extra-solar planet discoveries suggest that planetary systems are quite common, renewing the notion that life could be widespread.

The hundreds of billions of comets in the Oort cloud that surround the solar system could serve as a likely primordial reservoir of life in the solar system. Primitive microbial life contained and amplified within comets, could be dispersed as individual microbes or clusters of microbes to reach nascent planet forming nebulae. Additionally, evolved microbial ecologies on the surface of the Earth could be expelled by comet impacts into the zodiacal dust cloud which in turn would disperse them into molecular clouds where new stars and planets form. I intend to explore the role of comets in the spread of life on an interstellar scale.

1.2 History of panspermia

The concept of panspermia, that life is ubiquitous within the Universe, dates back to ancient Greece. In the 19th century an important experimental basis for panspermia was discovered by Louis Pasteur. His classic experiments showed that microorganisms are always derived from pre-existing microorganisms, an idea which was expanded upon by Lord Kelvin: *"Dead matter cannot become living without coming under the influence of matter previously alive. This seems to me as sure a teaching of science as the law of gravitation..."* The idea of interplanetary panspermia was discussed by Kelvin in 1871

and involved the transport of life-bearing rocks between objects within the solar system. It was his opinion that such transfers of life between the inner planets could occur sporadically as a consequence of asteroid and comet impacts. In 1874 the German physicist Hermann Von Helmholtz made the following statement:

"It appears to me to be fully correct scientific procedure, if all our attempts fail to cause the production of organisms from non-living matter, to raise the question whether life has ever arisen, whether it is not just as old as matter itself, and whether seeds have not been carried from one planet to another and have developed everywhere where they have fallen on fertile soil...."

In the beginning of the twentieth century this idea was expanded upon by Arrenhius. His hypothesis (1903) that bacterial spores were transported across the galaxy by the radiation pressure of starlight was met with much criticism. The long-term viability of the microbes subjected to the effects of UV and ionising radiation during transit was questioned. Although such criticisms continue to re-surface in modern times, on closer examination they are found to be without foundation. We shall return to this point in later sections.

Claims of the presence of microbial fossils in the Martian meteorite ALH84001 in 1996 (McKay et al.) led to a revival of interest in Kelvin's limited version of panspermia – lithopanspermia as it has come to be known. However the direct slingshot transfers of life-bearing rocks from the inner planets to the outer planets, satellites and beyond might represent a relatively inefficient form of panspermia. According to Melosh (1988) a solar system boulder has an extremely low capture probability into an Earth-like environment.

The recent development of interstellar transport mechanisms (Napier, 2004; Wallis and Wickramasinghe, 2004) makes the likelihood of life-transfer much greater. Napier describes how boulders are ejected from the Earth following a comet or asteroid impact. Eroded by zodiacal clouds into dust particles and transported due to the effects of radiation pressure, they are subsequently reincorporated into nascent protoplanetary

systems as the solar system moves in its ~240My period orbit around the centre of the galaxy, encountering molecular clouds and giant molecular clouds as it does so.

1.3 The ultraviolet problem

Becquerel (1924) argued on the basis of laboratory experiments that bacteria could not survive space conditions, particularly exposure to ultraviolet radiation. Deactivation and damage of naked space-travelling individual bacteria was thought to occur due to the ultraviolet light of stars, and such criticisms have persisted into modern times (Mileikowsky et al., 2000; Horneck et al., 1993). However it has been shown (Lewis, 1971) under normal laboratory conditions that microorganisms are not easily destroyed by ultraviolet. Instead they are frequently deactivated due to the dimerization of pyrimidine bases, a reversible process in which no genetic information lost. (Dimerization of bases distorts the DNA configuration and impedes transcription. Repair takes place by exposure to visible sunlight or by the operation of specialised enzymic systems)

Conditions in interplanetary or interstellar space (cryogenic conditions in the absence of air and water) are found to be less damaging. Most relevantly, perhaps, we note that it is possible to shield microorganisms against ultraviolet light. Molecular clouds in the galaxy can remove the glare of ultraviolet radiation and enable the growth of protective coatings around bacterial particles. In Chapter Six we will demonstrate how thin skins of carbonised material around individual bacteria, only 0.02 μm thick, would also shield the damaging ultraviolet radiation.

1.4 Resilience of bacteria

Survival against ionising radiation has been a common objection to panspermia, with claims that exposure to cosmic rays in space over hundreds of thousands of years would prove fatal to microorganisms. These criticisms are not borne out by direct experiments under appropriate conditions, and likewise overlook the huge replicative power of bacteria. According to the Hoyle-Wickramasinghe theory of cometary panspermia

(1979, 1981), even the minutest rate of survival ($\sim 10^{-21}$) would ensure the propagation of microbial life across vast cosmic distances. We shall return to this point in Chapter 7.

During an average residence time of 10 million years the cumulative radiation dose (at a very low flux) received by a bacterium in a typical location in interstellar space is estimated as $\sim 10^{6}$ rad (1 rad = 10^{-2} joules of energy absorbed per kg of matter). Ionising radiation dislodges electrons, causing bond breaks in the DNA and forms reactive free radicals. Although many terrestrial bacterial species may not survive this process, some almost certainly would. Under laboratory conditions, doses of 2 megarads (2Mrad) delivered over minutes limited residual viability of *Streptococcus faecium* by a factor of a million (Christensen, 1964), but similar doses have had a negligible effect on cultures of *Deinococcus radiodurans* or *Micrococcus radiophilus* (Lewis, 1971).

It is difficult to estimate the dose of cosmic rays received by a naked bacterium in a typical location in interstellar space, over a fraction of a million years. Within the solar system it is possibly in the range 10-45 Mrad per million years and depends on the distance from the sun and the phase of solar activity, highest at times near the peak of the solar sunspot cycle. Such doses are higher than the integrated doses that have been delivered within the laboratory, where the survival of bacteria is well-attested. Yet there is great uncertainty as to whether the terrestrial experience of radiation susceptibility could be directly translated to interstellar conditions. In anaerobic conditions with low O_2 pressures the effects of ionising radiation are diminished. Reducing H_2O content has a similar effect since it is the oxidation of free radicals, in particular OH^{-} that causes over 90% of DNA damage. Low temperatures, which immobilise and prevent the diffusion of free radicals, lead to a similar outcome.

A question also remains as to whether radiation damage to bacteria is a linear process. Exposure to short pulses of high intensity radiation under laboratory conditions may be far more damaging than extremely low intensities of interstellar ionising radiation delivered to bacteria for millions of years in space. A terrestrial analogue is perhaps the microbial spores that have been exposed to the natural radioactivity of rocks over

geological timescales. In fact viable cultures of bacteria have been recovered from ice drills dating back 500,000 years, in amber over 25-40My (Cano and Borucki, 1995; Lambert et al., 1998) and from 120 million year old material (Greenblatt et al., 1999). Viable bacteria have also been recovered in salt crystals in a New Mexico salt mine dating back 250My (Vreeland et al., 2000). The present day dose rate of ionising radiation on the Earth arising from natural radioactivity is in the range 0.1-1 rad yr^{-1} (UNSCEAR, 2000). These well-attested recoveries of dormant bacteria/spores after 10^8 yr must therefore imply tolerance to ionising radiation with total doses in the range ~ 10-100Mrad. We shall discuss these issues further in Chapter 6.

1.5 Extremophiles

A hundred years ago the survival of microbes under space conditions may have seemed an improbable prospect. Recent developments in microbiology however, have shown the existence of many types of extremophile bacteria surviving in harsh terrestrial environments. The discovery of bacteria in conditions which may replicate those found in space has particular relevance to astrobiology.

Psychrophyllic microorganisms have been found to thrive in Antarctic permafrost (Karl et al., 1999), and Junge, Eicken and Deming (2004) have shown that some psychrophiles metabolise at temperatures below 100K, perhaps even as low as 50K. Thermophyllic bacteria were found to replicate in water heated to temperatures above 100°C in deep sea thermal vents (Stetter et al., 1990). An astounding total mass of microbes also exists some 8 kilometres below the surface of the Earth, greater than the biomass at the surface itself (Gold, 1992). A species of phototrophic sulfur bacterium that is able to perform photosynthesis at low light levels, approaching near total darkness (Overmann and van Gemerden, 2000) has been recovered from the Black Sea. Bacteria such as *D. radiodurans* have even been found to thrive within the cores of nuclear reactors (Secker, 1994), seemingly unaffected by radiation.

Thus microbiological research has revealed that microorganisms are incredibly space-hardy. These properties are now regarded as being crucial to astrobiology (Cowan and Grady, 2000). As the exploration of our solar system continues we will surely find

extraterrestrial bodies with environments analogous to many of the terrestrial environments where extremophiles are known to flourish (Cleaves and Chalmers, 2004).

1.6 Discovery of organics in cosmic dust

Dust abounds in the Universe - in interstellar space, in intergalactic space, in external galaxies, in planetary systems, in comets and on planets like the Earth. The amount of dust entering the Earth's atmosphere from interplanetary space is usually estimated to be about 20,000 tons per year (Love and Brownlee, 1993). The mean geocentric velocity of larger particles, visual or radar meteors, is about 40 km per second. If the small particles have this mean geocentric speed, an influx of 20,000 tons per year would imply an interplanetary density of about $\sim 10^{-22}$ gcm^{-3}.

The first identification of organic dust in space was made by Wickramasinghe (1974). The spectroscopic signature of a bacterium or bacteria-like material in the 2.9-3.5μm spectral region was found in interstellar dust (Allen and D. T. Wickramasinghe, 1981), signifying the first clear demonstration that over a third of the carbon in the galaxy was tied up in the form of organic dust grains (Hoyle et al., 1982). The infrared spectral correspondence unquestionably put a strain on any alternative inorganic processes for producing "bacteria-like" grains so efficiently on a galactic scale.

Another clear signal that may be indicative of biology is the λ=2175A ultraviolet absorption feature of interstellar dust which accords well with biologically derived aromatic molecules (Hoyle and Wickramasinghe, 1977; Wickramasinghe et al., 1989). Thus at least two striking spectroscopic features of dust seem to be consistent with living material being present everywhere in the Galaxy.

A connection of similar material with comets was also vindicated spectroscopically when the first infrared spectra of comet dust similar to interstellar dust were obtained at the last perihelion passage of Comet Halley in 1986 (D. T. Wickramasinghe et al., 1986). Other

comets studied since 1986 led to further confirmation of these results which will be discussed in Section 3.2.

With the launch of the Infrared Space Observatory (ISO) by ESA in 1995 a large number of unidentified infrared bands (UIB's) have been discovered in emission at well-defined wavelengths between 3.3 and 22μm in a wide range of types of astronomical object. Whilst polyaromatic hydrocarbons (PAH's), widely presumed to form inorganically, are the favoured model for the UIB's, it is the case that no satisfactory agreement with the available astronomical data has been shown possible, particularly if we require the UIB emitters and the 2175A absorbers to be the same. Biologically generated aromatic molecules will be seen in Chapter 2 to provide a better explanation of this set of data. Investigations of Guillois et al. (1999) have pointed to a promising model based on coal (anthracite), which is a degradation product of biology.

More recently Caltaldo, Keheyan and Heyman (2004) have shown that aromatic distillates of petroleum, another biological product, exhibits correspondence with the astronomical diffuse infrared bands (UIB's) as well as the λ=2175A ultraviolet absorption feature. As the resolving power of telescopes improves we will continue to discover more and more organics in molecular clouds.

In Chapter 2 we shall interpret data from the lens galaxy SBS 0909+532 at z=0.83 and also the far ultra-violet extinction of starlight in our galaxy and in external galaxies showing a biological provenance of both.

1.7 Comets

A comet taken in isolation is a rather insubstantial object. But the solar system possesses more than a hundred billion comets so that in total mass they equal the combined masses of the outer planets Uranus and Neptune, about 10^{29}g. If all the dwarf stars in the galaxy are similarly endowed with comets, then the total mass of all the comets in the Galaxy, with its 10^{11} dwarf stars, turns out to be some 10^{40}g. This is very close to the mass of all the interstellar grains.

When a new star system (eg. a solar system) forms from interstellar matter, comets condense in the cooler outer periphery as a prelude to planet formation. Cometary panspermia requires some small fraction of microorganisms present in the interstellar cloud to have retained viability, or to be capable of being reactivated after incorporation within newly formed comets. Radiogenic heating can maintain a warm liquid interior in each of the comets for thousands of years (Wallis, 1980; Hoyle and Wickramasinghe, 1985). If microbial replication can occur within the comet during its initial liquid phase, the previous history of interstellar destructive processes becomes irrelevant, because of the enormous capacity of even a single viable microbe to increase its number exponentially (See Chapter 7).

According to the Hoyle-Wickramasinghe theory, cometary activity in the outer regions of the solar system 4 billion years ago, including collisions between cometary bodies, would have caused the expulsion of a fraction of regenerated bacteria back into interstellar space. A fraction of comets would also be deflected into the inner regions of the solar system, thus carrying microorganisms onto the Earth and other inner planets. The first life on the Earth 4 billion years ago would, according to this model, have been brought by comets, and become established for the first time during the epoch of late heavy bombardment between 4 and 3.8 billion years ago. Because comets have continued to interact with the Earth throughout the past 4 billion years, a strong prediction of the model is that cometary injections of microbial life must be an ongoing process.

We know from observations of comet Halley near perihelion in 1986 that comets do eject organic particles, typically at a rate of a million tons per day. An independent analysis of dust impacting on mass spectrometers aboard the spacecraft Giotto also led to a complex organic composition that was generally consistent with the biological hypothesis (Wickramasinghe, 1993). Thus one could conclude from the astronomical data that cometary particles, just like the interstellar particles, are *spectroscopically* similar to biological material.

Recent collections of dust from comet Wild 2 in the NASA *Stardust* mission have revealed organic structures that could be interpreted as either prebiotic molecules or degradation products of biology (Sandford, 2006). However, it should be stressed that the *Stardust* mission was planned in the late 1980s, before life in comets was considered an option. As a result, no life-science experiments were properly planned, and the aerogel collection strategy involved high-speed collisions so that no microbes would be recovered intact.

In 2000, Krueger and Kissel reported the discovery that a mass spectrometer aboard *Stardust* had intercepted five interstellar dust particles. The shattered residue of these particles, impacting the instruments at a speed of 30 km/s, was found to include structures described as 'cross-linked hetero-aromatic polymers'. Such molecular fragments are consistent with the break-up products of bacterial cell walls – arguably the only types of biological structures that could survive the high impact speeds. These results are consistent with spectroscopical identifications discussed earlier.

On July 4th 2005, NASA's *Deep Impact* probe collided with comet Tempel 1. The resulting ejecta was analysed using mass spectroscopy and an increased amount of organics was found to have been released after the collision (A'Hearn et al., 2005). Evidence of clay minerals was also discovered, this material being unable to form without the presence of liquid water.

Thus we can conclude without hesitation that the pristine cometary interior of Tempel 1 contains both organics and water. The spectroscopic results will be examined more fully in Chapter 7.

1.8 The origin of life

One of the earliest theories of the origin of terrestrial life is the ancient principle of spontaneous generation. According to this theory life was claimed to arise from inorganic matter spontaneously under 'suitable' conditions. For instance the Greek

philosopher Aristotle (384-322BC) stated that fireflies emerge from a mixture of warm earth and morning dew.

Biological material contains about twenty different types of atoms, the most important being carbon, nitrogen, oxygen and phosphorus. The ultimate source of origin of these chemical elements is stellar nucleosynthesis – the process by which the primordial element H is converted first to He and thence to C, N, O and heavier elements in the deep interiors of stars (Burbidge et al., 1957). So at the level of constituent chemical elements our origins can undeniably be traced to astronomy.

The standard theory of the origin of life was that due to Haldane (1929) and Oparin (1953) in which it was proposed that life began in a 'primordial soup' of organic chemicals that developed on a primitive Earth. Starting from a mixture of inorganic molecules such as water, methane, ammonia and hydrogen cyanide, they proposed that flashes of lightning occurring in thunderstorms and the ultraviolet rays from the sun could break up these inorganic molecules into fragments that could recombine to form a trickle of organics. The organics then rain down into the primitive oceans, and life could then begin through a multitude of chemical reactions over tens of millions of years.

This theory gained ground after the classic experiments of Miller and Urey (1959) where it was shown that organic chemicals that may serve as the building blocks of life (amino acids, sugars and nucleotide bases) could form from suitable mixtures of inorganic gases such a H_2O, CH_4, NH_3 when subjected to electrical discharges or energetic radiation.

F. Crick (1973) and Hoyle and Wickramasinghe (1982) amongst others have pointed out that the transition from chemical building blocks to microbial life is an exceedingly improbable step. Numerically, the odds against life emerging within a small terrestrial pond are estimated as some 10 raised to the power of many thousands, against one. In other words, the transition from the organic building blocks (such as sugars and amino acids) to life itself is not easily achieved, and surely not in the limited confines of our planet, and in a timescale available. The Earth being physically connected to material

distributed on a much wider scale throughout the Galaxy, there is no logical reason to confine the origin of life to our planet. A galactic or cosmic setting for the first origin of life would appear far more plausible.

1.9 Modern advances

In recent years, modern developments which favour a cosmic connection for life have emerged. By measuring carbon isotope ratios in sedimentary rocks, Mojzsis et al. (1996) have detected evidence of microbial life on the Earth before 3.83 Gya. This corresponds to the end of the Hadean Epoch, a period of late heavy bombardment of the Earth by comets and meteorites when *in situ* development of a primordial soup would have been impossible to achieve. In addition Mojzsis et al. (2001) have discovered evidence of a possible Hadean ocean as early as 4.3 Gya, while Nisbet and Sleep (2001) have argued that such intense bombardment during this same period would have periodically led to the complete evaporation of oceans.

Therefore, whilst *in situ* prebiotic evolution may not easily occur under such hostile conditions, perhaps the cometary collisions themselves injected life onto the Earth during the period 4.0-3.83Gya. One could speculate that the bacterial phyla that survived under such episodes of recurrent evaporation were thermophiles, found at the base of the phylogenetic tree. Such lifeforms would have had the ability to survive the harsh prevailing conditions and from these lifeforms a very much larger set can evolve.

A requirement of panspermia models is that all the higher members of the tree of life came in the form of genetic components that could be assembled in response to the Earth's varying physical conditions. The perceived evolution in the phylogenetic tree (Woese and Fox, 1977) of terrestrial life within its branches, Archaea, Bacteria and Eukarya, then becomes a relic of the re-assembly process of cosmically-derived genes. Recent studies of DNA sequence phylogenies show that sequences corresponding to higher life forms and multiple domains of life are present even at the very root of the "tree of life" (Olsen and Woese, 1997). The search for convergence to a single Last Universal Common Ancestor (LUCA) is thus proving elusive, and the search should

more logically be directed to a "Last Universal Common Community" (LUCC). Tepfer and Leach (2006) have argued persuasively for an ensemble of genes preserved in the form of plant seeds (which may even be partially degraded) as a model for panspermia. This is consistent with the idea of a Last Universal Common Community rooted firmly in the cosmos.

1.10 Protoplanetary nebulae and extra-solar planetary systems

Panspermia implies the transference of life between habitable locations widely separated in the cosmos. The requirement therefore is that habitable abodes of life must exist in abundance on a galactic scale. Do astronomical observations support the existence of planetary systems outside our solar system?

The starting point of all theories of solar system formation is a fragment of an interstellar cloud, a central condensation of which ends up as a star. Surrounding a newly-formed star in an embryonic planetary system is a flattened, rotating, protoplanetary disk within which planets eventually form. Whilst an outer shell of icy cometary bodies could be expected to surround a planetary disk, such a shell which is optically thin would be more difficult to observe using present day observational techniques. Some of the most active regions of star formation in our immediate vicinity are to be seen in the Orion molecular clouds. Hubble telescope images have revealed the presence of many proto-planetary disks which show nebulae seen edge-on. Two nebulae that have been actively investigated at both infrared and millimetre wavelengths are β-Pictoris, and TW Hydrae, the latter showing evidence of mm- or cm-sized accumulations of planetary material in the disk (Wilner, 2005). Injection of viable bacteria and spores into disks such as in Figure 1 would lead to seeding with life from an external source (see Chapter 5).

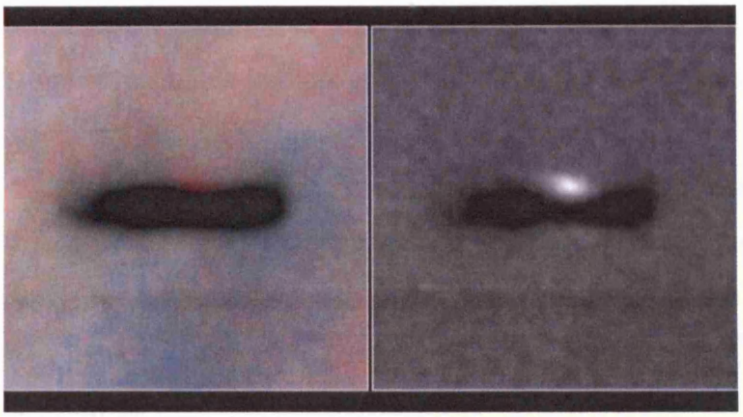

Figure 1: Edge-on protoplanetary disks in the Orion Nebula (McCaughrean and O'Dell, 1996)

Theories of planet formation suggest that planets must be a commonplace occurrence, at least for stars of masses between $1M_{\Theta}$ and $\sim 10M_{\Theta}$. Stability of planetary systems within a habitable zone around a parent star for timescales that are long enough for life to evolve is a separate issue which I shall not address in this thesis. The presence of any extrasolar planet, within which or on the surface of which microbial life can survive and replicate, would be of interest for panspermia and astrobiology.

Detection of extrasolar planets telescopically stretches modern astronomical technologies to the limit. If a planetary system like ours existed around our nearest neighbour α Centauri, its Jupiter counterpart would lie only 1" away from the central star, which would not be detectable against the brilliance of the central stellar disk even with our most powerful modern telescopes. Clearly indirect methods of extrasolar planet detection are required.

One such method that has been successfully deployed over the past decade is the use of the Doppler motions of central stars possessing Jupiter-mass planets. Viewed from the vantage of α Centauri our own Sun-Jupiter system would be detectable from dynamical effects. The star (Sun) and planet (Jupiter) would move around their common centre of mass with the period of the planet (11.8 yr), and this effect will be visible as a small regular Doppler wobble in the star's apparent path in the sky.

Since 1995 G. Marcy, P. Butler, M. Mayor, D. Queloz among others have used the Doppler technique to discover over 200 extrasolar systems, starting with the initial discovery of a planet around 51 Peg in the constellation of Pegasus (Mayor and Queloz, 1995; Marcy and Butler, 1996). Figure 2 sets out the characteristics of planetary systems discovered up until 2006, mainly using the Doppler technique.

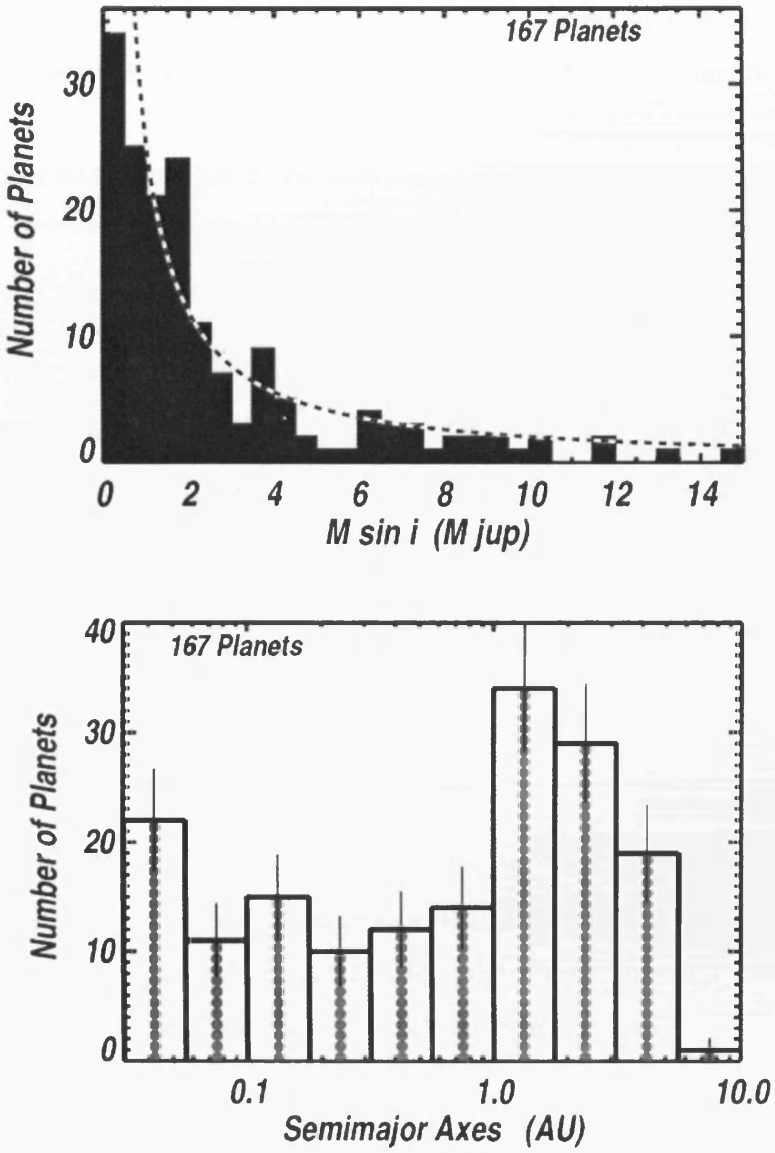

Figure 2: Histograms showing the distributions of exoplanets discovered upto 2006; their minimum mass with $M \sin i < 15$ (upper panel), and their distance from star with $0.03 < a < 10$ in logarithmic distance bins (lower panel) (Butler et al., 2006), i being the inclination.

We note that the Doppler method has a selective bias to find Jupiter-sized planets in relatively close proximity to the central star. However, an exception to this rule has recently emerged with the deployment of an ultra sensitive planet-hunting spectrograph HARPS on the ESO 3.6 metre telescope. Using this instrument several Neptune-sized planets and an Earth-sized one have so far been discovered. The most significant is the discovery of planets around the red-dwarf star Gliese 581 located at a distance of ~ 7pc in the constellation of Libra. Its mass is $0.31M_{\Theta}$, its radius $0.38R_{\Theta}$ and its effective temperature 3480K. The planets around this star have characteristics listed in Table 1.

Table 1: Characteristics of Gliese 581 planetary system

	Mass (M_E)	Orbital period (days)	Semi-major axis (AU)	Eccentricity, e
Gliese 581b	15.6	5.4	0.041	0.02
Gliese 581c	5.1	12.9	0.073	0.16
Gliese 581d	7.6	94	0.25	0.20

The smallest planet discovered upto May 2007 is Gliese 581c (1.5 times the Earth's radius) and it lies just within the habitable zone of its parent star as defined in the section below. However, von Bloh et al. (2007) have argued that Gliese 581d, which is tidally locked to the parent star, is a better candidate for habitability if a CO_2 greenhouse atmosphere is present.

1.11 Habitable zone

A habitable zone around a star is defined as the range of radial distance in which a planet can maintain conditions needed for life. This includes the requirement for liquid water at or near the surface, and ideally also a planet that can retain an atmosphere for timescales during which life can evolve. If the planet is too close to the star, surface temperatures would exceed the critical value for liquid water and if it is too far away the water will be in the form of solid ice. Other conditions for a stable habitable planet is that it is not too close to a Jupiter-sized planet whose interactions could lead to it being perturbed inwards or outwards (away from the habitable zone) on timescales that are too short. More restrictive, but perhaps more realistic conditions for Earth-type habitable zones have been

discussed by Franck et al. (2003). The calculations based on the simplest assumptions lead to the plot in Fig. 3 that shows the habitable zone for stars of various temperatures, assuming a main sequence mass-luminosity relationship (Underwood et al., 2003). Extrapolating the blue band in Fig. 3 to a mass of $0.31M_{\Theta}$ at its lower end we see that Gliese 581c might fall in the habitable zone.

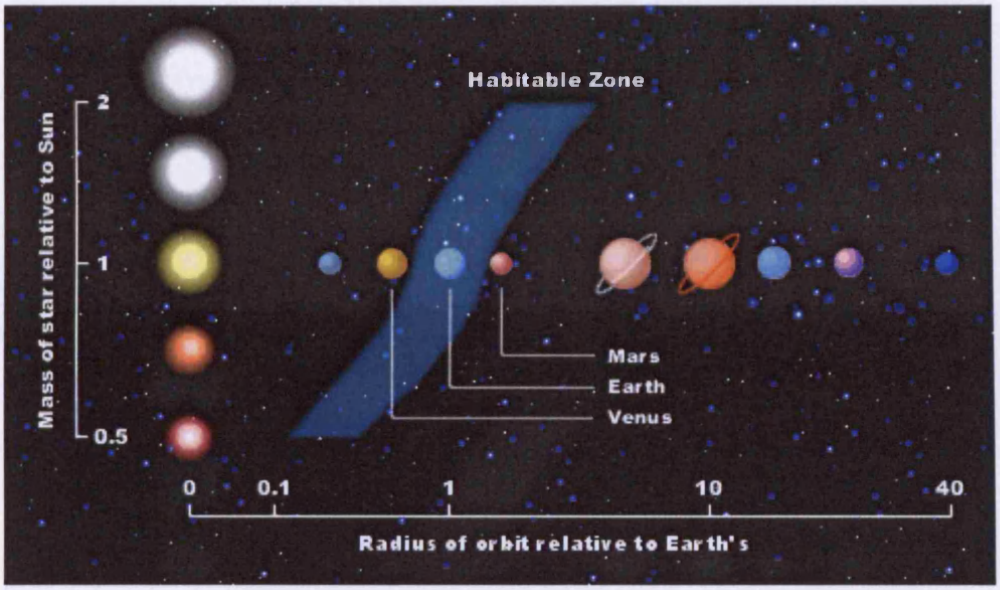

Figure 3: The habitable zone calculated by Barry Jones

The COROT mission led by the French national space agency CNES was launched in December 2006 with one of its objectives being to investigate the existence of exoplanets using the transit method (The transit method detects minute dips in the stellar brightness, as the planet partially eclipses its disk). Around 120,000 Main Sequence stars will be studied by COROT during its 2½ year mission in the hope that many more exoplanets will be discovered. The Kepler Mission due to be launched in 2008 will also study 100,000 Main Sequence stars continuously over 4 years using the transit method.

Confidence is growing that we may soon find that 'solar systems' like our own are commonplace. If so, the exceedingly improbable event of life's origins does not need to be replicated independently in every planetary abode that arises in the cosmos. According to panspermia theories, and the work described in this thesis, the life legacy will be out

there in space, ever-ready to be taken up by habitable comets, satellites or planets as they emerge. ESA's Darwin mission currently scheduled for launch in 2015 aims to detect biochemical signatures (H_2O, CH_4, O_3 etc.) on Earth-sized exoplanets by deploying a flotilla of orbiting 3-metre telescopes. New technologies have to be developed in time for this important project. Optimistic projections are that about 1% of stars in our neighbourhood have habitable planets. Since the average distance between stars is ~1.7 pc, the average distance between habitable planets would be ~ 8 pc.

Chapter 2: Interstellar Dust

2.1 Introduction

In this chapter we review the subject of interstellar and cometary dust in so far as it relates to panspermia. The revival of the ancient ideas of panspermia in the latter part of the 19th century by Kelvin, Helmholtz, Arrhenius and others was essentially driven by a biological imperative as discussed in Chapter 1. For Kelvin and Helmholtz the motivation stemmed from Pasteur's failure to produce microorganisms *de novo*; for Arrhenius an added incentive came from the growing evidence that bacterial spores and plant seeds have properties which enable them to endure extreme cold and ultraviolet radiation. A major modern revival of panspermia followed from the efforts of Hoyle and Wickramasinghe to identify the properties of interstellar dust.

Dust is all-pervasive in the Universe. Perhaps the most striking evidence for its existence is the conspicuous dark patches and striations which show up against the stellar background. As early as 1785, Herschel recognised and mapped this phenomenon in the Milky Way without the aid of photography. The concentration of infrared emission in the plane of the galaxy is a more modern indication of the presence of dust. Dust particles with radii mostly in the range $10^{-6} - 10^{-4}$ cm are concentrated within clouds – molecular clouds and giant molecular clouds with densities in the range 10 to several million atoms per cubic cm. Such interstellar clouds (gas and dust) occupy about 1% of the total volume of the galactic disc in the spiral arms and probably make up a few percent of the total mass of the Galaxy. New stars, planetary systems and comets all condense from such clouds of dust so its role is by no means trivial. We will show in a later section that there is spectroscopic evidence for the organic nature of cometary dust and of a general similarity between cometary and interstellar dust. It now becomes necessary to make further study of the interstellar dust from which comets are formed.

From 21cm data on neutral hydrogen emission which was available since the 1950's the average mass density of hydrogen in the solar vicinity is found to be 3×10^{-24}gm cm^{-3}. Together with hydrogen in molecular form (which exists inside denser clouds) the total hydrogen density can be reckoned to be about 5×10^{-24}gm cm^{-3}.

It is possible to set upper limits to the mass densities of the various types of grain materials proposed so far. The nuclear composition of the outer layers of a star is closely similar to that of the interstellar cloud from which it is condensed. This is true in particular for the case of the Sun for which the best data on relative abundances of the elements are available (see Table 2).

Table 2: A compilation of the relevant relative abundances in the Sun (Allen, 2000)

Element	AW	Relative Abundance
H	1	2.6×10^{10}
O	16	2.36×10^{7}
C	12	1.35×10^{7}
N	14	2.44×10^{6}
Mg	24	1.05×10^{6}
Si	28	1.0×10^{6}
Fe	56	8.9×10^{5}
Al	27	8.51×10^{4}

Table 2 together with the condition $\rho_H \approx 3 \times 10^{-24}$g cm^{-3} and the atomic/molecular weights of the various proposed materials leads immediately to Table 3.

Table 3: Upper limits of mass densities of various types of grain

Species	Max Density (g cm^{-3})
H_2O (ice)	4.8×10^{-26}
C	1.9×10^{-26}
Fe	0.6×10^{-26}
$MgSiO_3$ (ice)	1.2×10^{-26}
SiO_2	2.6×10^{-26}
Organic/Biologic $(H_2CO)_n$	4.7×10^{-26}

To the observational astronomer the most negative attribute of interstellar dust is its effect in dimming and reddening the light from distant stars. In the directions of dense, dark dust clouds in the galaxy, distant stars and extragalactic sources are completely blocked from view.

The first interstellar extinction observations were made by Stebbins, Huffer and Whitford (1939) using the techniques of photographic filter photometry. They measured

monochromatic magnitude differences between a reddened and unreddened star of the same spectral type (B) in the same galactic region over 3 distinct wavelengths. From their pioneering work followed further observations of interstellar extinction which currently span the wavelength 100μm in the infrared to 1000A in the ultra-violet and involves many tens of thousands of individual stars and includes the use of space telescopes and a variety of new observational techniques.

2.2 Modelling with spherical particles

The problem of light scattering by a spherical particle is essentially one in classical electromagnetic theory and involves a solution of Maxwell's equations with the appropriate boundary conditions on the sphere. Formal solutions were worked out independently by Mie (1908) and Debye (1909). The basic problem is as follows: a plane polarised electromagnetic wave is incident on a sphere of radius a, refractive index m. A long distance away the forward beam has lost a certain amount of energy. Part is *scattered* out of the forward beam and part *absorbed* by the sphere. The effective cross-sections for these processes are denoted $Q_{sca}\pi a^2$, $Q_{abs}\pi a^2$, where Q_{sca}, Q_{abs} are scattering and absorption efficiencies. The total cross-section for extinction is thus $Q_{ext}\pi a^2 = Q_{sca}\pi a^2 + Q_{abs}\pi a^2$, and we also define an albedo $\gamma = Q_{sca}/Q_{abs}$.

One of the objectives of the solution by Mie is to calculate Q_{sca}, Q_{abs} as functions of $x = 2\pi a/\lambda$, a dimensionless size parameter, and

$m = n - ik = \sqrt{\varepsilon - 2i\sigma\lambda/c}$

where λ is the wavelength of the incident radiation, n is refractive index, k is absorptive index, ε is the dielectric constant and σ is the conductivity of the grain. The solution gives

$$Q_{sca} = \frac{2}{x^2}\sum_{n=1}^{\infty}(2n+1)\left[|a_n|^2 + |b_n|^2\right] \qquad (2.1)$$

$$Q_{abs} = \frac{2}{x^2}\sum_{n=1}^{\infty}(2n+1)\,\mathrm{Re}\left(a_n + b_n\right) \qquad (2.2)$$

$$Q_{abs} = Q_{ext} - Q_{sca} \qquad (2.3)$$

If we write $y = mx$, the coefficients a_n , b_n are given by

$$a_n = \frac{x\Psi_n'(y)\Psi_n(x) - y\Psi_n'(x)\Psi_n(y)}{x\Psi_n'(y)\zeta_n(x) - y\zeta_n'(x)\Psi_n(y)} \tag{2.4}$$

$$b_n = \frac{y\Psi_n'(y)\Psi_n(x) - x\Psi_n'(x)\Psi_n(y)}{y\Psi_n'(y)\zeta_n(x) - y\zeta_n'(x)\Psi_n(y)} \tag{2.5}$$

Ψ_n, ζ_n, χ_n are Riccatti-Bessel functions defined by:

$$\Psi_n(z) = \left(\frac{\pi z}{2}\right)^{1/2} J_{n+1/2}(z) \tag{2.6}$$

$$x_n(z) = (-1)^n \left(\frac{\pi z}{2}\right)^{1/2} J_{-n-1/2}(z) \tag{2.7}$$

$$\zeta_n(z) = \Psi_n(z) + i\chi_n(z) \tag{2.8}$$

The material of the grain is dielectric for m real and is a metal or semi-conductor for m complex. In both cases a_n and b_n can be calculated using standard computational procedures. Computer programs for dealing with this problem are now in the public domain, and my own work involved adapting and modifying one that was being used at Cardiff University.

For $x = 2\pi a/\lambda \ll 1$ equations (2.1) and (2.2) take on the relatively simple form

$$Q_{ext} = -4x\,\mathrm{Im}\left\{\frac{m^2-1}{m^2+2}\right\} \tag{2.9}$$

$$Q_{sca} = \frac{8}{3}x^4\,\mathrm{Re}\left\{\left(\frac{m^2-1}{m^2+2}\right)^2\right\} \tag{2.10}$$

$$Q_{abs} = Q_{ext} - Q_{sca} \tag{2.10a}$$

We shall compute these quantities for the model /models of interstellar dust that were used for the purposes of this thesis.

2.3 Reflectivity of surfaces

Another quantity that we shall use later in the thesis refers to the fraction of electromagnetic radiation incident on a bulk surface (e.g. a comet) that is reflected rather than absorbed. Standard Electromagnetic Theory again provides a simple computational procedure. The coefficient of reflection R is given by

$$R = \frac{(n-1)^2 + k^2}{(n+1)^2 + k^2} \tag{2.11}$$

$$n^2 = 1/2\left[\left(\varepsilon^2 + 4\sigma^2\lambda^2/c^2\right)^{1/2} + \varepsilon\right] \tag{2.12}$$

$$k^2 = 1/2\left[\left(\varepsilon^2 + 4\sigma^2\lambda^2/c^2\right)^{1/2} - \varepsilon\right] \tag{2.13}$$

where ε is the dielectric constant (Abraham and Becker, 1950).

2.4 Equation of transfer

In order to assess the plausibility of theoretical interstellar dust models we require to know the relationship between extinction cross-sections of individual grains and the astronomically observed extinction of starlight. This involves solution of the equation of transfer in an optically thin approximation including the effect of scattering and absorption of starlight by grains, thus connecting model computations of Q_{ext} with $\Delta m(\lambda)$, the interstellar extinction at wavelength λ in magnitudes.

Consider an assembly of identical spherical grains of a given material and single radius a in the line of sight of a star. Suppose $I_0(\lambda)$ is the intensity of starlight received if no grains were present and $I(\lambda)$ the intensity actually received. If N denotes the column density of grains (cm^{-2}), a the radius of the grain and Q_{ext} is their average extinction efficiency, the equation of transfer yields

$$I(\lambda) = I_0(\lambda) \exp\left[-N\pi a^2 Q_{ext}\right] \qquad (2.14)$$

Using the definition of stellar magnitudes we then have the change in magnitudes due to extinction given by

$$\Delta m\,(\lambda) = 1.086 N\pi a^2 Q_{ext} \qquad (2.15)$$

For a distribution of particle radii defined so that $n(a)da$ is the column density in the radius range $a,a+da$ equation (2.15) is modified to

$$\Delta m\,(\lambda) = 1.086 \int_0^\infty \pi a^2 Q_{ext}\left(a,\lambda\right) n\,(a)\,da \qquad (2.16)$$

Since $\Delta m(\lambda)$ is proportional to $\langle\, Q_{ext}(\lambda)\,\rangle$ the normalised extinction determined observationally could be directly compared with a theoretical normalised extinction curve

$$\overline{Q(\lambda)} = \frac{\left\langle Q_{ext}(\lambda)\right\rangle - \left\langle Q_{ext}\left(\lambda_0\right)\right\rangle}{\left\langle Q_{ext}\left(\lambda_1\right)\right\rangle - \left\langle Q_{ext}\left(\lambda_0\right)\right\rangle} \qquad (2.17)$$

where λ_0 and λ_1 are two reference wavelengths (e.g. B & V filters).

For individual clouds of dust (interstellar clouds, or comet's coma) heated by ambient stellar radiation, infrared *emission* can be easily modelled in the optically thin case. The flux F_λ emitted by grains of radii a, absorption efficiency Q_{abs} is given by

$$F_\lambda \propto Q_{abs}(\lambda)\pi a^2 B_\lambda(T) \qquad (2.18)$$

where $B_\lambda(T)$ is the Planck function at temperature T. For a particular type of grain material with n, k determined in the laboratory, Q_{abs} is given by (2.10a) and the model

can be tested against an observed spectrum F_λ. We shall use this formula later in my thesis.

2.5 Modelling the interstellar extinction curve

Consider now the interstellar extinction curve in the Galaxy. The invariant properties of Galactic dust include the diffuse interstellar absorption bands at optical wavelengths like the 4430A band and the broad ultra-violet absorption feature centred at 2175A. Interstellar grains also exhibit a characteristic absorption band over the 2.9-3.5μm waveband, and a set of diffuse unidentified infrared emission features (Fig. 4) consistent with biologically-derived aromatics (Table 4) (see refs in Hoyle and Wickramasinghe, 1991).

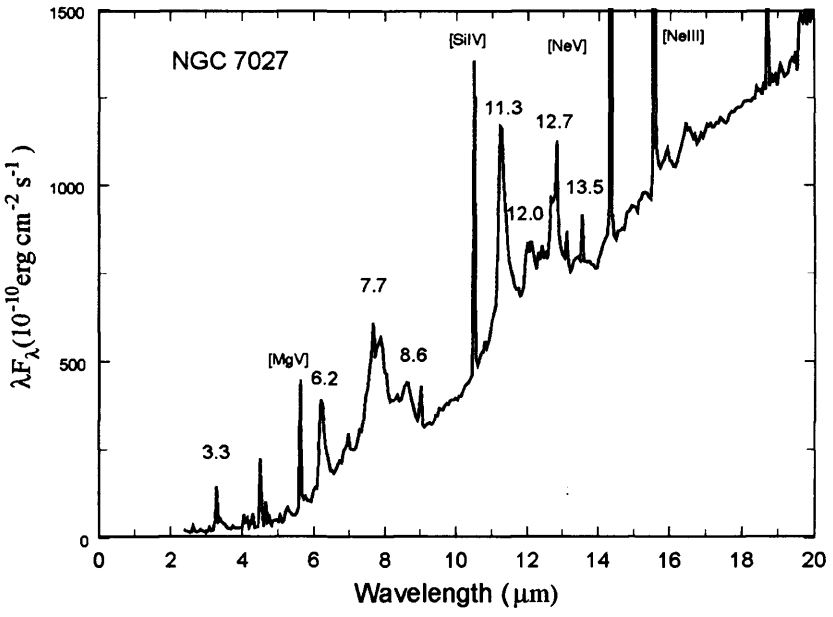

Figure 4: Emission spectrum of planetary nebula NGC 7027 obtained by ESA ISO satellite

Table 4: Wavelengths of principal emission peaks (μm)

NGC 7027		3.3	3.4		6.2	7.7	8.6	11.3
115 aromatics	2.9	3.3	3.4	5.25	6.2	7.7	8.8	11.25

The smoothed-out mean extinction curve for the Galaxy is shown by the curve marked "Obs" in Fig.5. Modelling this data requires three basic components in general: (1) dielectric grains of average radii 3000A; (2) a molecular absorber to account for the peak of extinction at 2175A and (3) dielectric grains of radii less than 200A. The 'dielectric' requirement for the components (1) and (3) permits any material with n~1.2-1.6 and k~0 in the visual band and near the ultra-violet spectral region. Inorganic ices and silicates are possibilities, but the infrared absorption of interstellar dust tells a different story.

From infrared absorption measurements it can be inferred that components (1) and (2) must be comprised predominantly of organic polymers which arguably may have a biological connection (see Figure 6). Although a mineral (largely silicate) admixture is also feasible, it is unlikely that such material contributes more than 10% to the mass of (1) and (2) in view of the abundance constraint listed in Table 3.

A schematic decomposition of the extinction into three such components is shown schematically in Fig.5. If curve (3) is assigned to organic particles of refractive index m=1.4, radius a=20nm and density 1.5g cm^{-3}, the mass extinction coefficient at wavenumber λ^{-1}= 9.4μm^{-1} is calculated from Mie theory as 9.875x10^{4} $cm^{2}g^{-1}$. To obtain the required contribution to interstellar extinction of 5 mag/kpc at 106nm with this material one therefore requires a mean mass density of 1.67x10^{-26} g cm^{-3}, which implies over a quarter of the total carbon density in interstellar space in the form of nanometric sized organic particles. We shall return to this point using my own calculations later in this chapter.

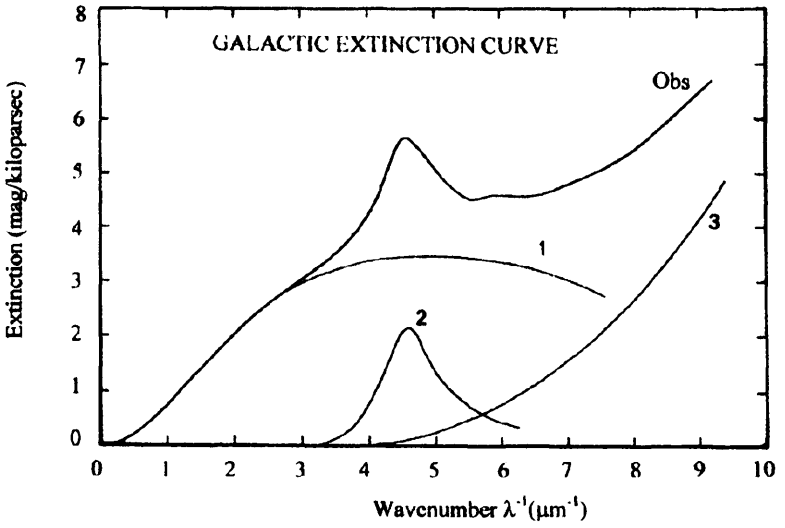

Figure 5: Interstellar extinction curve in the galaxy decomposed into 3 components (Hoyle and Wickramasinghe, 1991)

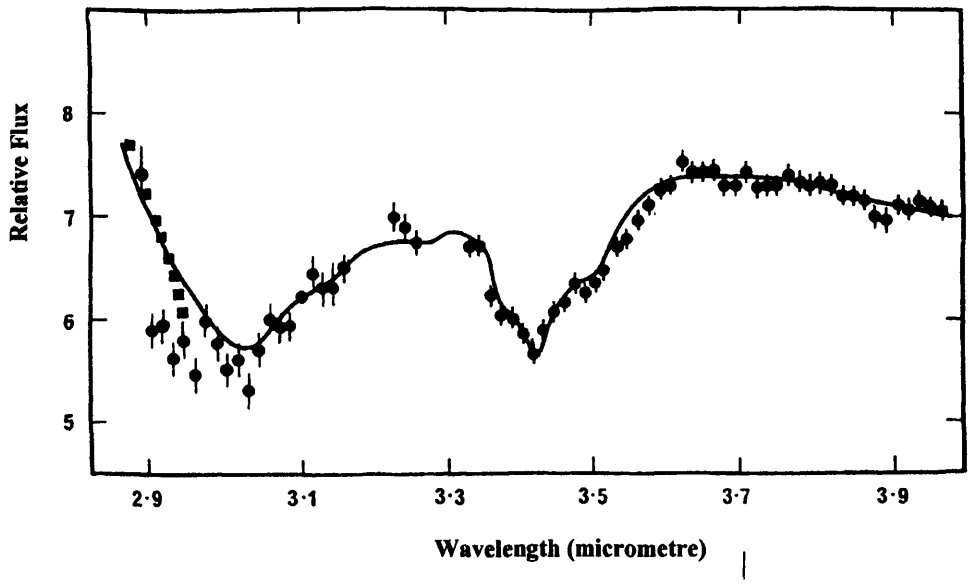

Figure 6: Infrared signature of dust over the 2.9-3.9 μm waveband. Relative flux data for GC-IRS7 from observations of Allen and D. T. Wickramasinghe (points) (1981) compared with S. Al-Mufti's predicted curve for dry *E.coli* type material (Hoyle et al., 1982)

2.6 Beyond the Galaxy

It has been known for many years that interstellar dust is not confined to our own galaxy. The best available data on extinction curves in external galaxies correspond to the Large Magellanic Cloud (LMC) and Small Magellanic Cloud (SMC). From observations of early-type supergiants Morgan and Nandy (1982), Kornreef (1982) and Nandy et al. (1984) obtained near infrared to visual extinction curves that were closely similar to that of the Galaxy. Ultraviolet extinction curves for these galaxies were also determined and found to be generally similar although not identical to the Galaxy: SMC and LMC show respectively a weak and middling 2175A extinction feature. Observations of many external galaxies have also shown evidence for diffuse infrared emission bands similar to the galactic bands, which may be reasonably interpreted in terms of polyaromatic hydrocarbons similar to those of biological origin as can be seen in the spectrum of the Antennae galaxies at 20Mpc (see Hoyle and Wickramasinghe, 1991). The similarity to anthracite is striking, anthracite being a degradation product of biology.

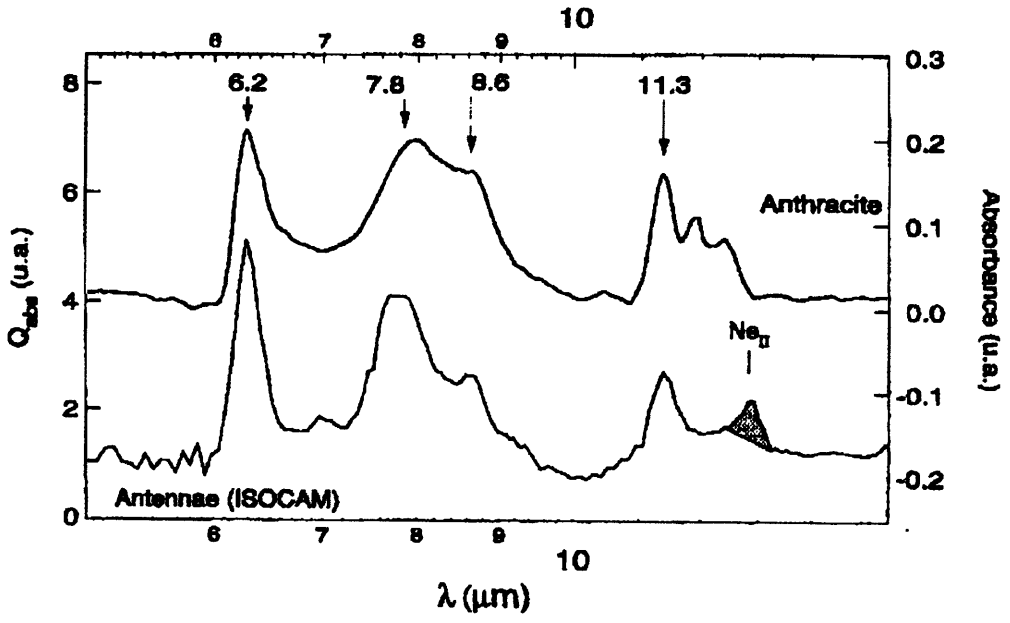

Figure 7: Spectrum of Antennae galaxies obtained by ISO compared with anthracite (Guillois et al., 1999)

2.7 Interpretation of a 2175A absorption feature at z=0.83

Following on from the work of Nadeau et al.(1991) and Falco et al. (1999), Motta et al. obtained spectra for a distant galaxy at redshift z=0.83 in 2002. The spectra showed a clear indication of a 2175A absorption feature. We shall compare these data with measured extinction curves from the Galaxy, LMC and SMC and with predictions from models. The observed extinction curve is found to be compatible with three-component models of classical grains and PAHs. Furthermore we note that the results can be interpreted in terms of products of a biological origin. This work will now be presented in greater detail.

The galaxy SBS 0909 +532 acted as a gravitational lens to amplify a quasar at a redshift z=1.38, yielding two distinct images. The two images correspond to slightly differing optical pathlengths through the lensing galaxy. The difference in apparent magnitudes observed at the lens galaxy $\Delta m(\lambda)$ then can be related to an average grain extinction efficiency $Q_{ext}(\lambda)$ for a spherical grain of radius a by the equation of transfer

$$\Delta m(\lambda) = \Delta M + 1.086 N \pi a^2 Q_{ext}(\lambda) L. \qquad (2.19)$$

Here λ is the wavelength at the lens redshift; N, is the number density of grains and L is an effective path length difference leading to the two distinct images. ΔM is a magnitude offset due to the difference between the amplifications of each image. The observations of Motta et al. (2002) yield magnitude differences $\Delta m(\lambda_1)$ where λ_1 is the redshifted wavelength $\lambda_1 = (1+z)\,\lambda$. Setting z=0.83 they made the remarkable discovery of an extinction peak at ~ 2175A, similar to the ultraviolet peak in the Galaxy, after the spectra were corrected appropriately to take account of the redshift.

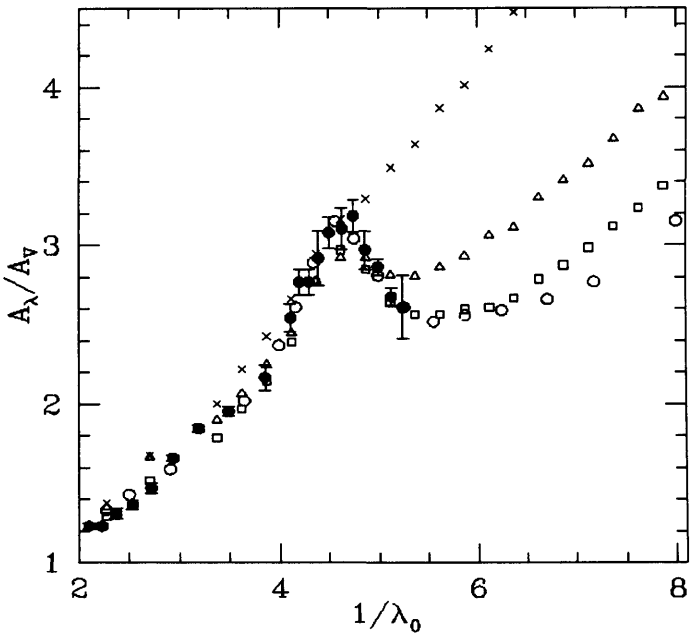

Figure 8: Extinction data for SBS 0909+532 (filled circles with error bars), for the Galaxy (open circles), LMC (squares), LMC shell (triangles) and SMC (crosses). The abscissae are wavenumbers in μm^{-1}.

To infer the A_λ/A_V values for the SBS 0909+532 extinction curve from the data of Motta et al. we need to perform the transformation

$$A_\lambda / A_V = \Delta m\,(\lambda) / A_V - \Delta M / A_V \qquad (2.20)$$

To determine A_V and ΔM we need to do a least squares fitting between the Motta et al. and the Galactic data in the 2.1 to 5.5μm^{-1} wavenumber range, obtaining A_V= 0.75 and ΔM=-0.55.

Fig. 8 shows the extinction curve, A_λ/A_V, of Motta et al. (open circles) compared with data for the Galaxy (Sapar and Kuusik, 1978; Hoyle and Wickramasinghe, 1991) and for the Small and Large Magellanic Clouds (Gordon et al., 2003). We have also included the LMC shell extinction curve. The detailed shape of the extinction over the entire wavelength range $2<\lambda^{-1}<5$ μm^{-1} agrees remarkably well with the Galactic curve, as was pointed out by Motta et al. (2002). However, as can also be seen in Figure 8, the

extinction curves from the LMC, LMC (shell), and Galactic are very similar for $\lambda^{-1} < 5$ μm^{-1}. Beyond this wavenumber value the curves from LMC (shell) and Galactic clearly separate. The points of the SBS 0909+532 extinction curve for $\lambda^{-1} > 5$ μm^{-1} seem to follow the trend of the Galactic and LMC curves but the error bars make the data also compatible with the LMC (shell) law. This effect will be interpreted in this thesis as a probable decline in the density of nanometric organic/biological particles.

2.8 Exploring models

Dust models that can fit an observational extinction curve over near infrared, visible ultraviolet spectral regions invariably require a mixture of compositions and sizes (Weingartner and Draine, 2001). The uniqueness of any such model is open to question, so the exploration of various grains size distributions and compositions becomes worthwhile. This is certainly true in the case of SBS 0909+532, a galaxy at z=0.83, the furthest galaxy for which a detailed extinction curve is available. In this section we consider mixtures of three grain components to fit the extinction curve in SBS 0909+532.

Component 1 (comprised of dielectric particles in the size range 0.1-0.7μm) contributes mostly in the visual spectral region; component 2 in the mid-ultraviolet region including the 2175A bump; and component 3 mainly in the far ultraviolet. This mixture can be built up under both the classical and the biological perspectives.

Under the classical point of view we would consider: (1) a size distribution of hollow dielectric grains (classical grains) with m=1.167 and $\langle a \rangle$=0.35μm, (2) aromatic molecules or spherical graphite grains of radii 0.02 μm both of which have a symmetric absorption band centred on 2175 A, and (3) dielectric grains with m=1.5, a=0.025μm (Rayleigh scatterers).

To adopt a biological point of view that we favour in this thesis we need reinterpret components (1) and (3) in terms of hollow and filled organic grains respectively. The three components of the biological model are generically similar to the ones considered earlier to model Galactic extinction data (Hoyle and Wickramasinghe, 1991). In this

earlier model component (1) was attributed to freeze-dried desiccated bacterial particles and components (2) and (3) to their degradation products.

The average $<Q/a>$ values (in units of μm^{-1}) for the several components are plotted in Fig. 9. The curve marked "Class" refers to a desiccated hollow organic grain model (Hoyle and Wickramasinghe, 1979) which can be also interpreted in terms of classical dielectric grains (it has extinction properties not unlike the general features of van de Hulst's curve #12 for classical dirty ice grains (Wickramasinghe, 1967)). The curve "Diel" calculated from the Mie formulae refers to component 3, whilst "Arom" and "Gr" refers to aromatic and graphite alternatives for component 2. The curve for graphite is calculated from the Mie formulae (Wickramasinghe, 1973) using the optical constants for graphite and a radius of 0.02μm, assuming spherical grains. The curve for aromatic particles is a normalised absorption curve for an ensemble of 115 biological aromatic compounds (Hoyle and Wickramasinghe, 1991).

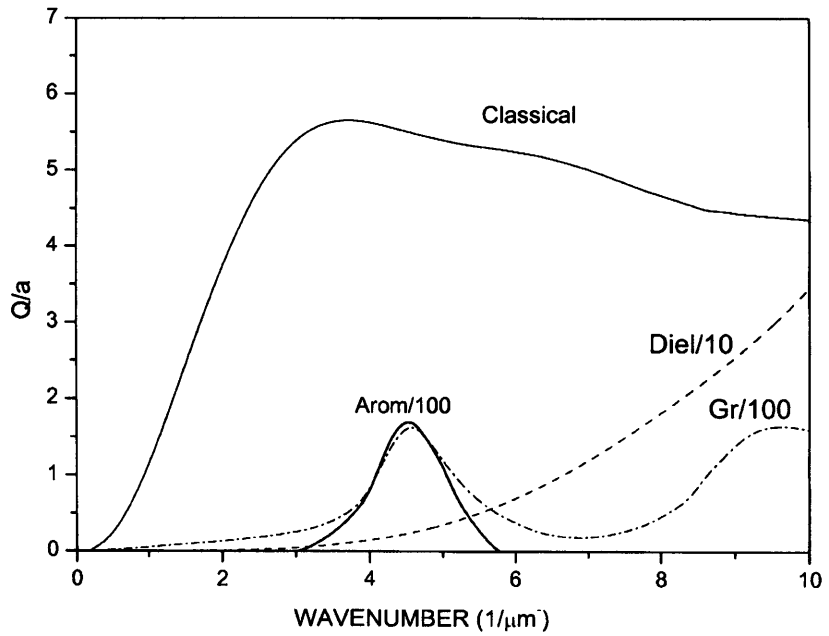

Figure 9: Mean Q/a curves for separate components of the mixtures of grains

We generate a two-parameter family of models with variable weightings of components 2 and 3 relative to component 1. A mean efficiency factor $Q(\lambda)$ for each case is calculated according to

$$Q(\lambda) = [Q_1(\lambda)/Q_1(4.6\mu m^{-1}) + bQ_2(\lambda)/Q_2(4.6\mu m^{-1}) + dQ_3(\lambda)/Q_3(4.6\mu m^{-1})]/(1+b+d) \quad (2.21)$$

Q_1, Q_2, Q_3 being the extinction efficiencies of each of the three components, with b and d being defining parameters of the model. Thus the relative extinction contributions at the $4.6\mu m^{-1}$ wavenumber are defined as

Class:Dielectric:Aromatic or Graphite = 1:b:d (2.22)

Table 5 lists the parameters we consider for a set of models involving classical grains (Class), small dielectric particles (Diel) and aromatic molecules (Arom)

Table 5

A	Class:Dielectric:Aromatic	1:0.00:0.7
B	Class:Dielectric:Aromatic	1:0.03:0.7
C	Class:Dielectric:Aromatic	1:0.05:0.7
D	Class:Dielectric:Aromatic	1:0.10:0.7
E	Class:Dielectric:Aromatic	1:0.15:0.5
F	Class:Dielectric:Aromatic	1:0.30:0.2

For each model in Table 5 we compute an average $Q(\lambda)$ from equation (2.21) and normalise the extinction according to equations (2.19) and (2.20) with $A(\lambda)$ being replaced by $Q(\lambda)$. Figure 10 shows normalised extinction curves for models A-F.

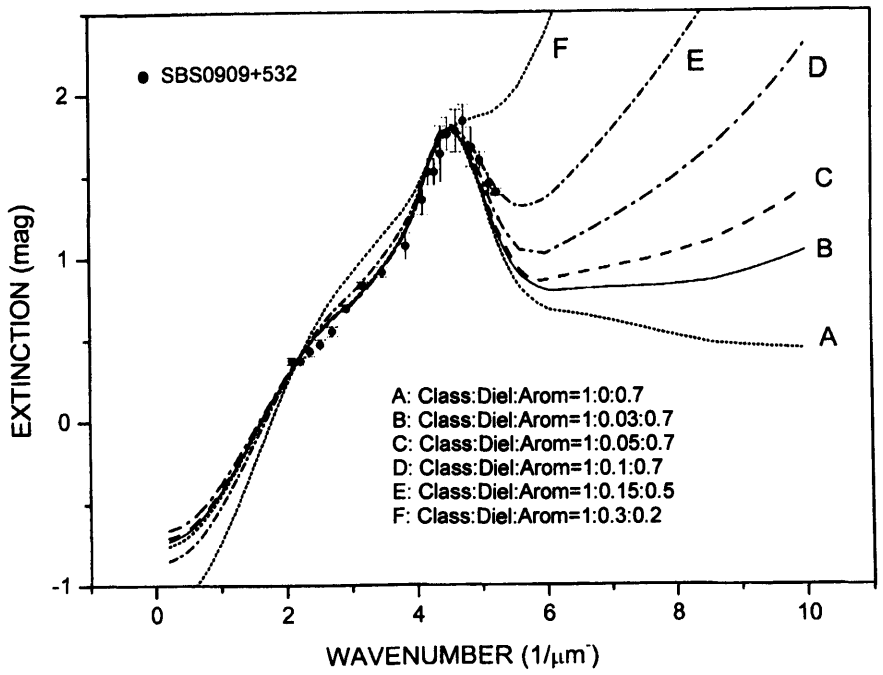

Figure 10: Normalised extinction curves for models A-F involving aromatic grains compared to the data for SBS 0909+532

Table 6 sets out the corresponding parameters for the same models as in Table 5 but with graphite replacing the aromatic component. Fig. 11 shows the normalised extinction curves for this set of models. Fig. 12 compares the cases for graphite vs aromatics in one particular instance.

Table 6

G	Class:Dielectric:Graphite	1:0.00:0.7
H	Class:Dielectric:Graphite	1:0.03:0.7
I	Class:Dielectric:Graphite	1:0.05:0.7
J	Class:Dielectric:Graphite	1:0.10:0.7
K	Class:Dielectric:Graphite	1:0.15:0.5
L	Class:Dielectric:Graphite	1:0.30:0.2

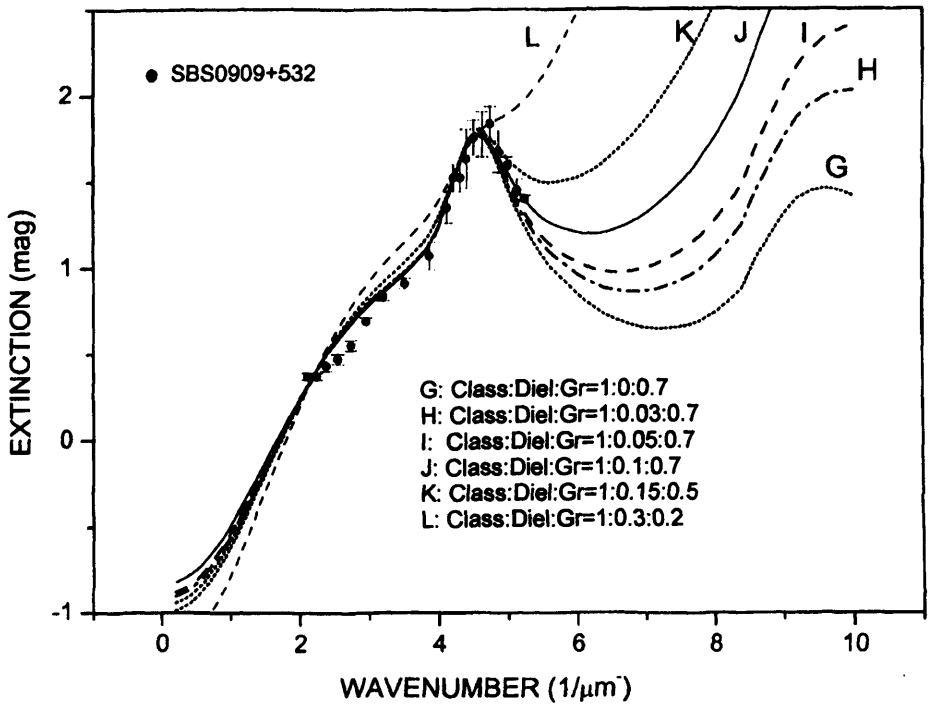

Figure 11: Normalised extinction curves for models G-L, graphite replacing aromatics in Fig. 10

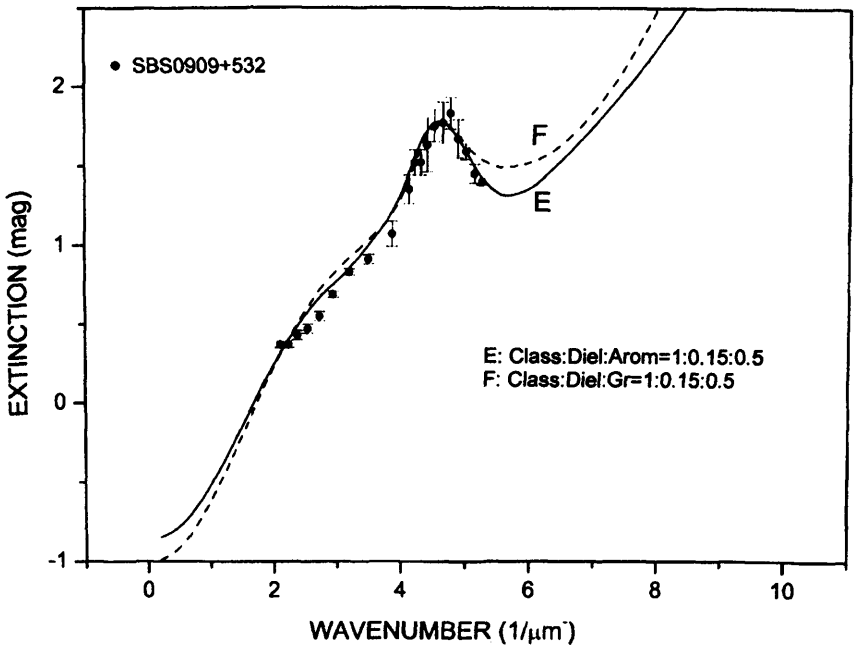

Figure 12: Comparison of normalised extinction curves for aromatic and graphite alternatives in one case

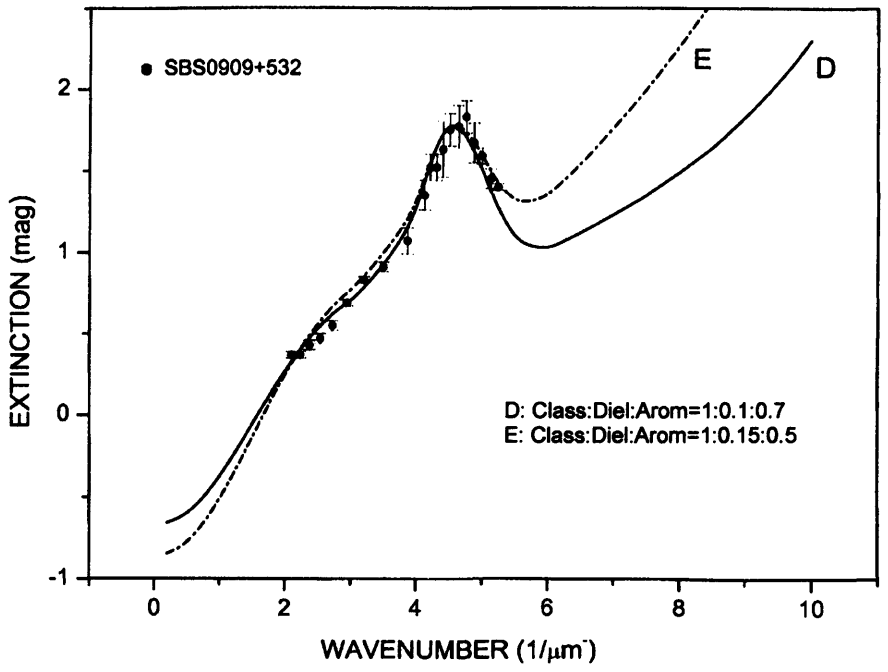

Figure 13: Two best fitting models to data for SBS 0909+532

We see that a simple three component grain model can reproduce all this range of properties. The data by Motta et al. are in principle, similar to the Galactic and LMC curves. However, the absence of far UV data makes them also compatible with the LMC (shell) and a variety of models. Two models (D and E) that are particularly satisfactory are shown in Figure 13.

The differences between aromatics and graphite for component 2 may seem marginal from a curve-fitting point of view. However, because of the highly artificial requirement for graphite grains of a single value of radius and spherical particles we prefer the option of aromatic molecules. If the 20nm radius dielectric grains of component (3) are arguably identified with nanobacteria it would imply that over half the mass of all interstellar grains in the galaxy SBS 0909 +532 are possibly nanobacteria, a very similar situation to that which, on the biological model, exists in our galaxy.

The prevalence of nanobacteria on such a vast cosmic scale would have profound implications for the problem of the origin of life. Particles of nanometric sizes are easily propelled by radiation pressure and have a greater resistance to radiation (Sommer et al., 2004), increasing the rate of viable transfers.

If such particles are associated with biology, as is likely to be the case, then the data of Motta et al. extends the range of cosmic biology/panspermia to a redshift of z=0.83, a considerable volume fraction of the observable universe.

2.9 Fluorescence

In addition to being responsible for extinction of starlight and thermal re-emission, interstellar grains are also associated with a fluorescence phenomenon leading to extended red emission over the waveband 5000-8000A. Such emission has been observed in planetary nebulae (Furton and Witt, 1992), HII regions (Sivan and Perrin, 1993), dark nebulae (Matilla, 1979) and high latitude cirrus clouds (Szomouru and Guhathakurta, 1998) in the Galaxy as well as in extragalactic systems (Perrin, Darbon and Sivan, 1995; Darbon, Perrin and Sivan, 1998). This phenomenon has a self-consistent explanation on the basis of fluorescence of biological chromophores (pigments), e.g. chloroplasts and phytochrome. Competing models based on emission by compact PAH systems are not as satisfactory, as is evident in Fig. 14. Hexa-peri-benzocoronene is one of a class of compact polyaromatic hydrocarbons that have been discussed in the astronomical literature. However, the width and central wavelength of its fluorescent emission leave much to be desired.

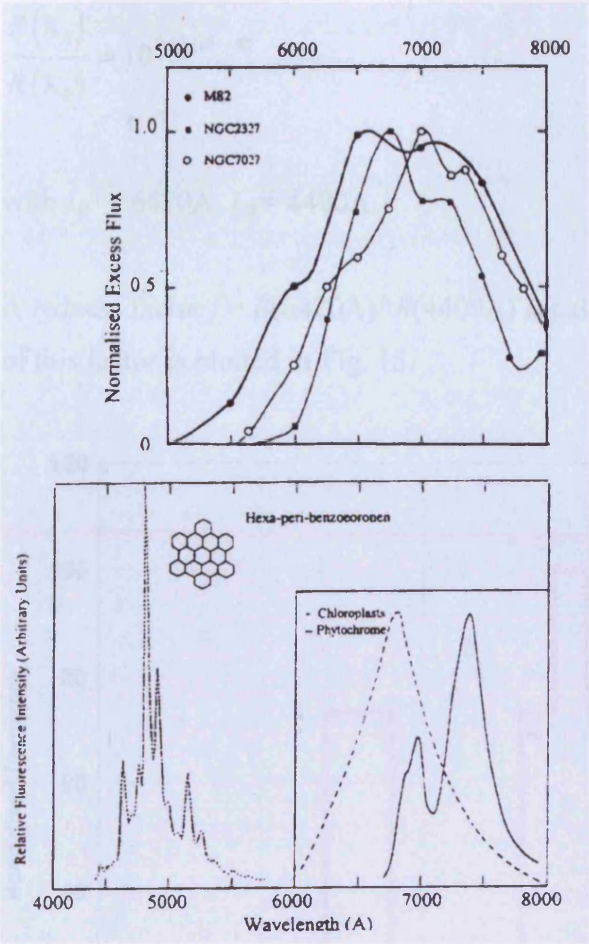

Figure 14: The points in the top panel show normalized excess flux over scattering continua from data of Furton and Witt (1992) and Perrin et al. (1995). The bottom right panel shows relative fluorescence intensity of spinach chloroplasts at a temperature of 77 K. The dashed curve is the relative fluorescence spectrum of phytochrome. The bottom left panel is the fluorescence spectrum of hexa-peri-benzocoronene.

I have already mentioned that cometary dust and interstellar dust have generic and compositional similarities. Besides extended red emission from galactic and extragalactic sources of dust there is also evidence of "excess redness" in objects within the solar system (Tegler and Romanishin, 2000). Some of the Edgeworth-Kuiper belt comets were found to have some of the reddest colours of any objects of the solar system. For the objects listed by Tegler and Romanishin we have taken B-V and V-R colours and calculated a reflectivity ratio given by

$$\frac{R(\lambda_R)}{R(\lambda_B)} = 10^{0.4\Delta(B-R)} \qquad (2.23)$$

with λ_R = 6420A, λ_B = 4400A.

A redness factor $f = R(6420A)/R(4400A)$ is calculated and a histogram of the distribution of this factor is plotted in Fig. 15.

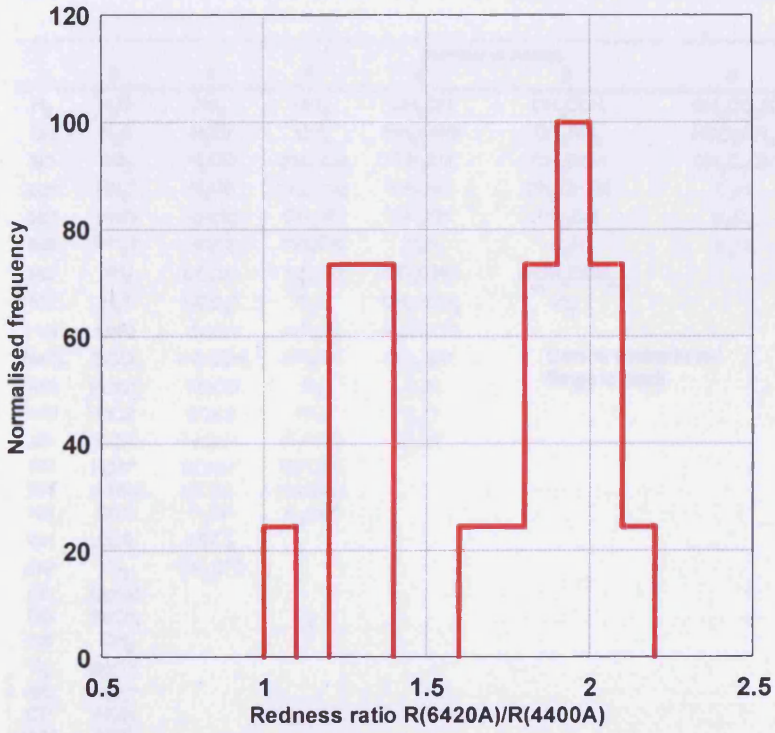

Figure 15: The distribution of the reflectivity ratio in Kuiper Belt Objects and Centaurs, from data given by Tegler and Romanishin

The two distinct peaks in this figure show that two classes of Kuiper belt objects can be identified, one red with $f = 2$, the other grey with $f = 1.2$. Asteroids and 'normal' comets have f in the range 1 to 1.26 (Wickramasinghe and Hoyle, 1998; Wickramasinghe, Lloyd and Wickramasinghe, J.T., 2002). A similar conclusion follows from Jewitt's study (2005) of a larger set of Kuiper Belt objects, to be discussed in Chapter 3. Significantly higher values of the redness factor f have a ready explanation in terms of fluorescence of

biological-type pigments generated by solar UV processing of the surfaces of Kuiper Belt objects.

2.10 The origin of organic molecules in space

Since the late 1960's interstellar clouds have been discovered to contain a large number of molecular species. The total number of molecules in the ISM total over 180 but this tally is dependent on the limitations of observational techniques, involving radio, mm and IR observations. A complete list upto 1999 is shown in Fig. 16.

Number of Atoms

2	3	4	5	6	7	8	9
H_2	H_2O	NH_3	SiH_4	CH_3OH	CH_3COH	CH_3CO_2H	CH_3CH_2OH
OH	H_2S	H_3O^+	CH_4	NH_2CHO	CH_3NH_2	HCO_2CH_3	$(CH_3)_2O$
SO	SO_2	H_2CO	CHOOH	CH_3CN	CH_3CCH	CH_3C_2CN	CH_3CH_2CN
SO^+	HN_2^+	H_2CS	HCCCN	CH_3NC	CH_2CHCN	C_7H	$H(CC)_3CN$
SiO	HNO	HNCO	CH_2NH	CH_3SH	HC_4CN	H_2C_6	$H(CC)_2CH_3$
SiS	SiH_2?	HNCS	NH_2CN	C_5H	C_6H	C_8^-?	C_8H
NO	NH_2	CCCN	H_2CCO	HC_2CHO	c-CH_2OCH_2		C_9^-?
NS	H_3^+	HCO_2^+	C_4H	CH_2=CH_2	C_7^-		
HCl	NNO	CCCH	c-C_3H_2	H_2CCCC			10
NaCl	HCO	c-CCCH	CH_2CN	HC_3NH^+	Carbon chains in red		
KCl	HCO^+	CCCO	C_5	C_5N	Rings in black		CH_3COCH_3
AlCl	OCS	CCCS	SiC_4	C_6^-?			$CH_3(CC)_2CN$?
AlF	CCH	HCCH	H_2CCC	C_5S?			
PN	HCS^+	$HCNH^+$	HCCNC				11
SiN	c-SiCC	HCCN	HNCCC				
NH	CCO	H_2CN	H_3CO^+				$H(CC)_4CN$
CH	CCS	c-SiC_3					
CH^+	C_3	CH_2D^+?					13
CN	MgNC						
CO	NaCN						$H(CC)_5CN$
CS	CH_2						
C_2	MgCN						Total: 124
SiC	HOC^+						
CP	HCN						
CO^+	HNC						
HF	KCN?						

Figure 16: Complete list of known interstellar molecules as of July 1999 (from Harvard Smithsonian CFA)

The list of observed interstellar molecules contains a significant fraction of organic molecules, and this is thought to represent just the tip of the iceberg with many remaining to be discovered. The biologically relevant molecules include H_2O, H_2CO (which could be a building block of polysaccharides) the amino acid glycine, acetic acid and a sugar

glycolaldehyde. Infrared observations of the diffuse interstellar medium (eg 3.3μm emission in the galactic cirrus) have also provided evidence of aromatic molecules (PAH's) as we have already discussed, and direct mass spectroscopy of interstellar dust in the *Stardust* Mission (Krueger et al., 2004) has shown the presence of cross-linked heteroaromatic structures in the degradation products of impacting grains. Evidence of fragments with atomic mass unit AMU>2000 consistent with pyrrole, furan substructures and quinones has been found (Fig. 17).

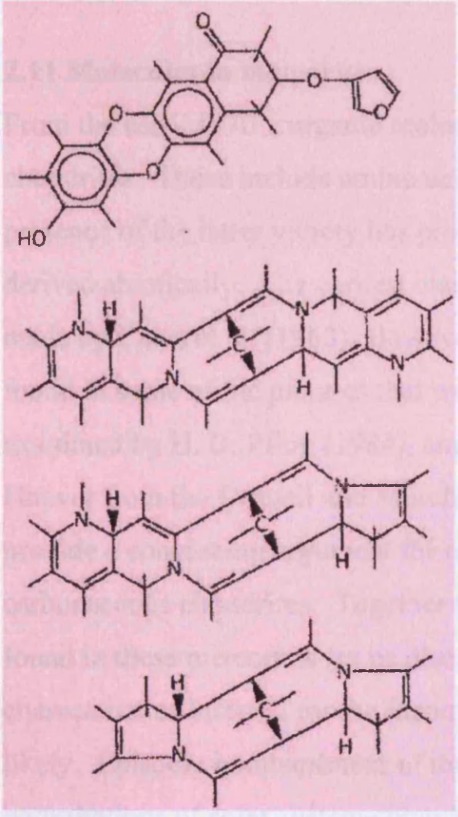

Figure 17: Functional groups in the break-up fragments of impacting interstellar dust grains, inferred by Krueger and Kissel from mass spectroscopy

In 1974 Wickramasinghe first proposed an organic polymeric composition of interstellar and cometary dust, and this idea was developed by Hoyle and Wickramasinghe (1977) to argue for the presence of biopolymers in interstellar grains. At the present time an organic composition for the bulk of interstellar grains is accepted without dissent. With an ever-growing list of gas-phase organic molecules in clouds associated with the

formation of new stars, the connection with astrobiology begins to appear self evident. Whilst attempts have been made to account for the observed interstellar molecules by processes involving ion-molecule reactions and surface chemistry on dust grains, the build-up of organic molecules of very high molecular weights may not be straightforward. Hoyle and Wickramasinghe (1989) have maintained that at least some of the organics in the ISM are degradation products of biologically derived material produced in the context of planetary systems, similar to the structures discovered by Krueger et al. (2004).

2.11 Molecules in meteorites

From the early 1970's organic molecules have also been identified in carbonaceous chondrites. These include amino acids, both biological and non-biological; and the presence of the latter variety has prompted the suggestion that all such molecules are derived abiotically. The earliest claim of organised elements (bacterial microfossils) was made by Claus et al. (1963). However, this was quickly rejected after ragweed pollen was found in some of the pictures that were published. The microfossil claim was re-examined by H. D. Pflug (1984), and in the last decade evidence obtained by R. B. Hoover from the Orgueil and Murchison meteorites (Hoover, 1997, 2005) would seem to provide a convincing argument for re-instating the 1960's claim of microfossils in carbonaceous chondrites. Together with the evidence of aqueous alteration in minerals found in these meteorites (to be discussed in more detail in Chapter 7), and the orbital characteristics inferred for the incoming bolide, a cometary connection seems to be likely. Episodic bombardment of the Earth by such objects could occur due to galactic perturbations of solar system cometary reservoirs, as we shall discuss in Chapter 4.

Chapter Three: Brief Overview of Comets

3.1 Introduction

Comets have been regarded with awe and fascination by civilisations throughout history. Their mysterious nature has long been a source of debate; from Babylonian times their status as celestial objects or atmospheric phenomena was already being discussed. From the 16th century onwards, certain fundamental discoveries relating to comets were made. In 1577 Tycho Brahe dispelled the myth that comets were atmospheric phenomena when he calculated the parallax of a comet and showed that it was at least 230 Earth radii away, well beyond the Moon.

In the 17th century Isaac Newton demonstrated that comets are subject to the same laws of motion and gravity that control planetary orbits. Applying this theory Halley compared the orbital elements of a number of well-observed earlier comets and successfully predicted the return of a comet in 1759, the comet which subsequently took his name. Earlier appearances of Halley's comet have now been identified from records dating back to 240 BC. In 1986, space probes Vega 1, Vega 2 and Giotto intercepted comet Halley as it once again approached the Sun and were able to collect extensive data on its physical composition. Recent explorations - the *Deep Space* Mission which impacted with comet Tempel 1 (2005) and the *Stardust* mission which intercepted comet Wild 2 (2006) – continue to enhance our understanding of comets.

An important role of comets could be in serving as probes of the most pristine, unchanged material in the Solar System. It is also becoming increasingly clear that comets interacting with the Earth over geological timescales had a profound influence on the development of terrestrial life, including mass extinction of species (Napier and Clube, 1979; Hoyle and Wickramasinghe, 1978a; Alvarez et al., 1980). There is growing evidence too that comets were connected with the origin of life, at the very least to the extent of providing prebiotic molecules that led to the assembly of a primitive self-replicating bacterium. More controversially, it can be argued that comets may even have provided the more complex genetic units that led to the introduction of life to the Earth.

3.2 The origin of comets and composition of comet dust

Comets are thought to have formed in the outer regions of the solar nebula about 4.5 billion years ago. The processes involved in the condensation of icy particles, their sticking together to form cometesimals, and finally the aggregations leading to cometary bodies are still under active discussion. Questions relate to the relative proportions of solar system material and pristine interstellar material that went to form the comets. If the first stages of comet formation occurred in the disc of solar material that was expelled from the primitive sun in the manner proposed by Hoyle (1978) the condensation process began when the gas cooled to 100K. This would have happened beyond the orbits of the present planets Uranus and Neptune. If the first stages of comet formation occurred in the more extended protosolar nebula the starting temperature would be below 30K. The observed distribution of the deuterium in water molecules may well hold a clue. The value of *D/H* in water in the Earth's oceans is ~ $40x10^{-6}$. The average value of *D/H* in water molecules in comets is $80x10^{-6}$ while that in interstellar clouds is about double, ~$720x10^{-6}$ (Bockelee-Morvan, D. et al., 1998; Robert, F. et al., 2000). The implication therefore is the cometary volatiles came in part from the inner solar nebula and in part from the interstellar cloud from which the solar system condensed. The *Stardust* results show that refractory high temperature minerals formed in the inner parts of the solar nebula are present in cometary dust. This is consistent with a comet comprised of a mixture of condensates from widely separated parts of the solar nebula. Because the interstellar clouds are known to be rich in organic material the inclusion of very similar material in comets does not come as a surprise.

The first confirmation of a cometary dust composition that was similar to biomaterial came with infrared spectroscopy of dust from comet Halley studied in 1986, and also from *in situ* mass spectroscopy using instruments aboard the Giotto spacecraft. The infrared spectrum of Halley dust in the 2.5-4μm waveband, showing similarity to bacterial material is shown in Fig.18. These correspondences have been discussed for many years (Hoyle and Wickramasinghe, 1985) and the critics have argued that such fits are not a unique indicator of bacteria. They are however consistent with a model

involving bacteria and their degradation products and/or complex organic polymers that mimic the spectroscopic behaviour of bacteria.

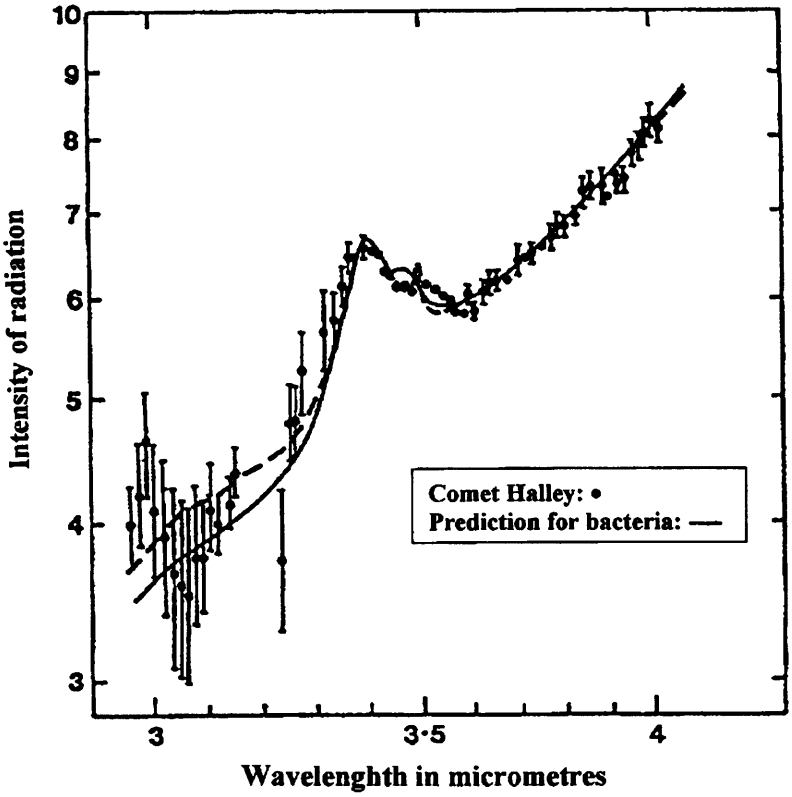

Figure 18: Observation (points) for comet Halley (data from D.T. Wickramasinghe and Allen, 1986) compared with predictions for a biological model involving *E. Coli* heated to 320K. The solid curve is the single temperature model in the small particle limit; the dashed curve uses the distribution of grain sizes as detected by the Halley probes (Hoyle and Wickramasinghe, 1991).

Similar features have been found in more recently studied comets as well (see Fig. 19), thus indicating, at the very least, that comet dust is largely organic in character, possessing spectroscopic properties indistinguishable from biomaterial.

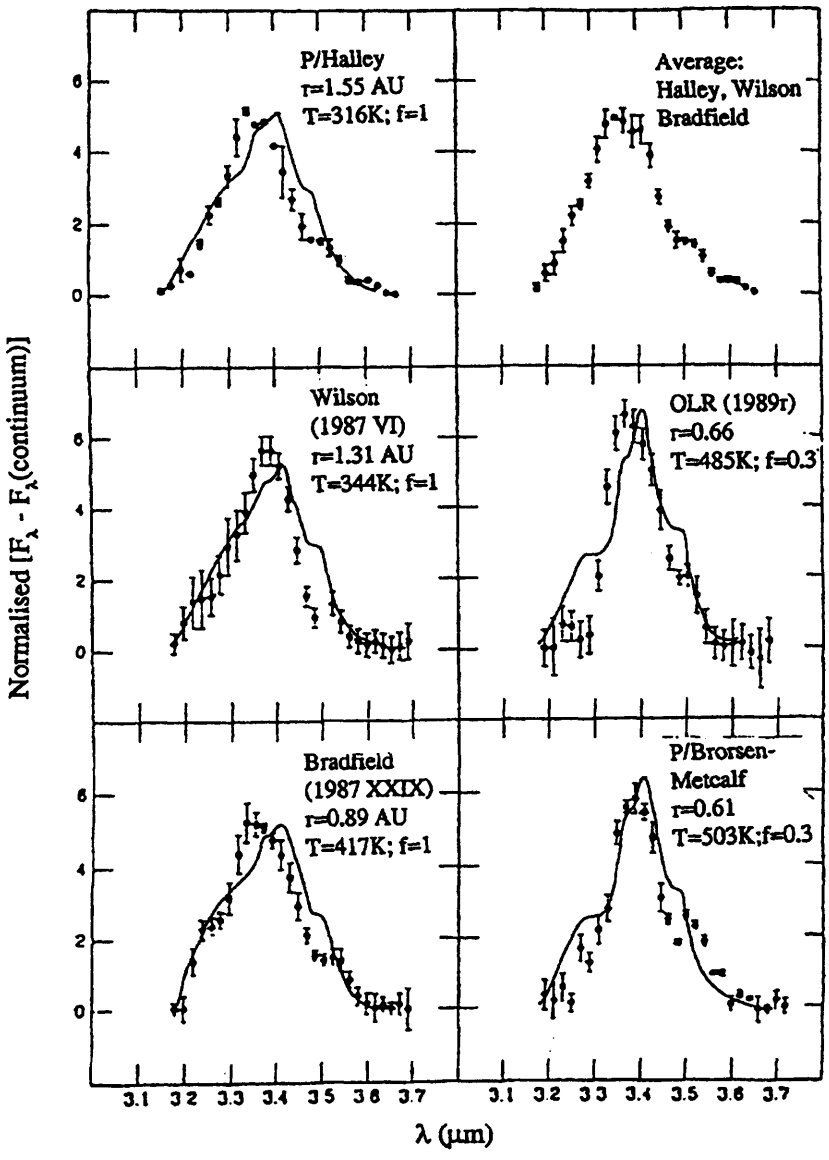

Figure 19: The profiles (points) represent the 3.4 μm feature as seen in several comets (Brooke et al., 1991). The curves are the proposed models involving the bacterial model (Festou et al., 1993).

Fig. 20 shows the infrared spectrum of dust over the 8-40μm waveband from comet Hale-Bopp at a distance of 5AU observed by Crovisier et al. (1997). The modelling of this spectrum by Wickramasinghe and Hoyle includes a mixture of olivine and biomaterial on a mass ratio 1:10.

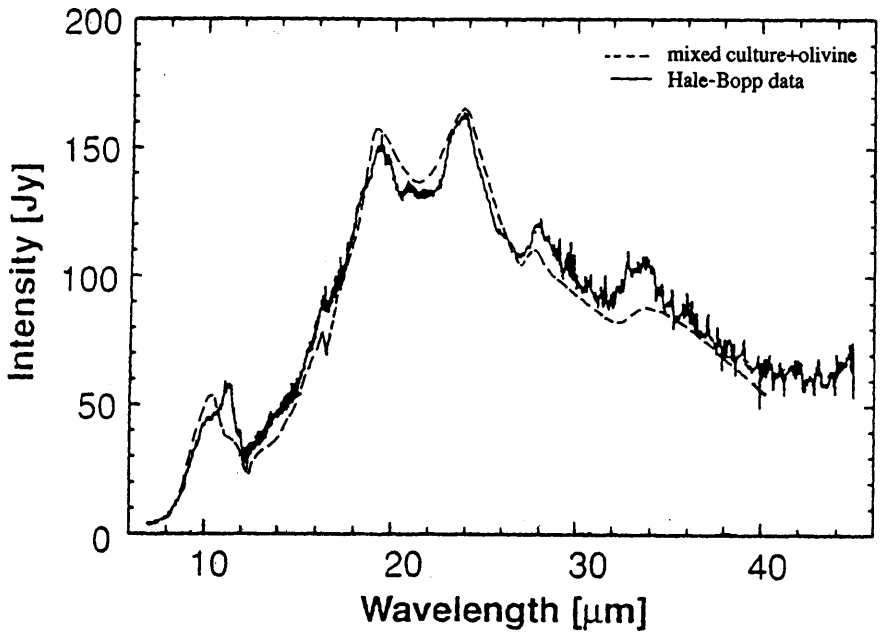

Figure 20: The dashed curve is a normalised spectrum calculated for a mixture of biomaterial and olivine dust. The olivine is assumed to have a temperature of 175K and the bioculture a temperature of 200K. The olivine comprises 10% of the total mass of the mixture (Wickramasinghe and Hoyle, 1999)

In Chapter 7 we shall carry out a similar modelling procedure in relation to data obtained recently for dust from comet Tempel 1.

The *Stardust* Mission to comet Wild 2 involved the collection of dust particles impacting a column of aerogel at velocity V~6km/s. Organic molecules/functional groups were found to be distributed along the trajectories of incoming grains in the aerogel. The molecules recovered along the tracks had heteroaromatic characteristics with high relative abundances of O and N, similar to what is found in biomaterial. It has been claimed that such structures delivered to a primitive Earth may have served as prebiotic molecules leading to an origin of life. On the basis of the *Stardust* results it cannot be excluded that some of these molecules represent degradation products of biology.

3.3 Theory of panspermia and comets

The cometary panspermia theory (Hoyle and Wickramasinghe, 1979, 1981) proposes that viable bacteria/bacterial spores exist in interstellar dust clouds, and that a component of these is included in comets at the time of their aggregation. The inclusion of radionuclides such as ^{26}Al leads to short-lived heat sources in comets that lead to internal melting of ices (see Chapter 7). A minute viable fraction of microorganisms is rapidly amplified and re-frozen into the cometary regolith once the initial heat sources become exhausted. In Section 7.3 we shall argue that transient cometary lakes form near perihelion due to solar heating, and biological activity can resume for short intervals of time.

We shall argue in this thesis that comets can play an even larger role in panspermia through their collisional interactions with life-bearing planets. We referred already to comet impacts on the early Earth leading to the formation of the oceans. Continuing episodes of impacts lead to the possibility of life-bearing material being 'splashed back' into interstellar space. Successful transfers of life to new born planetary systems take place most efficiently whenever the solar system encounters giant molecular clouds.

The freeze-dried bacteria/spores are expelled in cometary dust tails when cometary bodies approach the Sun. The possible expulsion of such biological particles (in clumps) from the entire Solar system is discussed in Section 6.9. Larger particles with ratio of radiation pressure to gravity < 1 generate cometary meteor streams in initially bound orbits. Such streams in Earth-crossing orbits can continue to inject material to Earth.

3.4 Basic dynamics of comets

Oort (1950) proposed the existence of a swarm of $\sim 10^{11}$ comets surrounding the solar system as the source of long-period comets. Since then the concept of the Oort cloud has grown more complex, now referring to a reservoir of some $\sim 10^{11}$-10^{12} comets with aphelia in the range 3000-200,000 AU, and with an increasing space density towards the inner regions. In addition several other populations of comets have been identified and will be enumerated in Section 3.5.

The mean active lifetime of a comet that passes inside Jupiter's orbit is ~10^4 yr (Levison and Duncan, 1997), small compared to the 4.6 Ga age of the solar system. The implication is that currently active comets must have arrived in the inner solar system relatively recently from more distant reservoirs, otherwise they would have exhausted their volatile material by now.

Comets from the Oort cloud are injected into the inner Solar system due to gravitational interaction with stars at a rate of a few per year. When such an 'injected' comet comes under the gravitational influence of Jupiter and Saturn its orbit evolves. Orbital evolution could produce several end states: it could plunge into the sun; it could lead to collisions with planets; it could be expelled entirely from the solar system (Fernández, 2005).

In the absence of other interactions a comet such as comet Halley moves in an elliptic orbit around the Sun with semi-major axis a, eccentricity e with period T given by

$$\frac{T}{\mathrm{yr}} = \left(\frac{a}{\mathrm{AU}}\right)^{3/2} \qquad (3.1)$$

The polar equation of the orbit follows from solving the equation of motion:

$$\frac{l}{r} = 1 + e\cos\theta \qquad (3.2)$$

where the semi latus rectum is $l = a(1-e^2)$

Relevant to the discussion in Chapter 5 is a determination of the time a comet spends within angular distance $\pm\theta$ of the line of apses. The equation for conservation of angular momentum $r^2\dot{\theta} = h$ can be re-written in the form

$$\frac{dt}{d\theta} = \frac{r^2}{h}$$

$$= \frac{l^2}{h(1+e\cos\theta)^2} \qquad (3.3)$$

using (3.2) Thus the time taken to go from θ=0 to a general apsidal angle θ is from (3.3)

$$t = \frac{l^2}{h}\int_0^{\theta} \frac{d\theta}{(1+e\cos\theta)^2} \qquad (3.4)$$

But the orbital period (twice the transit time from θ=0 to $\theta=\pi$) is

$$T = 2\frac{l^2}{h}\int_0^{\pi} \frac{d\theta}{(1+e\cos\theta)^2} \qquad (3.5)$$

Hence the fraction of time spent between $\pm\theta$ of the line of apses is

$$t/T = \int_0^{\theta} \frac{d\theta}{(1+e\cos\theta)^2} \Big/ \int_0^{\pi} \frac{d\theta}{(1+e\cos\theta)^2} \qquad (3.6)$$

Numerical integrations of (3.6) for the case of Halley's comet e=0.96 and also e=0.8, 0.9 are displayed in Fig. 21 and also in Table 7. It is seen that the comets spend most of their time at large heliocentric distance.

Table 7: Fraction of time spent within $\pm\theta$ of the initial apse line

Angle, θ	Fraction of time, t/T
0	0
10	0.0003
20	0.0007
30	0.001
40	0.0014
50	0.0018
60	0.0023
70	0.0029
80	0.0036
90	0.0047
100	0.0061
110	0.0083
120	0.0117
130	0.0178
140	0.03
150	0.0581
160	0.1359
170	0.3842
180	1

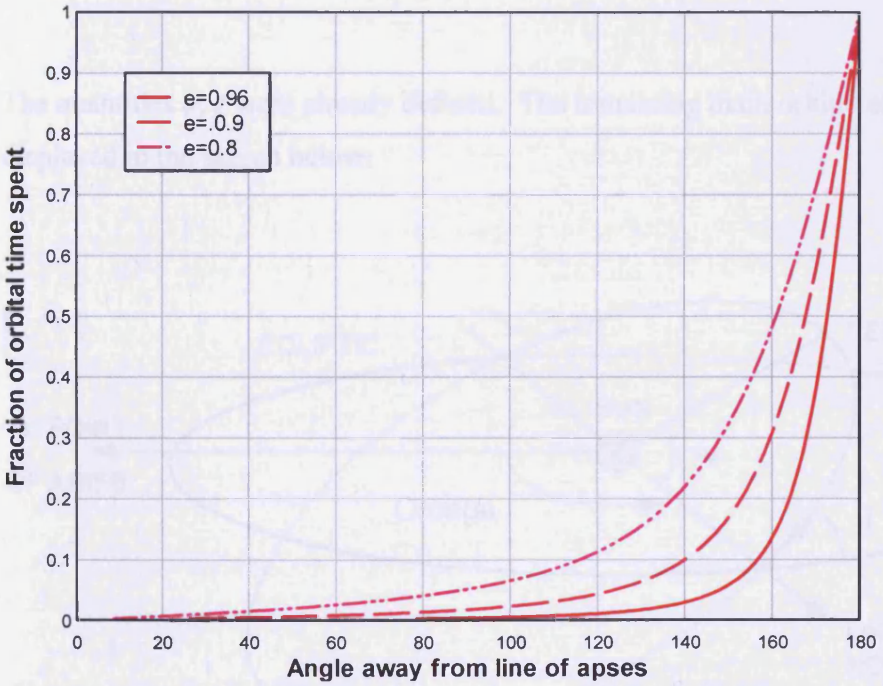

Figure 21: Fraction of orbital period a comet spends within $\pm\theta$ of the initial apse line, for various values of eccentricity.

The above considerations relate to the motion of a comet in its own plane. In reality the comets in our solar system (e.g. in the Oort cloud) have a wide distribution of inclinations and orientations of the line of apses. To a first approximation the distribution of semi-major axes may be taken to be random. Comets are also intermittently perturbed by Jupiter, and affected by interactions with molecular clouds and galactic tides. To discuss these interactions, as we shall do in Chapters 4 and 5, it is necessary to define the dynamical parameters characterizing a comet in its orbit. These are defined thus:

i = inclination

Ω = longitude of ascending node

ω = argument of periapsis

e = eccentricity

a = semi-major axis

Mo = mean anomaly

The quantities a, e were already defined. The remaining main orbital elements i, Ω, ω are displayed in the sketch below:

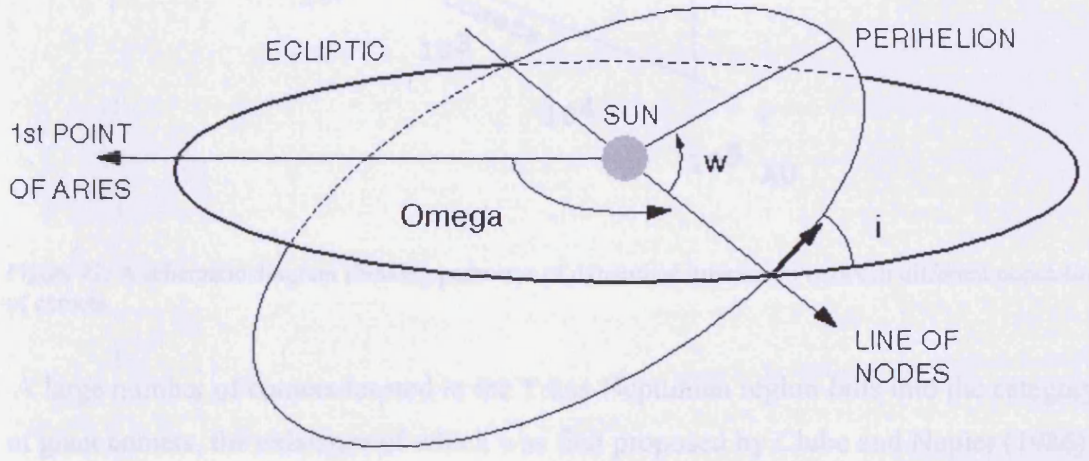

3.5 Classes of comet

Comets have classically been divided into two groups: the Jupiter family comets with period P≤20 yr, the Halley family comets with 20<P≤200 yr (collectively referred to as short period comets), and the long-period comets with P>200yr. Classes and populations of comets can be distinguished by their dynamical characteristics as well as by physical properties such as size, colour and albedo. Long period comets, of which comets Hayukatake and Hale-Bopp are examples, originate ultimately from the Oort cloud. But the distribution and sites of origin of comets that have been recently observed is far less clear. Fig. 22 reproduced from Brandt and Chapman (2004) shows schematically how the various types and classes of comet described in this section are interconnected in terms of dynamical evolution.

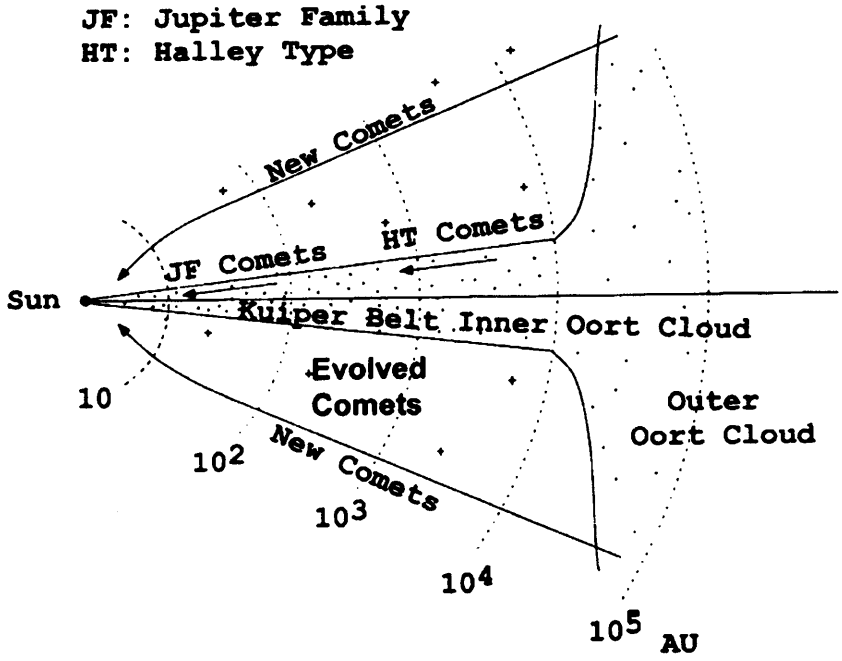

Figure 22: A schematic diagram showing pathways of dynamical interaction between different populations of comets

A large number of comets located in the Trans-Neptunian region falls into the category of giant comets, the existence of which was first proposed by Clube and Napier (1986) prior to the discovery of Chiron. All comets that come under the gravitational influence

of Jupiter can on occasion be fragmented into a variety of sizes, as for instance was seen in the case of comet Shoemaker-Levy in 1997. The Kreutz Sungrazers are a family of similarly-fragmented comets with orbits possessing very small perihelion values. Their orbits thus take them close enough to the sun to be destroyed, as can be seen in a photograph taken by the satellite SOHO that was launched in 1992 (Fig. 23).

Figure 23: SOHO photo of a Kreutz Sungrazer plunging into the sun

The Kreutz Sungrazers have been observed in large numbers since the launch of SOHO. Jupiter-fragmented giant comets could also be important in producing meteor-streams, such as the Taurids, and Earth-crossing fragments that could strike the Earth, as in the case of the K-T extinction event (Wallis and Wickramasinghe, 1995).

Kuiper belt population

In 1951 G. Kuiper proposed that some comet-like debris from the formation of the solar system should reside beyond Neptune. Kuiper's hypothesis received theoretical support in the 1980s when computer simulations of the solar system's formation predicted that a disk of icy debris should naturally form around the edge of the solar system. In such a scheme, planets agglomerate quickly in the inner region of the Sun's primordial circumstellar disk, and gravitationally swept up residual debris (Hoyle, 1978). However, beyond Neptune, the last of the gas giants, there should be a debris-field of icy planetesimals that never coalesced to form planets.

Fernández (1980) proposed the Kuiper (or Edgeworth-Kuiper) Belt, between 35-50 AU, as the source of Jupiter family comets. However the Kuiper Belt remained a theoretical speculation until the detection of a 240 km wide body in 1992, called 1992QB1 (Jewitt and Luu, 1993). Several similar-sized objects were discovered in rapid succession, all with orbital elements in agreement with what was expected for bodies in the Kuiper Belt, thus establishing the reality of the G. Kuiper's proposed belt. Pluto is now considered to be the largest member of this class of comets.

With periods less than 20 years (as opposed to a few million years for an Oort member), the comets in the Kuiper belt have orbits that lie near the ecliptic plane. In addition, all these comets go around the Sun in the same direction as the planets.

Scattered disc objects

A disk of cometary bodies in high eccentricity orbits in the ecliptic plane beyond Neptune has recently been discovered. These comets (SDO's) may represent escapees from the Kuiper Belt and/or scattered Uranus-Neptune planetisimals. Fernández, Gallardo, and Brunini (2004) have showed that nearly half of SDO's are transferred to the Oort cloud.

Centaurs

The recognition of a class of comet occupying the region between Saturn and Uranus/Neptune followed the discovery of 95P/Chiron. Originally thought to be an asteroid, 95P/Chiron behaved like a comet in 1989 when its brightness increased by 1 magnitude. The orbit of the centaur Chiron is highly eccentric with its perihelion just inside the orbit of Saturn and aphelion just inside that of Uranus. The sizes of known Centaurs range from a few tens to a few hundreds of kilometers across. Centaurs are not in stable orbits and will eventually be removed by gravitational perturbation by the giant planets.

However, about 0.5% of Centaur type objects in low eccentricity, low inclination orbits in the region 24-26 AU survive for the age of solar system. It has been estimated that the number of Centaur-sized bodies in such a restricted belt could be an order of magnitude

greater than the steady-state population of Centaurs scattered from the Kuiper belt. Furthermore, such a belt would add a significant fraction to the flux of Centaurs and short-period comets from the Kuiper belt (Fernández, Jewitt and Sheppard, 2002).

Since the discovery of Chiron, many other Centaurs have been discovered, but nearly all are still classified as asteroids, although they are being observed for possible cometary behavior. Thus far only one other Centaur has been observed to have a cometary coma: 60558 Echeclus.

Damocloids

Damocloids were originally defined as a class of asteroid in orbits with long periods and high eccentricities. They are considered to be related to comets because some objects identified as Damocloids have subsequently developed comae. Of the few studied, the median radius is 8km. The distribution of inclinations is indistinguishable from that of the Halley family comets. About 25% of the Damocloids possess retrograde orbits, unlike any other asteroids.

The Damocloids are extremely dark. Albedos of four Damocloids measured by Jewitt et al. have the lowest recorded for any Solar System objects (Fernández, Jewitt and Sheppard, 2001). Their surface properties are also peculiar. They are redder than sunlight but extreme redness found for many Kuiper Belt Objects and Centaurs, as discussed in Chapter 2, is not present. This is evident in the colour-colour plot from Jewitt (2005) reproduced below. Fig. 24 is also interesting in that we note how the distribution of a particular photometric parameter can be used to define classes or groups of comets. Redness can be taken as an indication of chemistry or even biochemistry occurring near the surface. The red pigments evidently generated by some photochemical/biochemical process may be similar to pigments recently discovered in the coloration of the cracks of the Jovian satellite Europa.

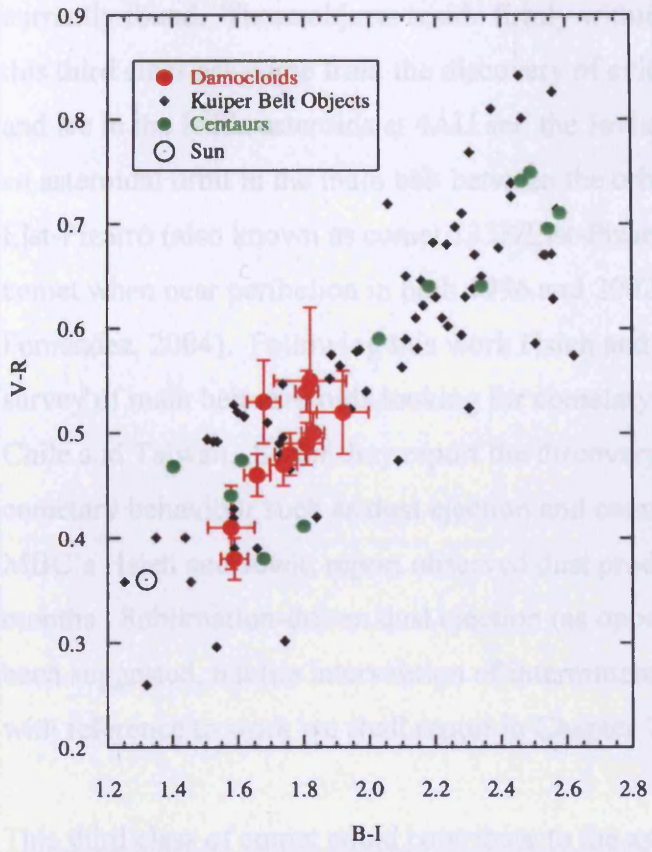

Figure 24: Colour-colour plot of centaurs, K-B objects, Damocloids and Centaurs.

Main belt comets

So far we have identified only two reservoirs of comets located in the Kuiper belt (30-50AU) and the Oort cloud (3000-50,000AU). These two reservoirs are likely to be generically linked to the processes whereby the outer planets Uranus and Neptune originated. The Kuiper belt comets may be regarded as the main reservoir supplying the so-called Jupiter family comets, whilst the Oort cloud supplies the Halley family and long-period comets, but the dynamical evolution of orbits is by its nature complex, and this distinction is by no means clear-cut (Emel'yanenko et al., 2005). It is mainly the latter class of object that we shall be concerned with in later chapters of this thesis.

A third source of comets has recently come to the fore, the so-called 'Main Belt' comets which are thought to form more or less in the orbital configurations in which they are

currently found. These objects reside firmly within the asteroid belt. The recognition of this third class has come from the discovery of evidence for possible cometary activity and ice in the Hilda asteroids at 4AU and the Jovian Trojans at 5AU. Despite occupying an asteroidal orbit in the main belt between the orbits of Mars and Jupiter, asteroid (7968) Elst-Pizarro (also known as comet 133P/Elst-Pizarro) was observed to eject dust like a comet when near perihelion in both 1996 and 2002 (Elst et al., 1996; Hsieh, Jewitt and Fernández, 2004). Following this work Hsieh and Jewitt (2006) carried out an ambitious survey of main belt asteroids looking for cometary behaviour using telescopes in Hawaii, Chile and Taiwan. So far they report the discovery of over 300 asteriods showing cometary behaviour such as dust ejection and coma formation. In 3 of the best-studied MBC's Hsieh and Jewitt report observed dust production to persist for several weeks or months. Sublimation-driven dust ejection (as opposed by impact generated activity) has been suggested, but the intervention of intermittent biological activity cannot be ruled out with reference to work we shall report in Chapter 7.

This third class of comet could contribute to the asteroidal/cometary impact history of the Earth. Cometary collisions occurring during the Hadean epoch lend support to the idea that such objects could have been a major source of terrestrial water (Hoyle, 1978), and possibly also of organic molecules and life.

Chapter Four: Disturbing the Oort Cloud and Panspermia

4.1 Introduction

The idea that viable organisms may be transferred between suitable habitats in the solar system has recently been revived following the discovery of relatively unshocked Martian meteorites on Earth, in particular ALH 84001; studies of impact cratering mechanics which show that terrestrial boulders can be ejected into interplanetary space with relatively little damage to any microorganisms within them; and the identification of dynamical highways connecting the Earth and Mars, with transfer times generally ~10^4-10^7 yr (but which could be as short as ~1yr) give further credence to the idea of such transference. Matters relating to the expulsion of unshocked boulders from an impact event and microbial survival in transit between habitats will be discussed in more detail in Chapter 6.

A fraction of ejecta with speeds exceeding planetary escape speed (5km/s for Mars, 11.2km/s for Earth) orbit the sun and diffuse through the solar system via successive gravitational perturbations by planets. Such gravitational perturbations involve diffusion in orbital energy $E \sim 1/a$, a being the semi-major axis (Bailey et al., 1990; Bailey, Clube and Napier, 1990). Numerical calculations have shown that larger perturbations, particularly by Uranus and Neptune, could lead to emplacement in orbits of aphelia between 5000 and 100,000AU (Wallis and Wickramasinghe, 2004). Such boulders will be easily dislodged and expelled from the solar system during molecular cloud encounters to be discussed in this chapter.

The transfer of life-bearing boulders from the solar system to exoplanets has seemed a much sterner proposition than transfers even to the outer regions of the solar system. Whilst emplacement of a boulder in the Kuiper belt could be accomplished in ~ 10^8-10^9 years by the cumulative effect of gravitational perturbations, the time between an expulsion event from the entire solar system and a passage within 1AU of a giant exoplanet in a passing molecular cloud could be much longer than a few billion years. The further step of a safe deflection onto the surface of a biofriendly planet, should one exist in that system, is negligible. It is unlikely, therefore, that a boulder containing

viable life from Earth has ever landed on the surface of an exoplanet by a simple ejection-capture process.

The solar system, located at a distance of ~8.5kpc from the Galactic Centre, moves in a Keplerian orbit with a period of 240My. The proper motion of the Sun at the present epoch is ~ 20km/s relative to the local interstellar medium. Boulders ejected from the solar system might be expected to enter nearby (passing) molecular clouds and protoplanetary nebulae at speeds typically in the range 15-20km/s. Such boulders would simply fly through the target cloud except in the rarest instances of planetary capture referred to above. The transfer of viable biomaterial from boulders to the target system could take place in several ways, for example as discussed by Napier (2004) and Wallis and Wickramasinghe (2004). In the mechanism proposed by Napier grinding collisions occur in the zodiacal dust cloud in the plane of the solar system, and life-bearing dust is expelled by the action of radiation pressure (see discussion in Chapter 6). This process ensures a fast and efficient transfer to a perturbing molecular cloud, the enhanced bombardment leading to boulder/dust expulsion being itself a consequence of the gravitational interaction between the molecular cloud and the Oort cloud of comets. Wallis and Wickramasinghe (2004) propose that larger life-bearing boulders released through impacts are more or less continuously added to the outer solar system from which they can be expelled. From here ~ 4 tonnes per year are expelled to reach passing molecular clouds and protoplanetary nebulae within which they become fragmented and stopped by frictional gas drag.

In the discussion that follows we assume the Napier transfer model on the grounds that the transfer is more efficient and, moreover, directly connected with Oort cloud perturbation. We shall show that significant numbers of viable microorganisms may indeed be deposited into the passing molecular cloud which must inevitably contain star-forming and planet-forming regions.

4.2 The effect of the vertical Galactic tide

The strongest perturbers acting on the Oort cloud are the vertical galactic tide (Byl, 1986) and passing molecular clouds (Napier and Staniucha, 1982). In the case of the Galactic tide, assuming a constant force field, energy is conserved and so the semi-major axis distribution remains unchanged; however the initial eccentricities and inclinations will relax towards some equilibrium distribution. We calculate the discrete changes in the orbital elements of comets under the influence of the vertical Galactic tide and the nebula, using analytic formulae such as those given by Fouchard (2004). The trajectory of the nebula is split into portions, for each of which changes in the orbital elements can be given by impulse formulae. This semi-analytic approach is orders of magnitude faster than direct numerical integrations, but involves some approximations. The results were verified using 4th order Runge-Kutta integrations.

In the analytical approach followed here the vertical galactic tide acting upon an ensemble of comets is modelled by formulae given by J. Byl (1986) and M. Fouchard (2004). An initial Oort cloud is assumed comprised of 25,000 individual comets with semi-major axes in the range a = 10,000-50,000 AU, a distributed as $n(a) \propto 1/a^2$, e randomly chosen between e = 0.01 and 0.999 and with angles l, Ω, ω, i randomly distributed over the appropriate ranges $(0, \pi)$ or $(0, 2\pi)$. At time $t = 0$ this initial cloud is acted on by a vertical galactic tide with acceleration constants:

$$\left.\begin{aligned} G &= -8.34 \times 10^{-15}\ \mathrm{yr}^{-2} \\ F &= 6.56 \times 10^{-16}\ \mathrm{yr}^{-2} \\ H &= 1.6 \times 10^{-15}\ \mathrm{yr}^{-2} \end{aligned}\right\} \qquad (4.1)$$

The Byl-Fouchard formulae give the following increments of orbital elements averaged over each cometary period $t = a^{3/2}$. With $q = a(1 - e)$ we have

$$
\left.
\begin{aligned}
\Delta q &= \frac{5a^{7/2}\sqrt{2q}}{8\pi}\sin b\cos b\cos\alpha\,(H-2G) \\
\Delta b &= -\frac{a^{5/2}\sqrt{2q}}{8\pi}\cos\alpha\left[-2H\sin^2\alpha\cos^2 b+3(H-2F)+\left(1-5\sin^2 b\right)(H-2G)\right] \\
\Delta\alpha &= -\frac{5a^{7/2}}{8\pi\sqrt{2q}}\sin b\cos b\sin\alpha\,(H-2G) \\
\Delta\omega &= \frac{a^{5/2}\sqrt{2q}}{8\pi}\frac{\sin\alpha}{\cos b}\left[-4\sin^2 b\,(H-2G)+3(H-2F)\right] \\
\Delta a &= 0
\end{aligned}
\right\} \qquad (4.2)
$$

where ω and b are longitude and latitude of perihelion in the fixed frame, and α is the angle between the orbital plane and the galactic polar great circle through perihelion. As t varies from 0 to 100 My we calculate the flux of comets into the planetary system ($q <$ 40 AU) displayed in Fig. 25. It can be seen that a quasi-equilibrium state is attained on a timescale of order 100My.

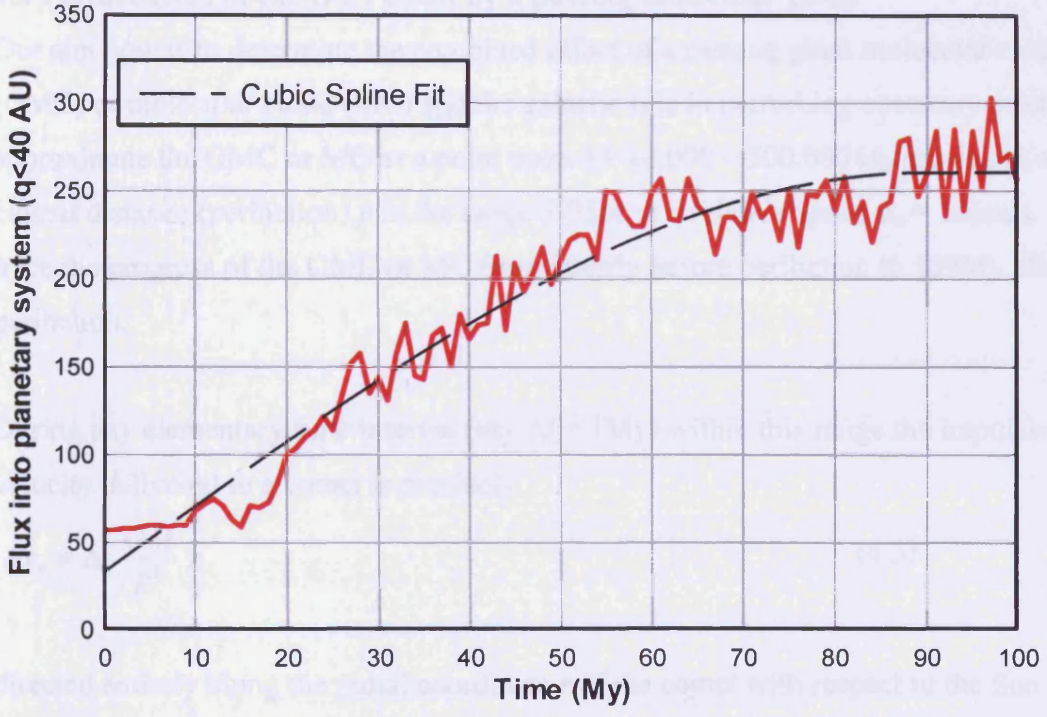

Figure 25: Flux into planetary system (taken as a sphere of radius 40 AU) due to interaction with the Galactic tide for 25,000 Oort cloud comets over 100 My

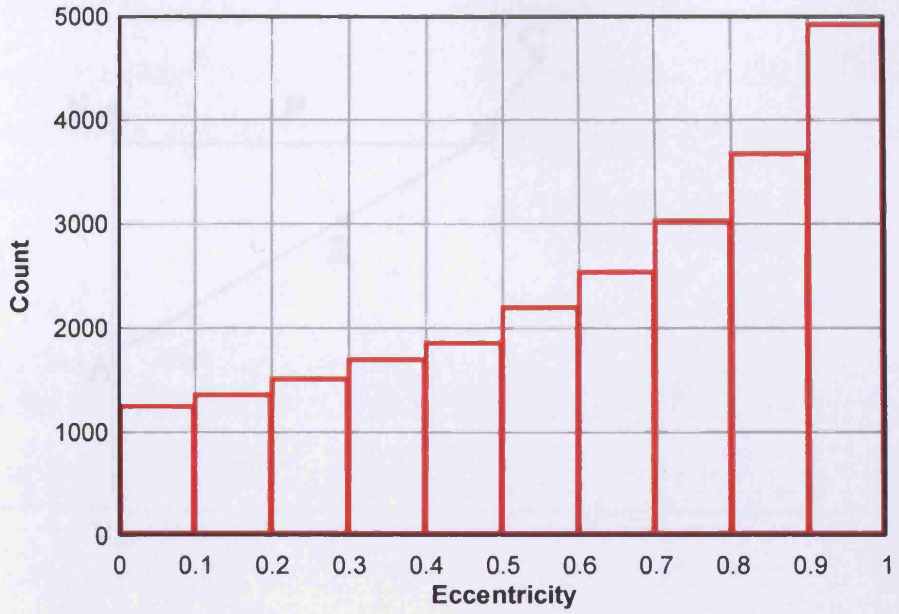

Figure 26: Histogram of eccentricities after 100 My interaction with the Galactic tide

4.3 Perturbation of the Oort cloud by a passing molecular cloud

Our aim now is to determine the combined effect of a passing giant molecular cloud (GMC) or molecular cloud (MC) and the galactic tide in perturbing cometary orbits. We approximate the GMC or MC as a point mass M=10,000 – 500,000M_Θ passing at a closest distance (perihelion) p in the range 5-25pc at a relative speed v_∞ = 15km/s. We trace the progress of the GMC or MC from 100My before perihelion to 100My after perihelion.

During any elementary time interval (say Δt = 1My) within this range the impulsive velocity delivered to a comet is precisely

$$\Delta v_s = \Delta t \frac{GM}{R^3} \boldsymbol{r} \qquad (4.3)$$

directed entirely along the radial coordinate $\boldsymbol{r}$ of the comet with respect to the Sun (see Appendix A and Fig. 27), R being the distance between the GMC (A) and the Sun at time t.

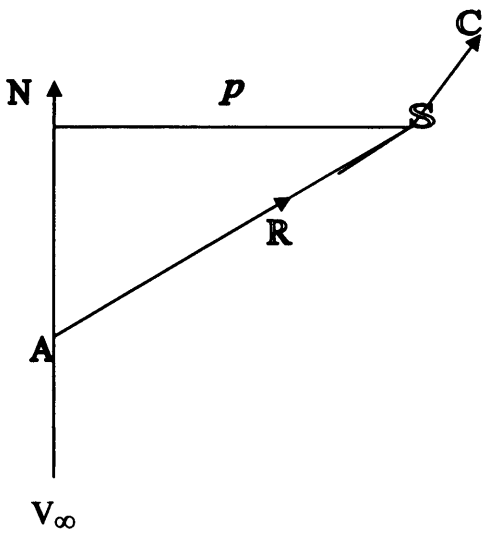

Figure 27: Schematic sketch of GMC/solar system geometry during encounter

If t is the time to go from A to perihelion N, then we have

$$R = \sqrt{(v_\infty t)^2 + p^2} \qquad (4.4)$$

with units properly taken into account (1km/s ≈ 1pc/My etc.).

We consider equal time-steps along the trajectory between $t = 0$ and 200 My with GMC/MC perihelion passage occurring at $t = 100$My. In successive time-steps impulsive velocity increments Δv_S are computed according to equation (4.3) with R given by equation (4.4). For every time-step we calculate changes in orbital elements in each of our 25,000 Oort cloud comets due to a superposition of the galactic tide and the GMC passage. Changes from the galactic tide are computed using the Byl-Fouchard formulae (4.1) and (4.2).

In the impulse approximation the elementary changes of orbital elements due to the GMC interaction can be calculated from formulae set out by A.E. Roy (1978) for a velocity

impulse $\Delta \underset{\sim}{v} = \left(\Delta v_S, \Delta v_T, \Delta v_W\right)$, Δv_S, Δv_T, Δv_W being components of the impulse velocity relative to the Sun. Here v_S, v_T are the components of the comet's velocity in the orbital plane in the radial and transverse directions and v_W is the component normal to the orbit.

$$\left.\begin{aligned}
\Delta a &= \frac{2}{n\sqrt{1-e^2}}\left(e\sin f \Delta v_S + \frac{p}{r}\Delta v_T\right) \\
\Delta e &= \frac{\sqrt{1-e^2}}{na}\left[\Delta v_S \sin f + \left(\cos E + \cos f\right)\Delta v_T\right] \\
\Delta i &= \frac{r\cos u}{na^2\sqrt{1-e^2}}\Delta v_W \\
\Delta\Omega &= \frac{r\sin u}{na^2\sqrt{1-e^2}\,\sin i}\Delta v_W \\
\Delta\varpi &= \frac{\sqrt{1-e^2}}{nae}\left[-\Delta v_S \cos f + \left(1+\frac{r}{p}\right)\Delta v_T \sin f\right] + 2\sin^2\frac{i}{2}\Delta\Omega \\
\Delta\varepsilon &= \frac{e^2}{1+\sqrt{1-e^2}}\Delta\varpi + 2\sqrt{1-e^2}\,\sin^2\frac{i}{2}\Delta\Omega - \frac{2r}{na^2}\Delta v_S
\end{aligned}\right\} \quad (4.5)$$

The quantity f is the true anomaly, $p = a(1-e^2)$, n is the mean motion such that $n^2a^3 = G(M+m)$ and $u = f + \varpi - \Omega = f + \omega$. r is the heliocentric distance given by

$$r = a(1 - e\cos E) \quad (4.6)$$

E being the eccentric angle. In our case $\Delta v_T = 0 = \Delta v_W$. At every time step, with Δv_S calculated from equations (4.3) and (4.4), equations (4.5) and (4.6) were used to change the orbital elements for every comet in our set, changes that were then added to those computed for the galactic tide. This procedure was sequentially carried out through time-steps from 0My to 200My, the GMC perihelion passage being placed at t =100My. At each time-step and for each comet, if the conditions q<40 AU *and* r<5000 AU were simultaneously satisfied, that comet was removed from the set with 50% probability. The reason is that a comet satisfying this condition has ~50% chance of being

gravitationally perturbed by Jupiter and Saturn into a hyperbolic orbit ejecting it from the solar system, or flung inwards and destroyed (Fernández, 2005). The flux of comets entering the planetary system to perihelia q<40AU at each time-step was recorded and is shown in Fig. 28 (a, b,c,d) for several representative cases.

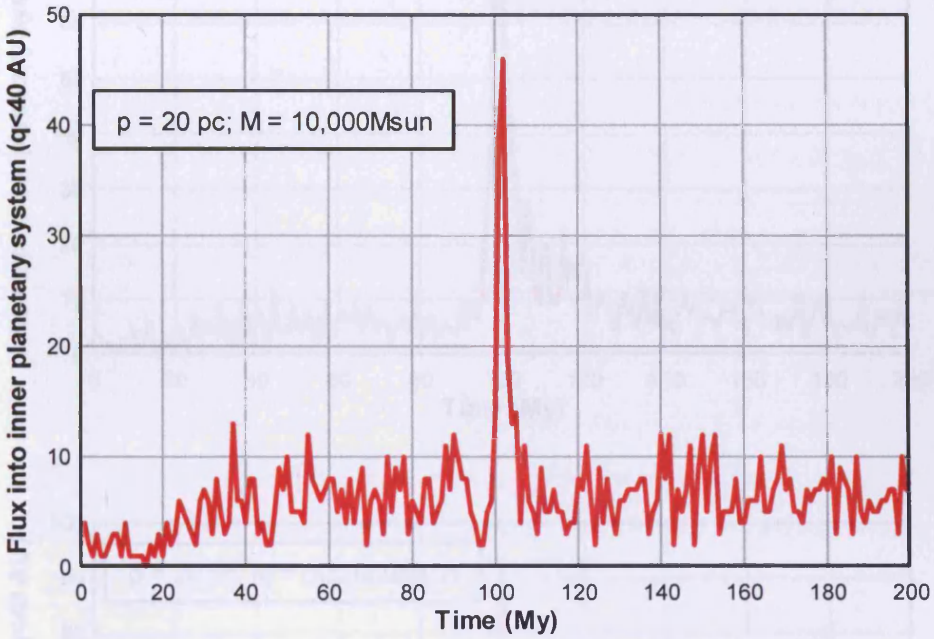

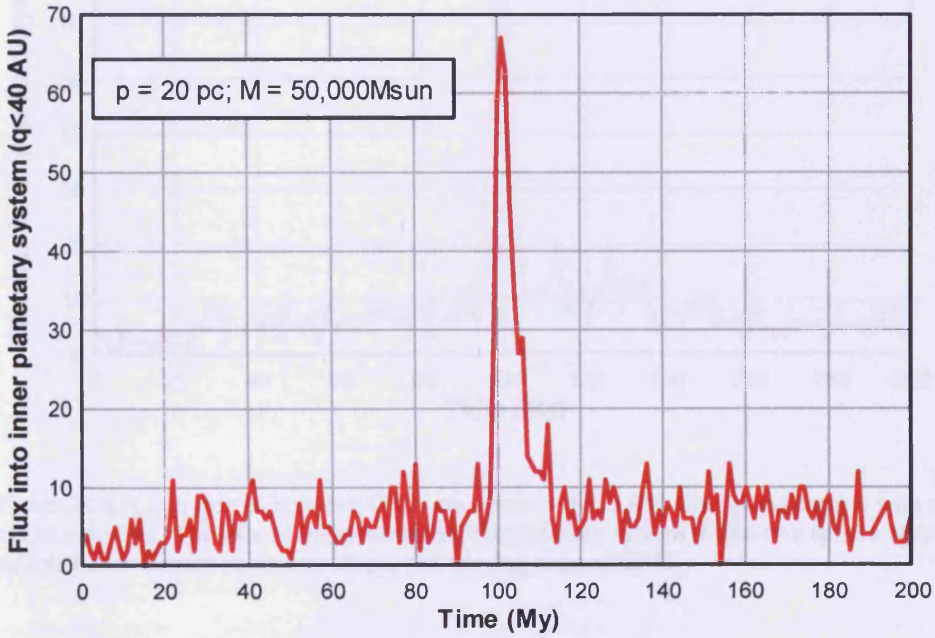

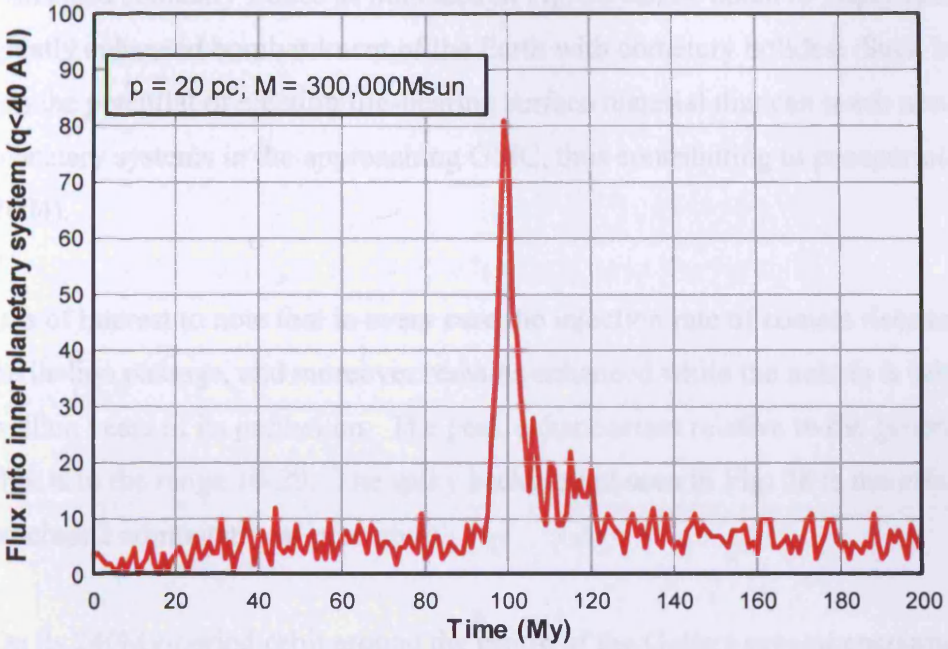

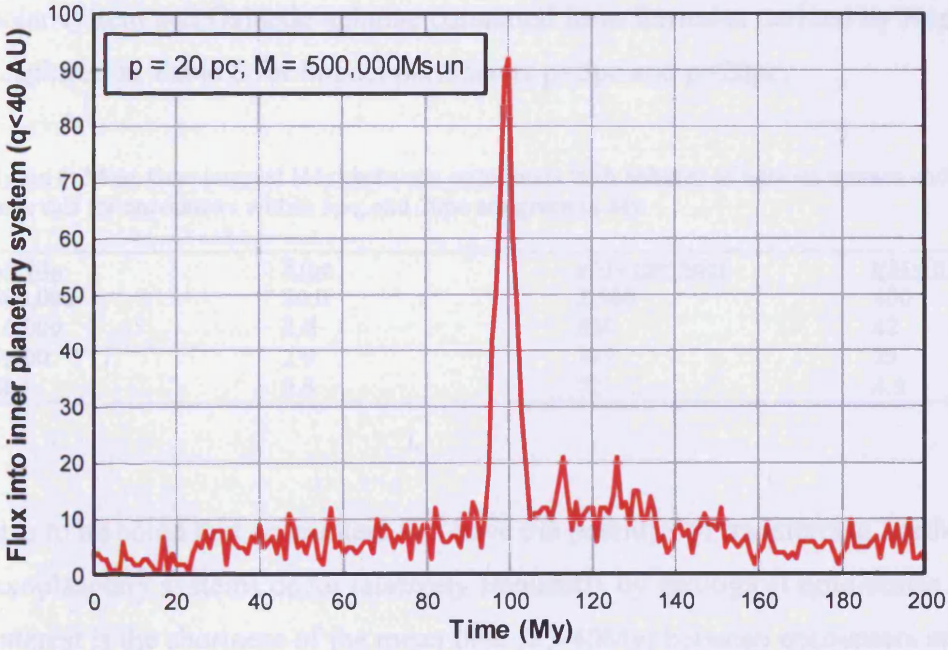

Figure 28 a, b, c, d (top to bottom): GMC encounter with 25,000 Oort cloud comets with continued effect of Galactic tide. The flux of comets entering the planetary system (taken as a sphere of radius 40 AU) is calculated for impact parameter 20 pc, and varying mass of GMC.

Enhanced cometary fluxes as indicated in Fig. 28 can be taken to imply episodes of greatly enhanced bombardment of the Earth with cometary bolides. Such bombardment has the potential of ejecting life-bearing surface material that can reach newly-forming planetary systems in the approaching GMC, thus contributing to panspermia (Napier, 2004).

It is of interest to note that in every case the injection rate of comets rises to a peak at perihelion passage, and moreover remains enhanced while the nebula is within a few million years of its perihelion. The peak enhancement relative to the general background flux is in the range 10-20. The spiky background seen in Fig. 28 is the effect of our stochastic computational procedure.

On its 240My-period orbit around the centre of the Galaxy several encounters with GMC's or MC's would have taken place. The frequency of such encounters between the solar system and Galactic nebulae computed from formulae derived by Napier (2007) are displayed in Table 8 for impact parameters p=5pc and p=20pc.

Table 8: Mean time interval (My) between encounters with nebulae of various masses and radii. Mean intervals for encounters within 5pc, and 20pc are given in My

$M/M_\odot$	R/pc	t/My (p= 5pc)	t/My(p=20pc)
500,000	20.0	2,560	400
10,000	2.9	630	42
5,000	2.0	389	25
500	0.6	72	4.5

It is to be noted that encounters that have the potential of transferring Earth-life to exoplanetary systems occur relatively frequently by geological time-scales. Of particular interest is the shortness of the mean time (25-40My) between encounters at 20pc with molecular clouds of masses in the range 5000-10000$M_\odot$. Fig. 28a shows clearly that such collisions are effective in causing significantly enhanced surges of cometary injections into the inner solar system. The correspondingly enhanced rates of impacts with Earth that occur during encounters would provide a very efficient mechanism for broadcasting terrestrial life to the approaching molecular cloud. Provided that, within a molecular

cloud, there are at an average of at least 1.1 exosystems with a receptive planet and an impact environment permitting the escape of microbiota, life and even the products of its evolution may propagate with a positive feedback throughout the habitable zone of the Galaxy within the lifetime of the Galactic disc.

4.4 Flux modulation due to the Sun's z-motion in the Galactic disc

On a more regular basis enhanced cometary injections into the inner solar system would be expected due to the Sun's periodic z-motion in the Galaxy, as it encounters higher ambient densities of gravitationally perturbing material near z=0 (Matese et al., 1995). The record of impact craters on the Earth shows evidence of a ~36 My periodicity (Yabushita, 2004; Stothers, 2006; Napier, 2006) and a tendency towards bunching in impact episodes (Napier, 2006). The latter is particularly conspicuous for impact craters with diameters greater than 40km, which are presumably the best preserved. Breakup of main-belt asteroids is inadequate to reproduce this observed pattern, and the question arises whether these properties are consistent with a model involving galactic perturbations of the Oort cloud, yielding impacts either directly through long-period comets or indirectly through periodic replenishment of the Halley-type comet population. A period in the range 34-39My is strongly suggestive of oscillations of the solar system normal to the galactic disc.

To test this proposition the Sun's vertical motion near in the disc could easily be calculated if the density distribution of ambient stellar and interstellar material $\rho(z)$ is known. The latter taken directly from Hipparcos data (Holmberg and Flynn, 2004) is as shown in the black curve (uppermost curve) of Fig. 29.

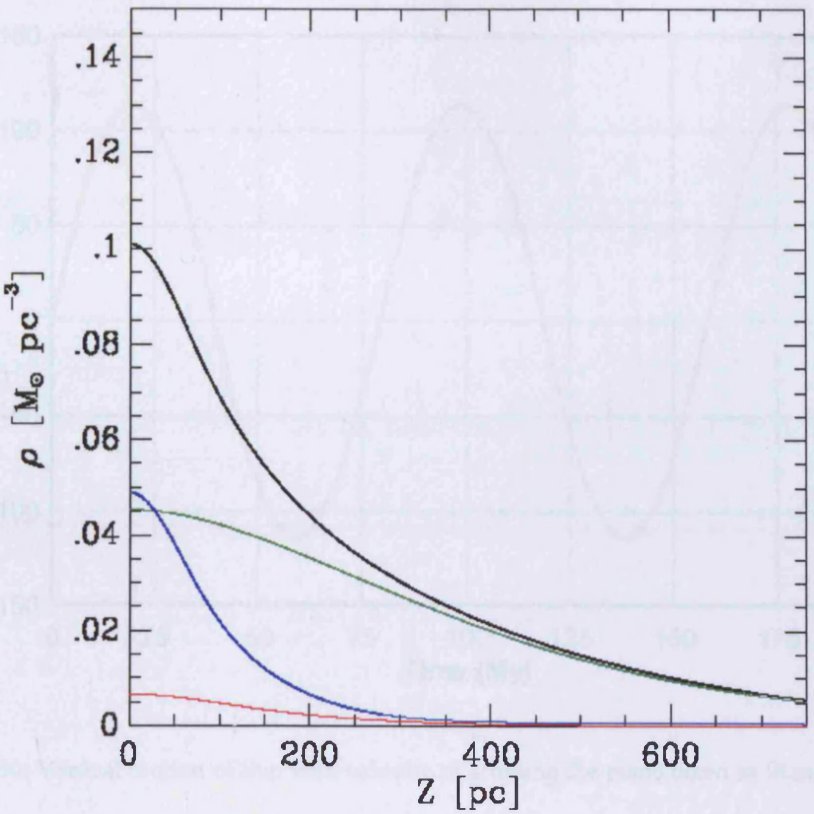

Figure 29: The density of galactic material as a function of height z. The black curve is the density of the total amount of matter, blue is the gaseous components, red is the young stars and green is the old stars.

The vertical motion of the Sun is then given by solving

$$\frac{d^2 z}{dt^2} = -4\pi G\rho(z) \qquad (4.7)$$

and the period and amplitude of the solar orbit may then be found for a given value of the vertical velocity at z=0.

Fig. 30 shows the numerical solution of this equation for the case v_0=9km/s and the $\rho(z)$ function defined by the black (uppermost) curve of Fig. 29.

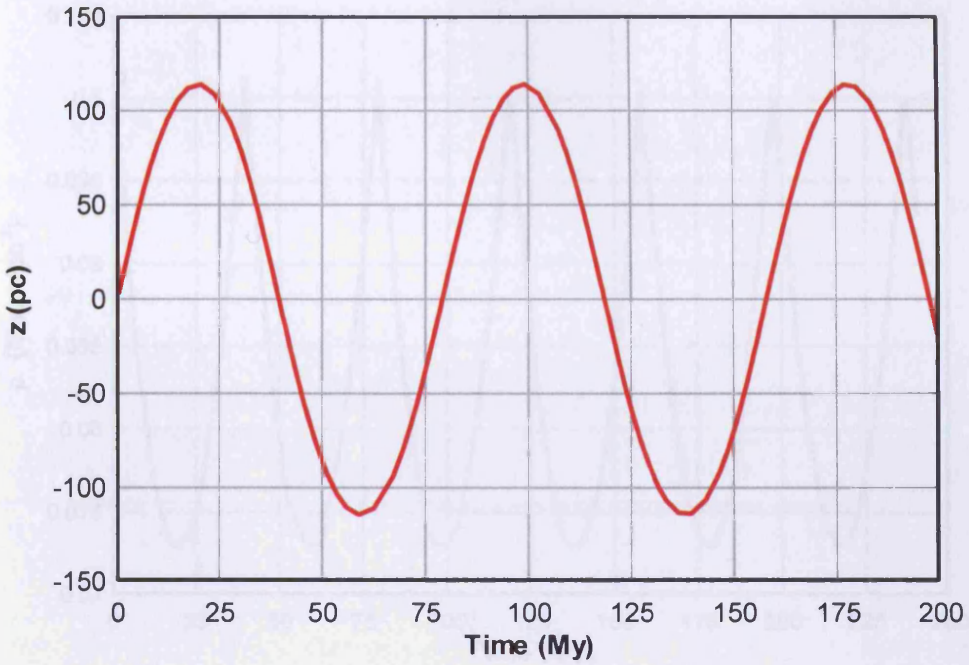

Figure 30: Vertical motion of Sun with velocity of crossing the plane taken as 9km/s

The tidal force on an Oort cloud comet with the potential of deflecting it to the inner solar system is given by

$$F \approx 4\pi G\rho'(z)\,\Delta z \qquad (4.8)$$

Where Δz represents the vertical height of the comet above or below the Sun. To a first approximation we may assume that the flux of comets into the inner solar system can be taken to be proportional to the density $\rho(z) = \rho(z(t))$ as shown in Fig. 31. Comets entering the inner solar system have a chance of fragmentation *à la* Shoemaker-Levy into meteor streams containing boulders and dust that can strike the Earth.

On the assumption that craters on the Earth are formed by such a flux we weight the function plotted in Fig. 31 with the known distribution function of crater ages (e.g. spline fit in Napier's crater-age distribution function). We then obtain the continuous distribution function shown in Fig. 32 from which synthetic data sets for comparison with observations can be extracted.

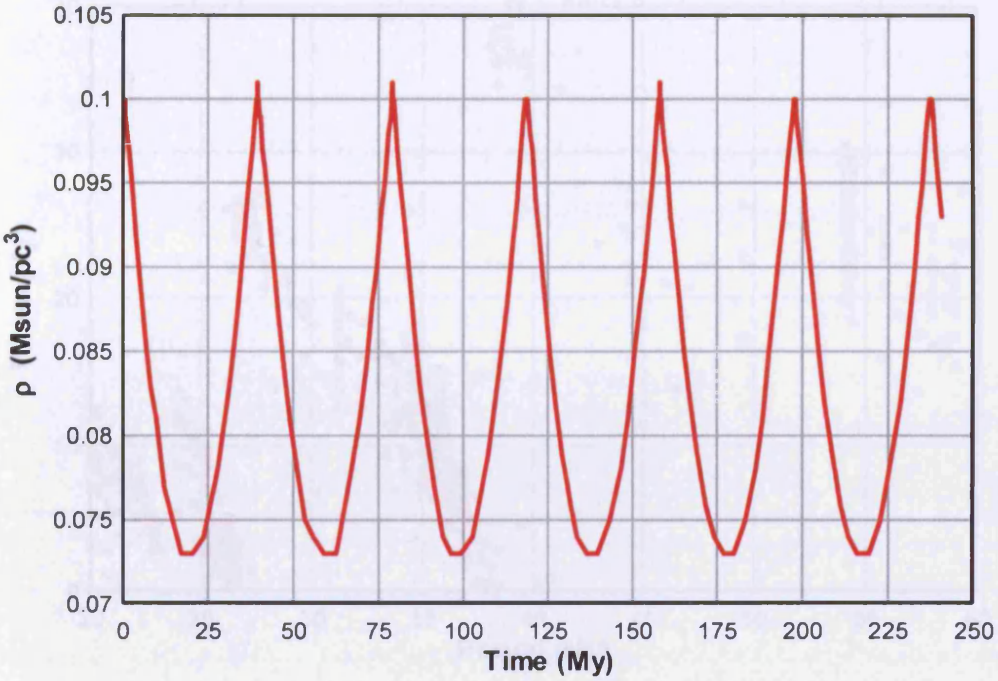

Figure 31: Flux of long-period comets into the inner solar system using curve of Fig. 30

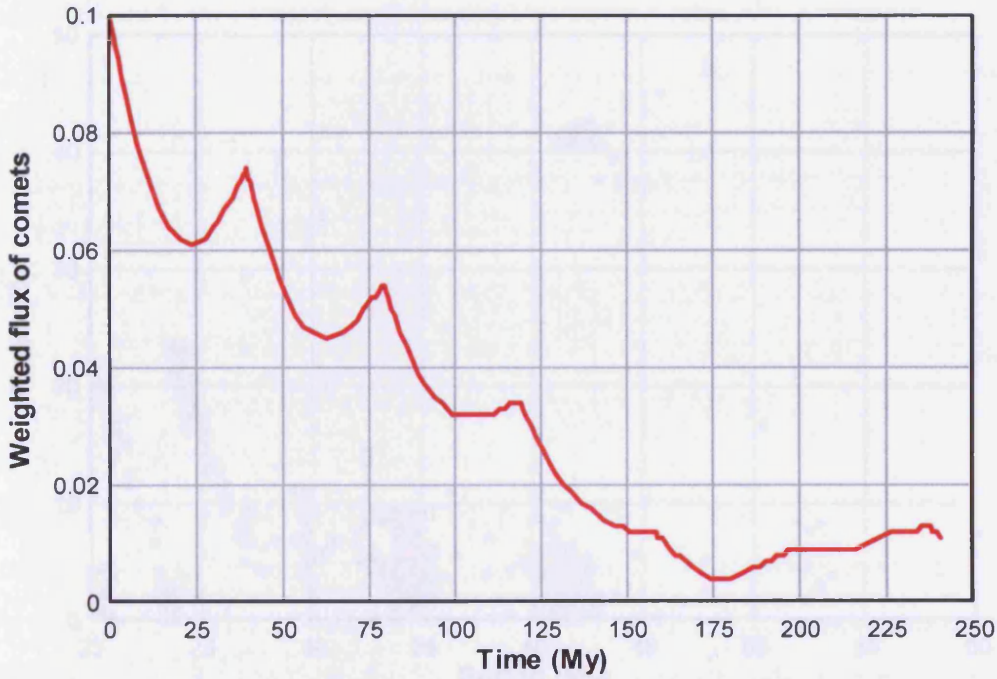

Figure 32: Weighted flux of long-period comets into the inner solar system assuming weighting function defined by crater age distribution

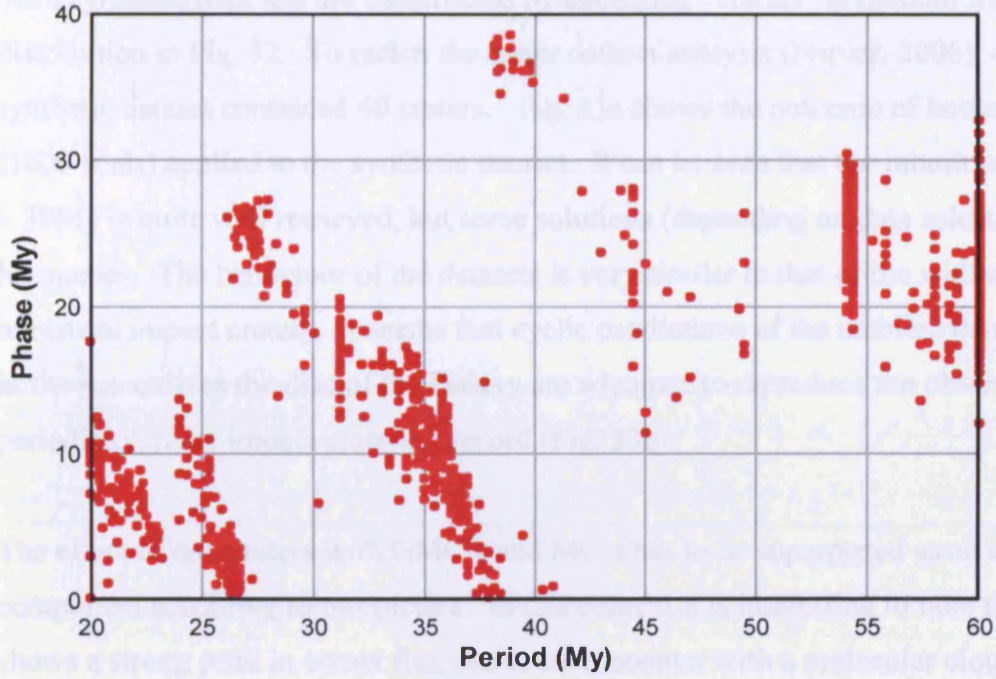

Figure 33a: Period/phase probability distribution of a synthetic dataset extracted from comet flux curve given in Fig. 32, derived by standard bootstrap analysis

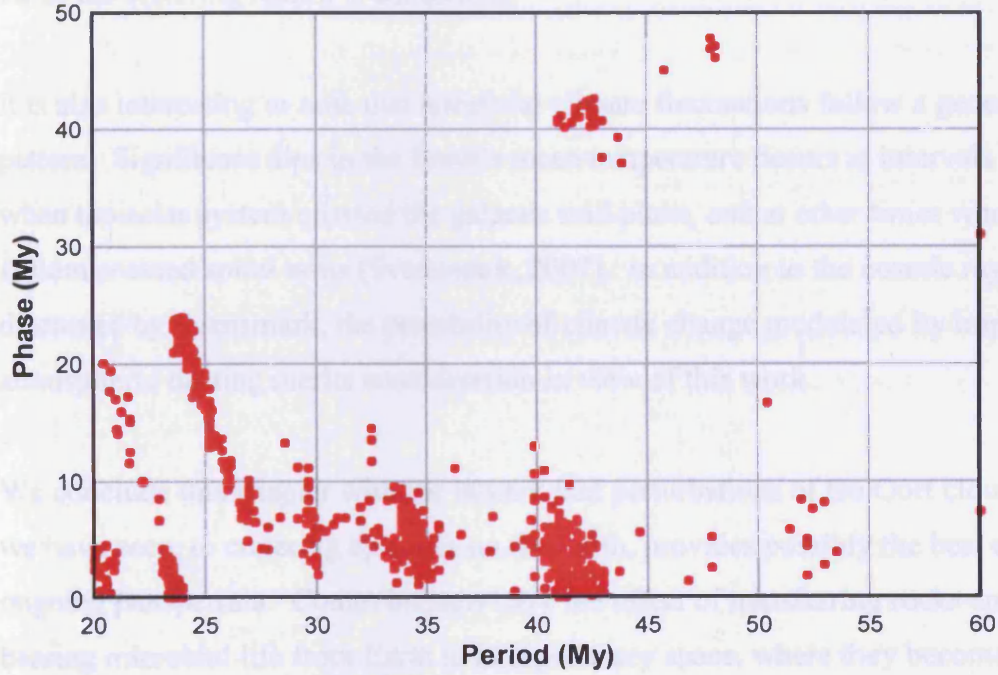

Figure 33b: Similar behaviour obtained from a bootstrap analysis of 40 well-dated impact craters (Napier, 2006)

Such synthetic data sets are constructed by extracting "craters" at random from the distribution in Fig. 32. To match the crater dataset analysis (Napier, 2006), each synthetic dataset contained 40 craters. Fig. 33a shows the outcome of bootstrap analysis (1000 trials) applied to the synthetic dataset. It can be seen that the inbuilt periodicity of ~ 39My is quite well retrieved, but some solutions (depending on data selection) yield harmonics. The behaviour of the datasets is very similar to that of the well-dated terrestrial impact craters. It seems that cyclic oscillations of the ambient density (Fig. 30) as the sun crosses the disc of the Galaxy are adequate to reproduce the observed periodicity in the impact cratering record (Fig. 33b).

The effect of encounters with GMC's and MC's has to be superposed as an erratic extra component according to our picture. In this context it is interesting to note that Fig. 28a shows a strong peak in comet flux due to an encounter with a molecular cloud of mass $10{,}000M_{\Theta}$ at a distance of 20pc. Table 8 shows that such encounters are relatively common, with a mean spacing of ~ 40My, suggesting that bombardment episodes rather than random arrivals of either asteroids or comets are overwhelmingly more important as far as the cratering record is concerned.

It is also interesting to note that terrestrial climate fluctuations follow a generally similar pattern. Significant dips in the Earth's mean temperature occurs at intervals of ~ 34My when the solar system crossed the galactic mid-plane, and at other times when the solar system crossed spiral arms (Svensmark, 2007). In addition to the cosmic ray effect discussed by Svensmark, the possibility of climate change modulated by impacts and atmospheric dusting merits consideration in view of this work.

We conclude this chapter with the remark that perturbations of the Oort cloud linked, as we have seen, to cratering episodes on the Earth, provides possibly the best evidence for ongoing panspermia. Comet impacts have the effect of transferring rocks and boulders bearing microbial life from Earth to interplanetary space, where they become collisionally ground and fragmented into dust that can be expelled by radiation pressure into nearby interstellar space. The passing molecular cloud, that caused the perturbation

in the first place, would have its share of nascent planetary systems within which life-bearing dust particles would become entrapped. In Chapter 6 we discuss the question of survival of space-travelling microbes, showing that a fraction adequate for our purposes will always survive in this transit process.

Thus panspermia outwards from Earth appears to follow logically from the known distribution of star-forming clouds in the Galaxy combined with well-attested celestial mechanics. Since Earth cannot be considered the "centre" of any such process, and because Earth-like planets are thought to be commonplace in the Galaxy, exchanges similar to those discussed in this chapter must also occur on a galactic scale. The microbial and evolutionary life legacy of our galaxy must accordingly be thoroughly mixed, and life everywhere therefore self-similar.

Whilst cometary impact episodes can transfer microbiota from Earth to nascent planetary systems in a nearby molecular cloud and thence efficiently onto exosolar-system comets, successful direct implantation on a habitable planet could be more restrictive. A planet in a habitable zone around a G-dwarf (or similar) main sequence star with masses in the range 0.8-1.2$M_{\odot}$ would appear to be required (Franck et al., 2000). Franck et al. (2007) have modelled the rate of Earth-like planet formation in the Galaxy making reasonable assumptions relating to star-formation rates, metallicity and other factors. A normalised plot of the number of Earth-like planets in the Galaxy from the instant of its formation is shown in Fig. 34. The clear peak around the moment of the Earth's formation shows that successful transfers of life by the processes discussed in this chapter are most likely to have taken place during the first 2-3 billion years of the establishment of life on the Earth.

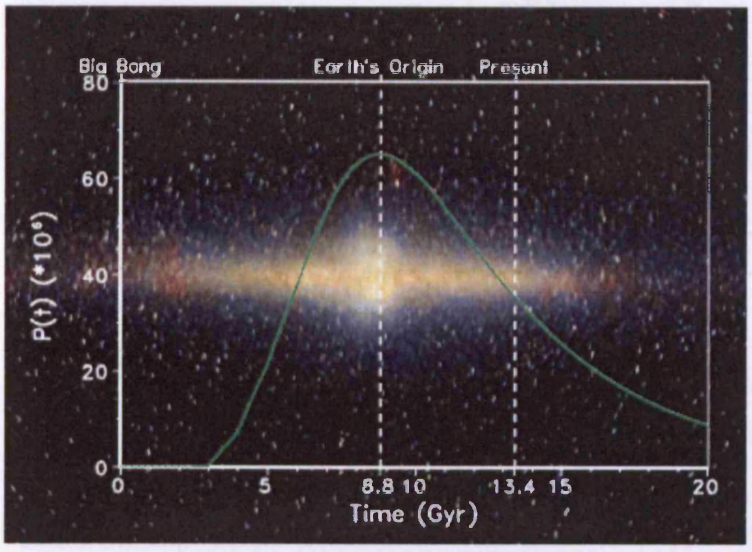

Figure 34: Number of habitable planets P(t) as a function of cosmological time for the Milky Way. The vertical dashed lines denote the time of the Earth' s formation and the present time (Courtesy, S. Franck)

Chapter Five: The Dark Halley Population – a Link in the Chain to Panspermia

5.1 Introduction

The principal source of long-period comets entering the inner solar system is the Oort cloud (Oort, 1950). The Oort cloud consists of ~10^{11} cometary bodies enveloping the planetary system at average distances of ~50 000AU. Individual comets are driven inwards primarily by galactic tides, which act continuously (Byl, 1986; Clube and Napier, 1996). As shown in Chapter 4, encounters with molecular clouds and stars during the solar system's motion through the galaxy gives rise to episodes of comet injection into the inner regions of the solar system on timescales of ~30-100My. Suppose that the absolute magnitude of an active comet is H_{10}. The absolute magnitude H_{10} of a comet (nucleus and coma) is defined as the visual magnitude of the comet placed at 1AU from the Sun and 1AU from Earth. Emel'yanenko & Bailey (1998) estimated the average present day flux of near-parabolic comets brighter than H_{10}=7 to be ~0.2 $AU^{-2}yr^{-1}$ at 1AU, while Hughes (2001) increased this estimate by a factor of four. Using the lower more conservative value the ingress of comets into a sphere of radius 4AU would be ~ $4\pi \times 16 \times 0.2$ yr^{-1}.

Once a long-period comet arrives at the outer reaches of the planetary system, its dynamical evolution comes under the control of the planets, with a chance of being perturbed into a Halley-type orbit. It then becomes possible to calculate the proportion of comets that are thrown into 'Halley-type' orbits (with period $20 < P < 200$ years). Emel'yanenko & Bailey (1998) found that with the perihelia range $0 < q < 4$ AU, the capture probability from the Oort cloud into a Halley-type orbit was ~1%, rising to ~2% if non-gravitational forces were allowed for. Adopting the 1% estimate and assuming a life-time of a Halley-type comet as being τ yr, we calculate that there should be a steady-state population of

$$N \sim 4\pi \times 16 \times 0.2 \times 0.01\ \tau$$

comets brighter than $H_{10} = 7$ in Halley-type orbits. From the observed degassing rate for comet Halley, Wallis and Wickramasinghe (1985) inferred a further lifetime of ~45-65 apparitions, giving a lifetime of 0.65×10^4yr for a period of 100 yr. Assuming a maximum upper limit $\tau \approx 0.75 \times 10^4$yr we obtain N~3000. This value is 400 times more

than is observed. A similar discrepancy was found by Levison et al. (2002). Recent discoveries of comets with the LINEAR telescope has been interpreted as reducing the value by an order of magnitude (Neslusan, 2007), but this claim has been challenged (Emel'yanenko, 2007).

Emel'yanenko & Bailey (1998) proposed that Halley-type comets become dormant after their first few perihelion passages through the inner planetary system. Assuming a mean albedo p=0.04 for the dormant comets, Levison et al. (2002) estimated that about 400 such bodies should have been detected, but at epoch January 2002 only nine were known. They proposed instead that at least 99% of Halley-type comets disintegrate completely during their first few perihelion passages, stating that a comet evolving into an orbit with q < 1AU has a 96% chance of disrupting before its next perihelion passage. No such process has been identified observationally, nor described in detail.

In the following sections we will show that the debris from such a hypothesised disintegration, if it were to occur, would create a bright, near-spherical cloud zodiacal cloud and some 15-30 annual meteor showers, neither of which has been observed. We shall put forward our own proposition (Napier et al., 2004) that the missing comets develop reflectivities that are vanishingly small in visible light, thus forming an unseen dark Halley population, and a collision threat to our planet.

5.2 Disintegration of Halley-type comets

Consider firstly the 3000 bright comets (with $H_{10} < 7$) which are supposed to be resident in Halley-type orbits but to have disintegrated to dust. The differential mass distribution of long-period comets may be fitted by a power law

$$n(m)dm \propto m^{-\alpha}dm \qquad (5.1)$$

where $\alpha \sim 1.47$ (Weissman & Lowry, 2001). This does not differ significantly from the best-fit $\alpha \sim 1.38$ obtained from the few known objects in Halley-type orbits (Levison et al.,

2002). In the calculation that follows we use $\alpha = 1.4$. A least-squares fit to the masses, m, and absolute magnitudes, H, of 27 long-period comets is given by

$$\log m = 21.13 - 0.48H \qquad (5.2)$$

assuming a mean albedo p=0.05 and density $\rho \sim 0.5$ g cm^{-3} (Bailey, 1990). This yields $m_1 \approx 5.9 \times 10^{17}$g for a comet with $H = H_{10} = 7$ at the lower brightness limit of our set. If we take the brightest comets in our set to have $H = H'$, say, then the upper limit of mass is given by

$$\log m_1 = 21.13 - 0.48\,H' \qquad (5.3)$$

and the average mass is

$$\overline{m} = \int_{m_1}^{m_2} m m^{-\alpha}\, dm \Big/ \int_{m_1}^{m_2} m^{-\alpha}\, dm$$

$$= \frac{m_2^{2-\alpha} - m_1^{2-\alpha}}{m_2^{1-\alpha} - m_1^{1-\alpha}} \cdot \frac{1-\alpha}{2-\alpha} \qquad (5.4)$$

using equation (5.1). With $\alpha = 1.4$ and the lower limiting magnitude set at $H' = -1.5$ we obtain $\overline{m} = 1.1 \times 10^{20}\, g$.

We now consider a sample of 3000 comets randomly extracted from this set. With an average mass ~ 10^{20} g, the total mass for the disintegrated Halley-type system is ~3000 $\times 10^{20} = 3 \times 10^{23}$ g.

In a typical case, taking period P=80 yr, semi-major axis a=18AU and eccentricity e=0.96, we find that the apsidal angles for which $r \leq 4$AU lie in the range $\pm 131^0$ (see Fig. 21 in Chapter 3). In this case the time that the cometary material spends within 4AU of the Sun is ~1.6yr. The mass of material within this sphere is of order $3 \times 10^{23} \times 1.6/80 \sim 6 \times 10^{21}$ g, which is 30–300 times the estimated total mass of the zodiacal cloud within 3.5AU (Hughes, 1996). Such a dust sphere would create a strong visible glow in the night sky, but this is not observed.

En route to joining the dust sphere, debris from the postulated disintegrations would form streams. Some of these would intersect the Earth to produce annual meteor showers. Levison et al. (2002) predicts that there would be 46,000 dormant and active Halley-type comets with q <1.3AU and absolute magnitudes (nucleus only) H <18 corresponding to diameters >2.4km. If we take 30,000 Halley-type objects with q <1.0AU and mean periods 60yr, then we expect 30,000/60 = 500 such bodies to pass within the Earth's orbit each year, and ~100 nodes of erstwhile dormant comets to come within ±0.05AU of the Earth's orbit. The characteristic width of a strong meteor stream is ~0.05AU, and so the number of recognisable streams from disintegrated comets is of order

$$N \sim 100 L_m / L_c \qquad (5.5)$$

where L_c ~100 kyr is the mean dynamical lifetime of the dormant comets and L_m is that of their associated meteor streams.

To estimate the mean lifetime of the meteor streams, we carried out simulations in which comets were randomly extracted from the 'dormant comet' parameter space computed by Levison et al. (2000). Each comet was broken into 27 pieces at perihelion, representing the meteoroids. These fragments were given random speeds up to δV in random directions. Laboratory experiments on simulated comet nuclei indicate that the ejection speeds of dust particles in the range 1 – 100 microns are a few meters per second when irradiated at a heliocentric distance $\lesssim$1.5 AU (Ibadinov, 1989).

By adapting the Mercury orbital integration programs developed by Chambers and Migliorini (1997) it was possible to follow the fragments for 100,000 years or until they had fallen into the sun, collided with a planet or been hyperbolically ejected.

We measured the coherence of the meteor streams using a standard similarity function defined by Southworth & Hawkins (1963). For two orbits A, B with Keplerian orbital parameters defined by the 5-vectors $O_k = \{q, e, \omega, \Omega, i\}_k$, $k = A, B$,

the orbital similarity function D is defined as

$$D^2 = [e_B - e_A]^2 + [q_B - q_A]^2 + \left[2 \cdot \sin \frac{I_{BA}}{2}\right]^2 + \left[\frac{e_B + e_A}{2}\right]\left[2 \cdot \sin \frac{\pi_{BA}}{2}\right]^2 \qquad (5.6)$$

Here I_{BA} is the angle made by the orbit's planes given by the formula

$$\left[2 \cdot \sin \frac{I_{BA}}{2}\right]^2 = \left[2 \cdot \sin \frac{i_B - i_A}{2}\right]^2 + \sin i_A \sin i_B \left[2 \cdot \sin \frac{\Omega_B - \Omega_A}{2}\right]^2 \qquad (5.7)$$

and π_{BA} is the difference between the longitudes of perihelion measured from the points of intersection of the orbits,

$$\pi_{BA} = \omega_B - \omega_A + 2 \cdot arc \sin\left[\cos \frac{i_B + i_A}{2} \cdot \sin \frac{\Omega_B - \Omega_A}{2} \cdot \sec \frac{I_{BA}}{2}\right] \qquad (5.8)$$

where the sign of the arcsin is changed if $|\Omega_B - \Omega_A| > 180^0$. The quantity D for our set of 27 meteors is calculated by averaging $<D_{AB}>^2$ given by equation (5.6) for all distinct pairs, and computing

$$D = \sqrt{<D_{AB}>^2} \qquad (5.9)$$

Fig. 35 shows a typical case of a comet with q=1AU, e=0.96, i=152°. The bottom three panels show the evolution of e, q and i for the 27 cometary fragments, and the upper panel shows the evolution of a coherence parameter defined by equations (5.6)-(5.7).

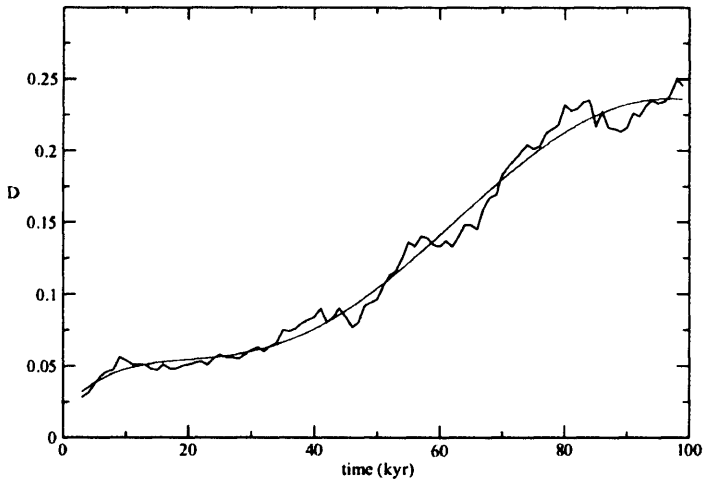
D
0.25
0.2
0.15
0.1
0.05
0
0
20
40
60
80
100
time (kyr)

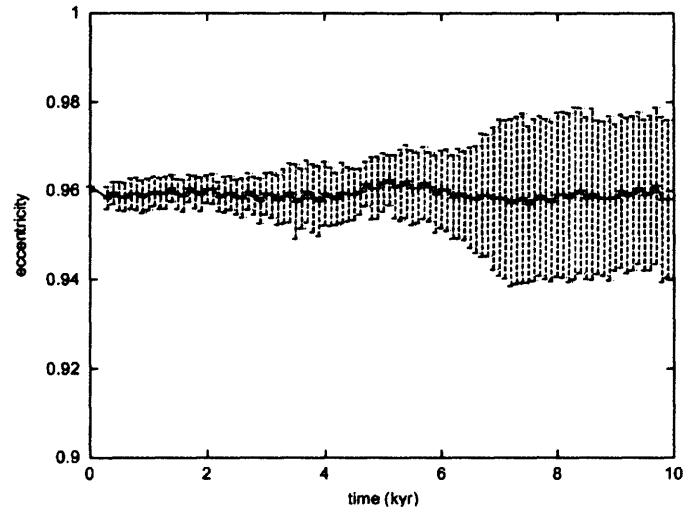
eccentricity
1
0.98
0.96
0.94
0.92
0.9
0
2
4
6
8
10
time (kyr)

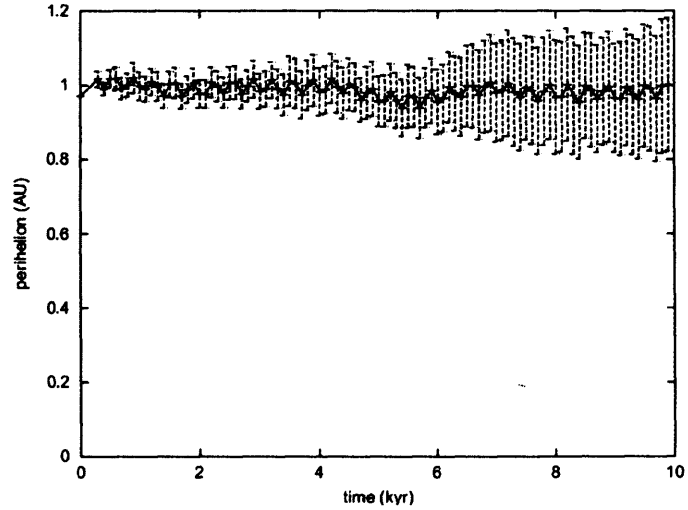
perihelion (AU)
1.2
1
0.8
0.6
0.4
0.2
0
0
2
4
6
8
10
time (kyr)

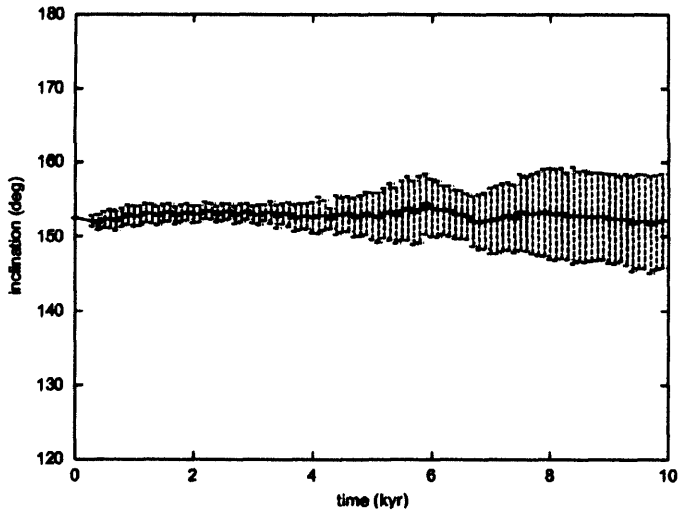

Figure 35: Evolution of a meteor stream. The orbital evolution of 27 fragments of a Halley-type comet assumed to have disintegrated at perihelion. A standard similarity function (the D-criterion) is computed for each of the 27 orbits taken in pairs, and the average is plotted. The orbits gradually diverge under the influences of the planets. Characteristically a meteor stream will be recognized as such when $D \leq 0.2$ and so in this case the disintegrated comet (initial $q = 1.0$, $e = 0.96$, $I = 152°$) would yield annual meteor showers over the full 10^5 yr of the integration.

The known strong meteor streams have $D \lesssim 0.2$. We found that a significant proportion of the meteor streams in our calculations remained coherent throughout their evolution. Adopting D_{crit}=0.2 as the cut-off for recognising a strong meteor stream, fig. 36 shows the lifetimes of meteor streams for initial velocity dispersions $\delta V = 2\text{ms}^1$ and $\delta V = 10\text{ms}^{-1}$. Weighting with the semi-major axis distribution of the dormant Halley-type comet populations (Levison et al., 2002), the overall mean ratio of lifetimes is given by L_m/L_c ~0.15 (Fig. 36). Thus if the characteristic width of a meteor stream is ~0.1 AU, the number of strong Halley-type meteor streams intersecting the Earth's orbit according to equation (5.7) is ~15.

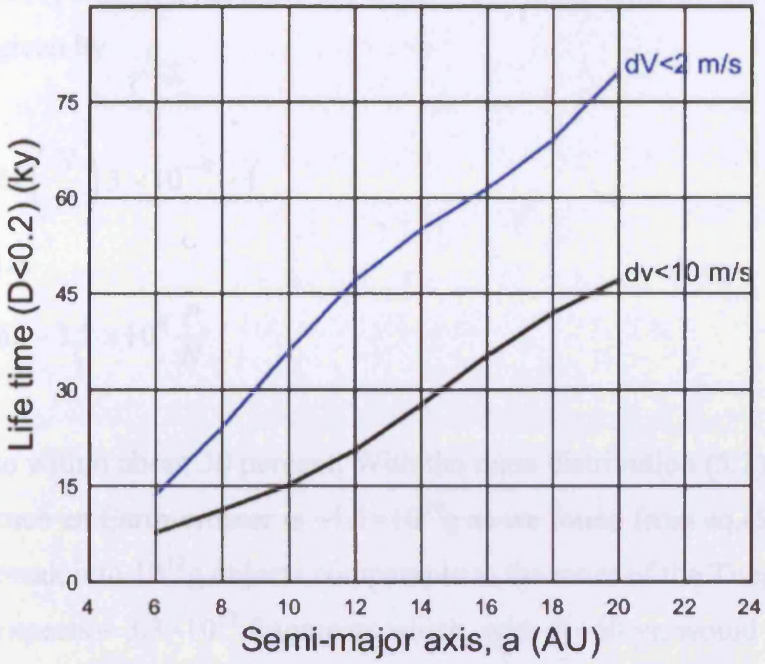

Figure 36: Lifetimes of meteor streams with initial eccentricities in the range $0.96 \leq e \leq 0.98$, averaged and smoothed. 'Lifetime' is here defined as in the text, with *Dcrit* = 0.2. Lifetimes are shown for initial velocity dispersions, at perihelion, of $\delta V \leq 2$ ms^{-1} (upper curve) and ≤ 10 ms^{-1} (lower).

A meteor stream may be observed as more than one annual shower. Comet Halley, for example, yields the Orionids and η Aquarids. The somewhat diffuse meteoroid stream associated with comet Halley has a mass estimated at $\sim 5 \times 10^{17}$ g (McIntosh and Hajduk, 1983). The 30,000 Earth-crossing comets which are supposed to disintegrate completely have mean mass of this order or greater. One would then expect to observe streams of Orionid or η Aquarid strength (hourly visual rate ~ 20), unconnected with any visible comet, at weekly to monthly intervals. Such a situation is of course not observed.

Instead of crumbling to meteoric dust, it is conceivable that the disintegration of the Halley-type comets would proceed to ~0.1 km 'Tunguska-sized' bodies, comparable with the dimensions of the smaller Kreutz sungrazers, or with the fragments such as were observed to split from Comet Hyakutake (Desvoivres et al., 2000), or for the comet Shoemaker Levy 9. Consider an isotropic distribution of N bodies of mean period P years, near-parabolic orbits and perihelia < 1 AU. The mean collision probability of the Earth with such bodies is $\sim 3 \pm 1 \times 10^{-9}$ per perihelion passage (Steel, 1993). Thus with

N/P perihelion passages per annum, collisions with the Earth occur at mean intervals δt yr given by

$$\delta t\left(\frac{N}{P}\right)3\times10^{-9}\sim 1 \qquad (5.10)$$

i.e.

$$\delta t\sim 3.3\times10^{8}\frac{P}{N} \qquad (5.11)$$

to within about 30 percent. With the mass distribution (5.1) and $\alpha = 1.4$, the mean mass of such an Earth-crosser is $\sim 1.1\times10^{20}$g as we found from eq.(5.4). If all 30,000 comets break into 10^{12}g objects comparable to the mass of the Tunguska impactor, then one expects $\sim 3.3\times10^{12}$ fragments which, with $P \sim 60$ yr, would yield more than one hundred Tunguska-like impacts on Earth every year!

Detection of the debris might be avoided if the comets disintegrate into sub-micron particles that do not contribute to zodiacal light. Entering at 50-70 kms^{-1} corresponding to Halley-type orbits, these would ablate in the high ionosphere and escape detection by both visual observations and radar. It would be necessary for 99% of comets in short-period orbits to be reduced to particles « 0.1 mm in diameter within a few perihelion passages, a requirement which hardly seems plausible and for which there is no independent evidence. There is therefore a paradox: assuming a steady-state, the case for a large discrepancy rests only on Newtonian dynamics and the rate of influx of long-period comets, which is known to within a factor of a few (c.f. Emel'yanenko and Bailey, 1998; Hughes, 2001).

One should thus expect to see thousands of Halley-type comets along with their decay products, either dormant bodies or annual meteor showers, along with a bright, near-spherical zodiacal cloud; but all these entities are either absent or under-represented by two or three powers of ten. There is no good reason to assume detailed balance between the long period and Halley populations. However to account for the discrepancy the imbalance must be extremely large, of order 400 – 1600. Surges of this magnitude may

occur at intervals ~ 10^8 yr when a star penetrates the hypothetical dense inner Oort cloud similar to the discussion in Chapter 4. However comets in such a shower would have aphelia strongly concentrated around the region of sky where the perturbing star made its closest approach (Fernández and Ip, 1987), and this is not observed. In addition the equilibration time between the long-period and Halley populations is only ~0.1 My and so the hypothesis would require us to live in a very special epoch, when a shower was under way but had not yet populated the Halley-type system.

5.3 Extremely dark comets

We propose, as a solution to the paradox, that the surfaces of inert comets become extremely dark. It is likely that the final stages of the accumulation of comets involved the mopping up of debris of micron or submicron sizes from the molecular cloud or a protoplanetary disc which was dominated by elongated refractory interstellar organic grains ~10^{-5} cm across, possessing volatile mantles (Bailey et al., 1990; Wickramasinghe,1974). Although silicate dust is also doubtless present, estimates of their mass fraction relative to the organic component could be as small as 15% (Crovisier et al., 1997; Wickramasinghe and Hoyle, 1999). This is also consistent with mass spectra of interstellar dust obtained on instruments aboard the NASA spacecraft *Stardust* which showed an overwhelming dominance of heteroaromatic polymers and no evidence of minerals (Krueger et al., 2004). On the grain model we consider, sublimation of volatiles would build up into a vacuous fairy-castle or aerogel structure. It is possible to envisage many metres of such a structure developing with little or no compaction, except perhaps through the agency of collisions with meteoroids. It is of interest in this connection that particles of probable cometary origin entering the ionosphere and stratosphere have a fluffy, porous structure, with vacuum filling factors ~ 0.75-0.95 (Rietmeijer, 2002; Wickramasinghe et al., 2003). A tarry medium of refractive index $m_1 = n_1 - ik_1$, within which are distributed vacuum spheres of refractive index 1 occupying a fraction f of the total volume of material, behaves as one of complex refractive index m given by

$$m^2 = m_1^2\left[1 + \frac{3f\left(1 - m_1^2\right)/\left(1 + 2m_1^2\right)}{1 - f\left(1 - m_1^2\right)/\left(1 + 2m_1^2\right)}\right] \qquad (5.12)$$

where $m = n - ik$, n, k being the real and imaginary refractive indices (Bohren and Wickramasinghe, 1977). For normal incidence the reflectivity R of a slab of this material is given by the formula from classical electromagnetic theory (Abraham and Becker, 1950)

$$R = \frac{(n-1)^2 + k^2}{(n+1)^2 + k^2} \qquad (5.13)$$

For a prescribed tarry matrix and for given values of the vacuum volume fraction f we can readily solve for m from (5.4), and thus compute R. We take $n = 1.45$, and $k = 0\text{-}0.1$ at optical wavelengths, as being representative of organic polymers (e.g. kerogen). The results of numerical calculations are given in Fig. 37.

It is evident that very low values of R can be achieved with vacuum fractions in line with existing estimates for loose aggregations of interstellar dust grains: the bulk porosities of interplanetary dust particles are ~0.75 and those of Type III fireballs of cometary origin are ~0.95 (Rietmeijer, 2002). The fading function required by the observations may thus be achieved when a comet's surface, comprising a loose aggregate of interstellar dust grains, loses ice between the interstices. An active periodic comet loses gas and dust primarily through active areas on its surface. Some of this falls globally back on to the cometary surface (Wallis and Al-Mufti, 1996). In due course, with depletion of volatiles, the comet loses its coma and becomes dormant. The ice remaining in the volume between the surface grains sublimates, without replenishment, the cometary surface becomes an aerogel, and the albedo rapidly falls to very low values (Fig. 37).

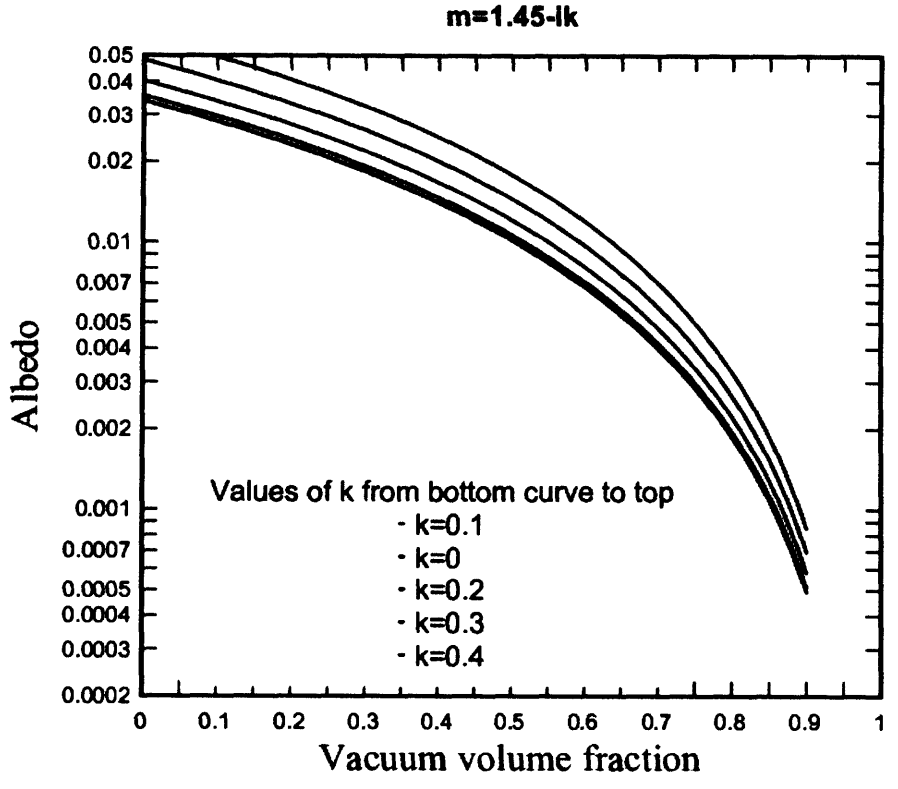

Figure 37: The reflectivity of an aggregate of organic particles 10^{-5} cm in diameter as a function of porosity. For comparison, the nuclei of active comets have albedos p ~ 0.02–0.04, while dark spots on comet Borrelly have p ~ 0.008 (Nelson et al., 2004). Brownlee particles and particles collected in statsospheric collections by Narlikar et al. (2003) are of probable cometary origin and have porosity of 75% or more.

With this model, it has been found experimentally that the thickness of the crust on the surface of a comet increases proportionately to the square root of the insolation time, while the gas production rate proceeds in inverse proportion to the thickness of the crust (Ibadinov et al., 1991). Laboratory and numerical work (Ibadinov, 1993 and references therein) shows that the rate of fading of short-period comets, and its dependence on perihelion distance, are well reproduced by a nucleus of graphite particles embedded in water ice, with 80 percent porosity and thermal conductivity 0.05 $W^{-1}K^{-1}$. In this case, for a comet in a Halley-type orbit, the crust grows at ~5 cm yr^{-1}. The pressure of the escaping water vapour is insufficient to break such a crust (loc. cit. Kührt and Keller, 1996).

The volume of space out to which a body of albedo p is detectable varies as $p^{3/2}$ and so, if there is an expectation that 400 dormant comets with canonical $p = 0.04$ should by now

have been detected, the actual number of detections when $p = 0.002$ say is ~5 (c.f. 9 detections to date): thus the expected albedos of the carbonaceous aerogels are consistent with the presence of a large dark Halley population. The nearest known extraterrestrial albedos of this order are the dark spots on Comet Borrelly, which have p ~0.008 (Nelson et al., 2004). If the predicted population of dark Halleys had this albedo, ~40 would by now have been discovered. There is clearly a strong selection effect against the discovery of astronomical objects in the solar system with albedos $p \ll 0.008$ (Jewitt and Fernández, 2001).

5.4 Current impact hazard

The above solution to the 'missing comet' problem leads to the supposition that there exists a large population of extremely dark comets in Earth-crossing orbits. They are undetectable with current NEO search programmes but are impact hazards nonetheless.

Levison et al. (2002) computed that, without disintegration, there would be a population of $N \sim 3\times10^4$ dormant Halley-type comets with diameters $D > 2.4$ km and perihelia $q \lesssim 1$ AU. For $\overline{P} \sim 60$ yr and mean impact speed ~60 kms^{-1}, then from (5.11) the mean interval between impacts of such bodies is ~0.67 My, with impact energies $\gtrsim 1.5 \times 10^6$Mt (Jeffers et al., 2001). This leads to the conclusion that impacts of at least 1.5×10^7 Mt energy are expected at mean intervals »2.3 My. This interval will of course be increased somewhat if we take account of the revised estimates of comet fluxes from the LINEAR data (Neslusan, 2007).

But these rates are well in excess of those expected from the NEO system currently being mapped out (mainly S-type asteroids: Morbidelli et al., 2002). Hughes (2003) has argued that there is no room for a significant cometary contribution, active or dormant, on the grounds that the impact rate from the near-Earth asteroid population is adequate to produce the known rate at which terrestrial craters are produced. This argument depends on a scaling relation between the diameter of the impactor and the crater which it forms, which is uncertain to order of magnitude. Rickman et al. (2001), on the other hand, find that comets yield a large, perhaps dominant, contribution to km-sized impactors. They

estimate that a terrestrial impact rate of about one Jupiter family comet (active or dormant) per My. The expected impact rate is also significantly higher than has been inferred from lunar cratering data (Neukum and Ivanov, 1994).

Current detection and deflection strategies involve the assumption that decades or centuries of warning will be available following the discovery of a threatening asteroid. However if the major impact hazard indeed comes from this essentially undetectable population, the warning time of an impact is likely to be at most a few days. A typical Halley-type dormant comet spends 99 % of its time beyond the orbit of Mars and so a full mapping of this population is beyond current technology.

If the Halley-type population is derived in large part by capture of comets from the long-period system (Bailey and Emel'yanenko, 1998), then perturbations of the Oort cloud (as discussed in Ch. 4) may yield an upsurge in the dark Halley population, and ultimately in the flux of impactors on the Earth. As we have pointed out earlier the Oort cloud is demonstrably sensitive to Galactic perturbers of various sorts – stars, nebulae and tides (Byl 1986; Napier and Staniucha, 1982 etc.). Nurmi et al. (2001) confirm that the flux of comets from the Oort cloud, and hence the impact rate, may fluctuate by an order of magnitude arising from the motion of the sun with respect to the Galactic midplane. Since we are at present passing through the plane of the Galaxy, it is expected that the current impact rate is several times higher than that deduced from the lunar cratering record, which is time-averaged over one or two Gy.

The significance for the panspermia thesis is that the dark Halleys are a present-day link in the chain between the Galactic disturbances discussed in Chapter 4, huge impacts that dislodge microbiota from the Earth. The idea that passages of the Sun through the spiral arms of the Galaxy might induce terrestrial disturbances has been discussed by a number of authors (e.g. McCrea, 1975). Napier and Clube (1979) specifically proposed that bombardment episodes might occur during such passages, leading to mass extinctions. Leitch and Vasisht (1998) have shown that, indeed, the Sun was passing through a spiral arm during the Cretaceous-Tertiary and Permo-Triassic extinctions of 65 and 250 million

years ago, which also coincided with the Deccan and Siberian trap flood basalts. On our model each of these was caused not by a stray asteroid, but by an episode of cometary bombardment due to interaction of the solar system with the galactic environment. Along with mass extinctions, comet bombardment episodes (e.g. the K-T impact event) would have the effect of directly contributing to panspermia by transferring life-bearing rocks containing even plant seeds (Tepfer and Leach, 2007) and surface dust from the Earth to nearby nascent planetary systems (Napier, 2004; Wallis and Wickramasinghe, 2004). It is also not impossible that new genera are introduced via impacting comet material. In this connection, the sudden appearance of diatoms in the fossil record at precisely the time of the K-T impact is worthy of note (Hoover et al., 1986).

Chapter Six: Creation, Survival and Expulsion of Micro-organisms from the Solar System

6.1 Introduction

Throughout geological history a significant exchange of boulders between Earth, Mars and the Moon has taken place. Exchange of material between the Earth and Mars would have been most common between 4.6 and 3.8 billion years ago during the first 800 million years of the Solar System's existence, when major impacts with asteroids and comets were frequent, the so-called Hadean epoch which was referred to in an earlier chapter.

Thirty-four meteorites have to date been identified as originating from the planet Mars, the most famous of which is meteorite ALH84001 (Hamilton, 2005). Studies of this Martian meteorite (Weiss et al., 2000) showed that the temperature of the rock never exceeded 41°C. This leads to the possibility that any bacteria lodged within the meteorite would retain its viability, hence its relevance to panspermia and the present thesis.

In this chapter we explore possible mechanisms for the exchange of life-bearing material between planets and also address the all-important question of survival of micro-organisms in transit.

6.2 Expectations from impact cratering mechanisms

The Earth accumulates an average of 20,000 tons of extraterrestrial material every year (Love and Brownlee, 1993). Most of this material enters Earth's upper atmosphere as small particles, but more rarely larger objects also strike Earth. These objects are rocky or metallic fragments of asteroids or large cometary bolides, large and solid enough to survive passage through Earth's atmosphere.

The formation of impact craters has been described by Melosh (1988,1989). A hypervelocity impact takes place when a cosmic projectile penetrates the Earth's atmosphere with little or no deceleration from its original velocity. The process by which the crater is formed and modified can be described in several stages.

The minimum impact velocity of a collision with a comet or asteroid whose perihelion is close to 1AU with Earth is 13.5 km/s. Velocities of impacting cometary bolides could be higher: for Earth-crossing bolides in Halley-family orbits we estimated average impact speeds of ~55 km/s (c.f. Chapter Four).

We consider here the specific processes discussed in relation to cometary bolides. The immense kinetic energy of the impactor is transferred to the target rocks via shock waves at the contact or compression stage (O'Keefe and Ahrens, 1993). Energy loss occurs as the radius of the shock front increases, and as the target rocks are heated and deformed. It lasts perhaps only a few seconds, until the shock wave reflected back into the impactor is dissipated as heat. This leads to the almost complete melting and vaporisation of the impactor.

Then follows the excavation stage in which a transient crater is formed. Shock waves which surround the projectile expand through the target rock. As they travel upwards the resulting release waves are reflected downwards. Once the transient crater has reached its maximum size this stage is concluded and the crater is then modified under the influence of gravity and rock mechanics.

In the near-surface region the target rock is fractured and shattered, and some of the initial shock-wave energy is converted into kinetic energy. The rock involved is accelerated outward in the form of individual fragments travelling at velocities that can exceed the escape speed from Earth (Melosh, 1988).

In this way, Melosh has described how impacts may throw meteorite-sized fragments of rock into space, a fraction of which could be transferred to other planets in the solar system and beyond.

6.3 Mechanisms for ejection and fragmentation of boulders

Lunar and martian meteorites provide evidence of actual material that has undergone this process, while the Chicxulub crater event 65 Ma ago provides evidence of the collisional ejection process. Wallis and Wickramasinghe (1995) showed that ejecta from such a terrestrial event readily reaches Mars. Mileikowski et al. (2000) discussed this transfer process, requiring individual metre-sized rocks to be ejected at very high speeds through an atmosphere of density $\sim 10^{4}$ kg m $^{-2}$. Wallis and Wickramasinghe (2004) discuss an alternative scenario. For an impact of a large comet, for example the Chicxulub impactor, the sheer bulk of ejecta exceeds the atmospheric mass by a large factor. Rocks and debris can reach escape speeds by being swept up with the high speed vapour and particles. Such a plume is produced by the collision that it essentially blows a hole through the atmosphere (Melosh, 1989). The implication is that rock fragments and debris down to mm sizes or smaller can be ejected along with larger rocks. This material could carry away entire micro-ecologies of life into space.

Napier (2004) discusses a mechanism for the fragmentation of unshocked boulders from the topmost layers of an impact site. Fragmentation and erosion of the boulders occur within the dense zodiacal cloud over 10^{4}years. The disintegrated particles are ejected from the Solar system as beta-meteoroids (particles for which the repulsion due to sunlight exceeds the attraction due to gravity) and are then reincorporated into protoplanetary systems during passages through dense molecular clouds.

6.4 ß-Particles

Whether in the model of Napier (2004) or in the scheme envisaged in cometary panspermia theories, the requirement is for small (micrometre-sized) grains (including bacteria) to be ejected entirely out of the solar system. Small grains generated in the inner solar system and leaving the solar system on hyperbolic orbits due to the dominating effect of the radiation pressure force were identified by Zook and Berg (1975). The ratio of radiation pressure force to solar gravity is designated β. Particles

with $\beta>1$ are called β -meteoroids. The existence of these particles was confirmed by Hiten satellite measurements (Igenbergs et al., 1991)

We shall now investigate the path of such particles.

For an attractive force of μr^2 per unit mass, the equations of motion integrate to give

$$\frac{d^2 u}{d\theta^2} + u = \frac{\mu}{h^2} \qquad (6.1)$$

where $u = 1/r$, h is angular momentum and θ is the angle in polar coordinates.

Integrating (6.1) gives

$$u + \frac{\mu}{h^2} = A\cos(\theta + \varepsilon) \qquad (6.2)$$

If a particle is projected from a distance c=1AU with velocity $\sqrt{2\mu/c}$ at angle α to the radius vector then by differentiating (6.2) we obtain

$$-\frac{1}{r^2}\frac{dr}{d\theta} = -A\sin(\theta + \varepsilon) \qquad (6.3)$$

It can be shown that initially, for θ=0,

$$r\frac{d\theta}{dr} = \tan\alpha \qquad (6.4)$$

which gives

$$\left(\frac{r}{c}\right)^{-1} = -\frac{\beta}{2\sin^2\alpha} + \frac{\cot\alpha}{\sin\varepsilon}\cos(\theta + \varepsilon) \qquad (6.5)$$

For given values of β and α we can therefore compute the trajectory of a particle as it is ejected hyperbolically. This is done in Sections 6.7-6.9.

6.5 Protective shielding in small β-particles

The effects of ultraviolet light and low energy galactic cosmic rays have continued to be discussed as a problem for the survival of bacterial particles in interstellar transit. The Hoyle-Wickramasinghe model of panspermia requires a fraction of bacterial particles to be available in viable form in order to seed embryonic cometary/planetary systems forming elsewhere in the galaxy (Hoyle and Wickramasinghe, 1981).

Here we shall show that the hazard of galactic cosmic rays is not sufficient to reduce viability of particles to the extent of compromising panspermia in any way. The best prospect for retaining viability is for small clumps (colonies) of bacteria travelling together as integral units. In such cases interior organisms would be well shielded from damaging ultraviolet radiation. Bacterial clumps of this kind with diameters in the range 1 - 10μm have been recovered from the stratosphere up to heights of 41 km and have been provisionally interpreted as being of cometary origin (Harris et al., 2002).

The question arises as to the confinement or otherwise of these clumps within the solar system. Under certain circumstances can desiccated bacteria, individually or in small clumps, be accelerated to the outermost regions of the solar system and beyond? And under what conditions do they survive long interstellar journeys before becoming incorporated in a new generation of comets? We attempt to address these issues in the following sections.

6.6 Carbonisation of the surface

A small clump of desiccated bacteria after prolonged exposure to solar ultraviolet radiation at ~ 1 AU, would inevitably become charred/graphitised at the surface. Taking the interior bacterial material to have an estimated volume filling factor of ~ 30%, its average refractive index will be $< n > \cong 1.0 + 0.3(1.5 - 1) = 1.15$, assuming $n = 1.5$ for the hydrated bacterial material (Hoyle and Wickramasinghe, 1979).

Solar ultraviolet photons acting on the surface would eventually lead to a thin layer of reduced carbon, but the growth of this layer would be self-limiting. A graphite sphere of

radius 0.02 μm has a peak extinction efficiency $Q_{ext} \approx 3.348$ at the ultraviolet wavelength of 2175A giving a mass extinction coefficient of 5.7×10^5 cm^2 g^{-1}, assuming a bulk graphite density of $s = 2.2$ g cm^{-3} (Wickramasinghe, 1973). A closely similar mass extinction coefficient will also be relevant for a thin layer of graphite (Wickramasinghe, 1967). A layer of thickness t comprised of such material will thus produce an optical depth

$$\tau = 5.7 \times 10^5 \times 2.2t \qquad (6.6)$$

A value $\tau = 3$ will be achieved for a graphite thickness of $t = 0.024\mu$m. Therefore it is unlikely that the overlying graphite layer will grow to much more than ~ 0.03μm before the ingress of ultraviolet photons is checked. In this case genetic material residing in the interior would be well protected from damaging solar ultraviolet light.

6.7 Radiation pressure effects

We next model the effects of radiation pressure on a spherical clump of hollow bacterial grains (or an individual bacterial grain) of radius a surrounded by varying thicknesses t of graphite mantle. We assume a refractive index m=1.15 consistent with the discussion in Section 6.6. (Here we ignore the effect of a small absorption coefficient that may apply within the cells.) For the overlying graphite mantle we adopt the wavelength dependent values of n, k from the laboratory data of Taft and Phillipp (1965) (see tabulations in Hoyle and Wickramasinghe, 1991).

Each particle is now regarded as an idealised concentric core-mantle grain. The dielectric core radius is defined as $r_c = a$, and the outer mantle radius is $r_m = a + t$. The rigorous Guttler formulae for coated spheres were programmed from equations set out in Wickramasinghe (1973). For given values of (a, t) we can calculate at any wavelength λ the optical efficiencies $Q_{ext}(\lambda)$, $Q_{sca}(\lambda)$, and the phase parameter $<\cos\theta>$.

The efficiency factor for radiation pressure $Q_{pr}(\lambda)$ is then given by

$$Q_{pr}(\lambda) = Q_{ext}(\lambda) - <\cos\theta> Q_{sca}(\lambda) \qquad (6.7)$$

For the purpose of evaluating the effect of solar radiation on grains we next compute an approximation to the ratio

$$\overline{Q}_{pr} = \frac{\int_0^\infty F_\lambda Q_{pr}(\lambda) d\lambda}{\int_0^\infty F_\lambda d\lambda} \qquad (6.8)$$

for each of the cases under discussion.

Here $F_\lambda d\lambda$ is the relative energy flux of sunlight in the wavelength interval $(\lambda, \lambda + d\lambda)$ and a simple quadrature procedure with truncations at λ = 0.25 and 1.0 μm is used in evaluating the integrals.

In all cases we found that the strongly dominant contribution to the average arises from a wavelength close to 4500A, and indeed $\overline{Q}_{pr} \approx Q_{pr}(4500A)$.

6.8 Ratio of radiation pressure to gravity

A bacterial grain (or grain clump) of external radius r_m located at a distance R from the centre of the Sun of radius R_Θ ($R \gg R_\Theta$) will experience a force directed radially outward due to radiation pressure of magnitude

$$P = \frac{L_\Theta}{c} \pi r_m^{\,2} \overline{Q}_{pr} \frac{1}{4\pi R^2} \qquad (6.9)$$

where L_Θ is the bolometric luminosity of the Sun and c is the speed of light. The oppositely directed gravitational attractive force to the sun is

$$G = k \frac{m M_\Theta}{R^2} \qquad (6.10)$$

where M_Θ is the solar mass, m is the grain mass and k is the universal gravitational constant. The mass m of the grain clump is given by

$$m = \frac{4}{3}\pi\left[(a+t)^3 - a^3\right]s + \frac{4}{3}\pi a^3\rho \qquad (6.11)$$

where s is the bulk density of graphite and ρ is the mean density of the hollow clump material. With s = 2.2 g cm^{-3}, ρ= 0.3 g cm^{-3} and L_Θ/M_Θ= 3.83/1.99 equations (6.9), (6.10) and (6.11) yield

$$\frac{P}{G} = 0.57\frac{(a+t)^2}{2.2(a+t)^3 - 1.9a^3}\overline{Q}_{pr} \qquad (6.12)$$

where a and t are in micrometres. Our computations of $\overline{Q}_{pr}$ described in Section 6.7 combined with (6.12) then gives P/G ratios for each of the grain models considered. The results are plotted in Figure 38.

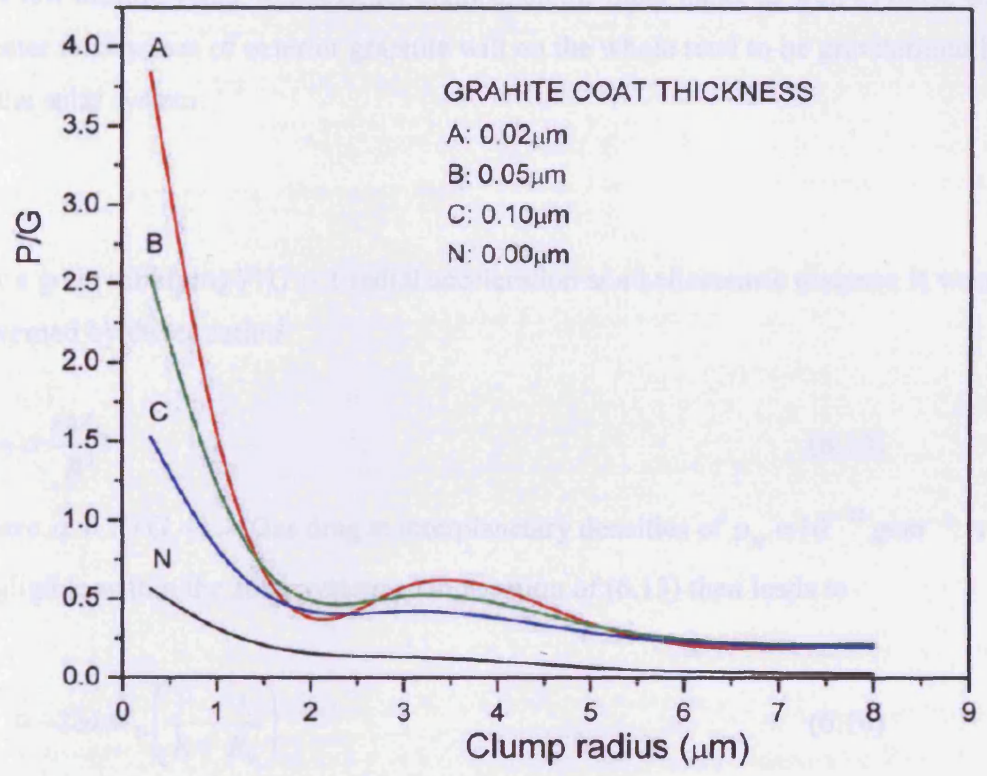

Figure 38: The ratio of radiation pressure to gravity for bacterial grains/grain clumps of radius a with concentric mantles of graphite of thickness t

6.9 Results and dynamical considerations

For particles without graphite coatings the curve marked (N) shows that the ratio *P/G* stays well below unity for all the cases we have considered. This means that such grains will remain gravitationally bound to the solar system and will not readily contribute to interstellar panspermia.

The curves A, B, C show, however, that this situation changes dramatically as the particles begin to acquire carbon coatings. For a graphite coating of thickness 0.02μm *P/G* exceeds unity for bacterial spheres of diameters in the range 0.6-2.5μm. The lower limit is appropriate to a single bacterium, or a few small bacteria and the upper limit to small clumps of bacteria. The smaller particles and clumps once carbonised at the surface are seen to be well suited as candidates for interstellar panspermia. Once expelled from the solar system they could reach nearby protosolar nebulae in timescales of a few million years. Much larger clumps, on the other hand, as well as those with greater thicknesses of exterior graphite will on the whole tend to be gravitationally bound to the solar system.

For a grain satisfying $P/G > 1$ radial acceleration at a heliocentric distance R would be governed by the equation

$$\ddot{R} = \alpha \frac{kM_{\Theta}}{R^2} \qquad (6.13)$$

where $\alpha = P/G - 1$. (Gas drag at interplanetary densities of $\rho_H \approx 10^{-22} gcm^{-3}$ is negligible within the solar system.) Integration of (6.13) then leads to

$$\dot{R}^2 = -2\alpha k M_{\Theta}\left(\frac{1}{R} - \frac{1}{R_0}\right) \qquad (6.14)$$

where R_0 is the heliocentric distance at which radial acceleration of the grain is assumed to begin. As $R \rightarrow \infty$ the asymptotic velocity given by (6.14) is

$$V_\infty = \sqrt{\frac{2\alpha k M_\odot}{R_0}} \qquad (6.15)$$

Taking $\alpha = 0.5$ (P/G = 1.5) as a typical case and R_0=1 AU, equation (6.15) gives $v_\infty \cong 3\times10^6$ cm/s. With this speed a bacterial clump would reach the outer edge of the Kuiper belt, ~ 100AU in ~ 15 years and a protosolar nebula in a perturbing molecular cloud (such as discussed in Chapter 4) at ~ 10pc in ~0.3My.

6.10 Surviving the hazards of galactic cosmic rays

Whilst a thin layer of graphitised carbon around a bacterium or clump of bacteria provides complete protection from ultraviolet light, exposure to galactic cosmic rays poses a more serious potential threat (Mileikowsky, et al., 2000). Radiation doses that limit viability are critically dependent on bacterial species. Below is a table showing the percentage of spores of *Bacillus subtilis* surviving after naked exposure to space vacuum in the solar vicinity (Mileikowsky, 2000).

Table 9: Survival of spores of *B. subtilis* (data from Horneck 1993, Horneck et al. 1995)

Mission	Duration of vacuum exposure (days)	Survival fraction at end of exposure (%)
Spacelab 1	10	70
EURECA	327	25
LDEF	2107	1.4 ± 0.8

Within the solar system the radiation doses received by an outward moving bacterium depend critically on the phase of solar activity, being highest at times near the peak of the solar cycle. The average radiation dose received at 1AU over a timescale comparable to the 11yr period of the solar cycle is less than 10Mrad, and so viability will not be expected to be drastically reduced. The LDEF experiment indeed shows a reduction to 1% for the extreme case of an unprotected, unfrozen (at ~1AU) bacterial culture. Cryogenically-protected clumps of bacteria or bacterial spores are expected to fare

significantly better. In a typical interstellar location a very much lower flux of ionising radiation would be delivered over astronomical timescales. There are indications that a higher tolerance would be expected in this case. We shall return to this point later in this chapter.

We next estimate theoretically the doses of ionising radiation intercepted by bacterial clumps in an unshielded interstellar cloud. To do this we compute the rate of deposition of ionisation energy E due to cosmic ray nuclei passing through a spherical grain of radius a (in microns) and density $s \approx 1$ g cm^{-3} :

$$\frac{dE}{dt} \cong Ja \qquad \text{MeV cm}^{-2}\,\text{s}^{-1} \tag{6.16}$$

where J is given by

$$J = (\sum_i f_i Z_i^2) \int_{1MeV}^{\infty} F(E)\frac{1MeV}{E}dE \tag{6.17}$$

Here f_i denotes the fraction of cosmic ray nuclei with atomic number Z_i, and $F(E)dE$ is the flux of cosmic ray protons with energy in the range $(E, E+dE)$ (Salpeter and Wickramasinghe, 1969). The value of J would vary from place to place in the interstellar medium, and is in general dominated by a low energy tail of the cosmic ray spectrum which is cut off here at $E = 1$MeV.

For a spherical grain of radius a equation (6.16) gives an energy dissipation rate into solid material $q = \dfrac{4\pi a^2}{4\pi a^3 s/3} Ja$ MeV g^{-1} s^{-1} which with $s = 1$ g cm^{-3} converts to

$$q \approx 1.5\text{x}10^4\, J \text{ r yr}^{-1} \tag{6.18}$$

remembering that a radiation dose of 1rad (1r) corresponds to a deposition of ionisation energy of 100 erg g^{-1}.

The much-publicised adverse effects of ionising radiation in space can be shown to be flawed from a number of standpoints. A value of J in the range 0.01-0.1 $cm^{-2} s^{-1}$ within interstellar clouds seems plausible in the light of available astronomical data (see, for example, arguments in Spitzer, 1978). A value J =0.01 $cm^{-2} s^{-1}$ thus delivers 15 Mr in 10^5 yr. Consider now the residual viability of a hypothetical microbial species that halves its viable fraction with a radiation dose of, say, 1.5Mr. Over the 0.3My timescale for reaching the cosy protection of a protosolar nebula located ~10pc away (see Section 6.9), and consequent inclusion in a new generation of comets, the integrated radiation dose received is 45 Mr, leading to our hypothetical species being attenuated by a factor $(1/2)^{30} \approx 10^{-9}$. For a more radiation-susceptible microbial species that halves its viable population with a radiation dose of 750kr, the corresponding viable fraction reaching the new protosolar nebula will be 10^{-18}.

To incorporate a million viable bacteria of this type in every comet condensing in the new system requires the accommodation of a total of 10^{24} itinerant bacteria, dead and alive. This would contribute only ~10^{11} g, which is less than one tenth of a millionth of the mass of a 10km sized comet. According to the present argument interstellar panspermia will be assured even with the most pessimistic of assumptions. But the experimental situation could be even more favourable.

Experiments done so far to determine viability as a function of total dose are most likely to be irrelevant for this purpose. Laboratory studies have invariably used high fluxes of ionising radiation delivered over short pulses, at room temperatures in the presence of air. Extrapolation from these to the astronomical case involves many uncertainties. In particular, most damage resulting from free-radical formation will be eliminated in an anaerobic environment, and low flux-long time intervals may not equate to short pulses of high-flux radiation in the laboratory case.

Similar conclusions follow from a re-evaluation of laboratory data by Horneck et al. (2002). They discuss experiments to determine the survival of *B. subtilis* spores subjected to encounters with simulated heavy nuclei in galactic cosmic rays. It has been possible to 'shoot' such nuclei to within 0.2 μm of a spore. The fraction of inactivated spores at various distances of the cosmic ray (CR) track are given as

$b \leq 0.2$ μm: 73 %

0.2 μm $< b <$ 3.8 μm: 15 – 30 %

These experiments show that even for a central hit by a high Z low energy CR particle a significant fraction would survive, and since the flux of such particles is low, a timescale of ~ 1 million years must elapse before a spore would be deactivated.

Citing other experiments, Horneck et al. (2002) point out that for spores embedded in a meteorite, the timescale for survival to a 10^{-4} % level (due to primary and secondary CR effects) at a depth of 2-3 m is ~ 25 Ma. The same surviving fraction is obtained for shielding at a depth of 1 m after 1 Ma, and for a naked spore the estimated timescale is ~0.6 Ma. Over timescales of 3×0.6 Ma the survival fraction is 10^{-18}. A clump of bacterial spores travelling at 10 km/s would traverse a distance of 18 pc during this time, comfortably less than the mean distance between cometary/planetary systems.

There are strong indications that even the survival rates quoted above are a gross underestimate. They are based on experiments conducted at atmospheric pressure with normal levels of humidity (Lindahl, 1993). There is evidence that bacterial endospores are resistant to inactivation by free-radical damage and chemical processes because their cytoplasm is partially mineralised and their DNA is stabilised (Nicholson, 2000). Most significantly it has been found that bacterial spores (genus *Bacillus*) in the guts of a bee preserved in amber for 25–40 Ma could be revitalised (Cano and Borucki, 1995). Similarly, bacterial spores in 250 Ma old salt crystals have also been revitalised (Vreeland et al., 2000). In both these studies the most stringent sterilisation techniques were used to avoid contamination of the samples, and the authors are confident that they have revived bacterial spores of great ages. With a natural background radioactivity (of

rocks) of ~ 1 rad per year, we have here evidence of survival with doses of 25-250 Mrad of ionising radiation. The importance of this result in relation to panspermia cannot be denied. To avoid this conclusion some scientists have used phylogenetic arguments. They point out that the revived organisms bear a close relationship to contemporary species, and so argue that they must be contaminants. What they fail to appreciate is that panspermia theories permit re-introductions of the same organism (stored in comets) separated by millions of years, so no evolutionary divergence is required. The phylogenetic modernity of the micro-organisms found as well as their survival over millions of years consistently point to an extraterrestrial origin.

6.11 Lithopanspermia vs Cometary Panspermia

In this section we discuss the relative merits/demerits of two versions of panspermia under discussion: lithopanspermia and cometary panspermia.

Lithopanspermia requires three conditions
(1) A planetary body with life present in the top metres of its surface
(2) An impact of a comet or asteroid
(3) Ejection of 'fertile' surface material some of which could reach escape velocity and become available for transport to another planetary body.

It is now accepted that cometary impacts essentially constituted the final stages of the formation of the Earth. Comets impacting the Earth between 4.2 and 4 Ga ago (including Main Belt Objects) brought the volatiles, including water that went on to form the Earth's atmosphere. The impacts are also thought to have brought large quantities of organics that could have served as precursors of life, or more likely in our view, feedstock for bacterial life that came in with comets.

Impacts on the Earth continued after the initial period of 'heavy bombardment' well after life got established. Such impact events (e.g. the K-T Chicxulub impact) have been associated with extinctions of species, but they could also be responsible for spreading life. This process becomes more effective and efficient during times when the solar

system has encounters with molecular clouds. Cometary impacts on the Earth and the inner planets are then more frequent and 'fertile' ejecta could reach nearby nascent planetary systems on timescales «1Ma.

Whilst cometary panspermia accounts for the dispersal of microorganisms, lithopanspermia permits the products of evolution on planetary surfaces to be shared on a galaxy-wide scale. Cometary panspermia requires that some fraction of freeze-dried bacteria and spores survive interstellar travel for typical timescales of $\sim 10^6$ years. Several hazards have to be endured: freeze-drying, exposure to ultra-violet radiation and cosmic rays. Freeze-drying (if done slowly, as would be the case for planetary or cometary escape) poses no problem, and UV radiation whilst potentially damaging is easily shielded against by surface carbonisation of clusters, as we showed earlier, or by embedding within porous dust particles. The main loss of viability would ensue from cosmic ray exposure, the high Z (atomic weight), low energy particles being potentially the most damaging. It will be shown in Section 7.1 that only the minutest survival fraction of microorganisms is required in order to make panspermia inevitable.

Impactors of diameters > 1km are most efficient in the process of lithopanspermia. Considerable amounts of rocks, soil and life-bearing dust are thrown up at high velocities, some fraction reaching escape speeds. Ejecta leave the Earth and orbit around the Sun for timescales varying from several hundred thousand years to mega years. A fraction (ground into micron sizes by impacts) leaves the solar system, a fraction reaches other planetary bodies, and if conditions are appropriate, terrestrial life will seed an alien planet.
There are, however, several bottlenecks to cope with before viable transfers take place:
(1) Residual survival in the impact ejection from the source planet
(2) Residual survival in transit – enduring radiation environment of space
(3) Residual survival on landing at a destination (Earth-like) planet

Shock damage caused by the ejection process could be substantial and leads to reduction of viability of any microbes embedded in rocks. Experimental data obtained by Burchell

et al. (2004) show that survival rates of $10^{-4} - 10^{-6}$ is assured in most cases where shock pressures upto ~ 30 GPa were used. Similar survival fractions are relevant for impacts of meteorites onto a destination planet. However, individual bacteria/ clusters of bacteria would survive entry into a planetary atmosphere more easily in shallow angle encounters which lead to incoming particles becoming satellites of the destination planet in the first instance.

The terrestrial analogue of panspermia is the dispersal of plant seeds across the surface of the planet. With many millions of seeds produced by an individual plant only a single viable seed needs to find a fertile landing site to re-establish the species in a different location. The similarity to the logic of panspermia cannot be overlooked. Indeed Svante Arrhenius (1908) cited the long-term cryogenic survival properties of plant seeds as one of his justifications for panspermia. Plant seeds have been known to retain viability in archaeological sites which are thousands of years old, and Tepfer and Leach (2006) has obtained further evidence for survival of seeds against many hazards of space. With lithopanspermia the possibility arises that plant species could be translocated on a galactic scale, or at any rate that genetic information in the DNA of plants could be safely and securely carried within seeds in small rocks and boulders.

Chapter Seven: Liquid Water in Comets

7.1 Introduction

Despite the fact that water-ice was known to make up a large fraction of a comet's composition, liquid water in comets was considered impossible for a long time. The dominance of Whipple's icy conglomerate model with comets sublimating from a perpetually frozen material prevented any discussion of a phase transition from ice to liquid water. The first discussion of liquid water in comets can be traced to Hoyle and Wickramasinghe (1978b):

"Typically a cometary body would acquire an organic mantle about a kilometre thick. The organic mantles (comprised of interstellar molecules) would initially be hard frozen like the ices below them... Internal heating and liquefaction inevitably occurred, however, as a result of chemical reactions among the organic materials, triggered perhaps by collisions of the comets with smaller bodies. Such reactions could release up to ten times the energy needed to melt cometary ices at a depth of a few hundred metres below the cometary surface..."

A necessary condition for liquid water to be stable within a comet is that the ambient temperature and pressure exceed the corresponding triple point values, T=273K and p=6mb. For a static uniform sphere of radius r and density ρ the central pressure is

$$p = \frac{2\pi}{3} G\rho^2 r^2 \qquad (7.1)$$

Assuming $\rho \approx 1$ g cm^{-3} and setting p>6mb equation (7.1) yields

$$r > 2\text{km} \qquad (7.2)$$

This is clearly the minimum radius of a cometary body that can sustain a liquid water core.

The phase change from ice to liquid water could produce dramatic biological consequences in a comet. The smallest mass of viable microbial material entering a nutrient-rich watery medium could be vastly amplified on a very short timescale.

The generation time (doubling time) of a microoganism depends on type and species, nutrient concentration as well as temperature. A naturally-occurring population of bacteria in Siberian permafrost is known to have a doubling time ranging from 20 days at -10^0C to 160 days at -20^0C (Rivkina et al., 2000). For a nutrient-poor cometary medium at a temperature close to 270K let us assume the doubling time for an anaerobic bacterium to be ~ 1yr (which is likely to be an upper limit).

If τ is the generation time of the bacterium, the biomass at a time t is given by

$$m \cong m_o 2^{t/\tau} \qquad (7.3)$$

where m_0 is the intial biomass. Equation (7.3) can be re-written to give

$$t = \frac{\tau \ln(m/m_0)}{\ln(2)} = 1.44\tau \ln\left(\frac{m}{m_0}\right) \qquad (7.4)$$

With $m_0 = 10^{-12}$ tonne (~ 10^6 bacteria) a million tonnes of biomass (representing less than 10^{-6} of a typical cometary mass) would be generated in a mere 60 years. Thus the smallest masses of viable bacteria/spores included within a newly-formed comet and the shortest time-spans for a liquid water core are enough to establish the importance of comets in relation to panspermia.

7.2 Primordial melting

Melting of cometary ices might occur due to heat generated by radioactive elements. Two short-lived nuclides that can be considered in this context are ^{26}Al (half-life 0.74My) (Wallis, 1980) and ^{60}Fe with a half-life 1.5My. The energy released by radioactive decay of ^{26}Al to ^{26}Mg, is 1.48×10^{13} J/kg. With an interstellar isotope ratio of $^{26}Al/^{27}Al \approx$

$5x10^{-5}$ and the known cosmic abundance ratios of C,N,O/Al we obtain a ^{26}Al mass fraction in pristine cometary material of ~ $3x10^{-7}$ (Mac Pherson et al., 1995; Diehl et al., 1997). The total energy available from radioactive decay of ^{26}Al within a comet is thus ~ $4.4x10^{6}$ J/kg, Recently the importance of ^{60}Fe in heating planetesimals has been discussed (Mostefaoui et al., 2004) and similar considerations apply to comets. With an order of magnitude higher value of relative abundance in cometary material, and a higher energy yield per unit mass, the heat available from the decay of the two shorter-lived nuclides ^{26}Al and ^{60}Fe could total $3x10^{7}$ J/kg. This energy yield is over two orders of magnitude higher than the heat of fusion of water-ice (~ $3.34x10^{5}$J/kg).

The feasibility of primordial liquid water cores is thus firmly established but estimating the duration of a liquid phase requires more detailed calculations. Such calculations involve several poorly-defined parameters, including the thermal conductivity of the cometary regolith and the time lapse between the injection of radionuclides into the solar nebula and the formation of comets. Such uncertainties are alleviated, however, by the extreme shortness of the required timescale for bacterial replication (see Eq.(7.4)).

Detailed model calculations of the thermal evolution of radiogenically-heated comets have been carried out by Wallis (1980), Yabushita (1993), Merk and Prialnik (2003) among others. A limiting factor for heating by short-lived nuclides (^{26}Al, half-life 0.74My; ^{60}Fe half-life 1.5My) is the time taken for the cometary bodies to accrete following the injection of radioactive nuclides into the solar nebula. If the process takes much longer than several million years, these radioactive heat sources would have become extinct. Uncertainties still exist in theories of comet formation but a consensus is growing that icy bodies in the inner solar system (Main Belt Asteroids) and comets in the inner Kuiper belt formed on timescales less than a few My. For comets condensing much further out in the solar system over longer timescales, a more secure source of radioactive heating would appear to come from the nuclides ^{232}Th, ^{238}U and ^{40}K.

Wallis (1980) considered a heat-conduction model with ^{26}Al. By integration of the diffusion equation he showed that a comet of radius ~ 3-6km containing a plausible

fraction of ^{26}Al would melt in the centre. A central low pressure water-droplet mixture was envisaged, insulated by a surrounding icy shell, the water phase being maintained against re-freezing for timescales of ~ My. Yabushita (1993) explored models involving longer-lived radioactive elements such as ^{232}Th, ^{238}U (with half-life > 1Gy). With appropriate mass fractions and on the assumption of a very low thermal diffusivity (10-100 times lower than for crystalline-ice) it was shown that relatively large comets, $r >$ 150km would be liquefied. Yabushita considered further the interesting possibility of chemistry leading to prebiotic molecules occurring within large liquid comets.

We now consider an approximate model of a radiogenically-heated comet to compute its thermal evolution. Merk and Prialnik (2003) derive the equation

$$C_p \frac{dT}{dt} = \tau^{-1} X_0 H e^{(-t_0+t)/\tau} - \frac{3\kappa T}{R^2 \rho} \qquad (7.5)$$

where T is the average temperature, C_p is the average specific heat, τ is the half-life of the radioactive element, H is the radioactive heat input per unit mass, κ is the average thermal conductivity, X_o is the mass fraction of ^{26}Al and R is the cometary radius. Here t_o (assumed to be ~ 1My) is the time between injection of ^{26}Al and the formation of comets, and t is the time after the comet was formed.

We assume $C_p = 10^3$ J/kg, ρ=0.3 g/cm^3, $d=\kappa/(\rho C_p)=10^{-6}$ m^2/s, for crystalline ice, and the previously assumed values of X_o and H relating to ^{26}Al. The adoption of values close to those appropriate to crystalline ice can be justified because the transition from amorphous ice to crystalline ice occurs at temperatures of ~ 120K (Merk and Prialnik, 2003). Any transport of energy through convection would be stalled once percolating water vapour re-condensed and effectively sealed pores in the cometary body.

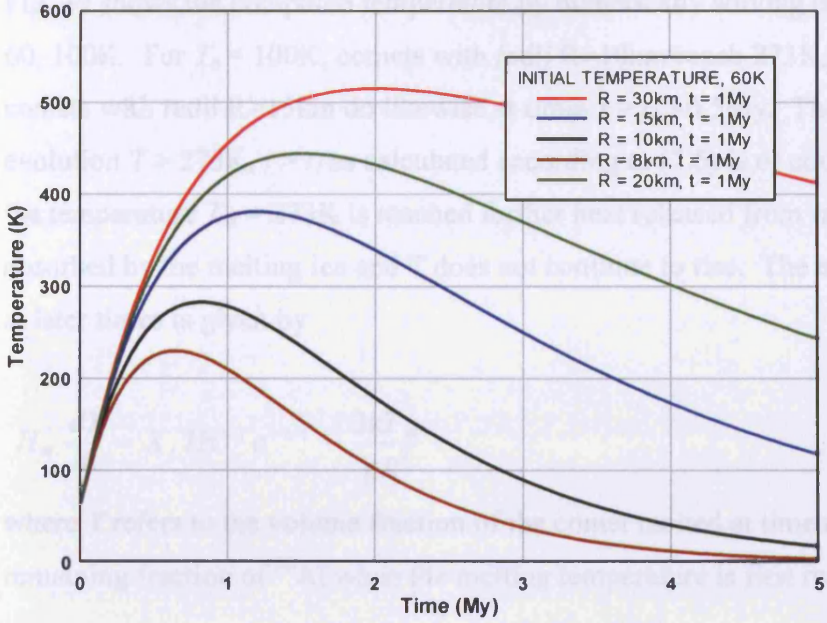

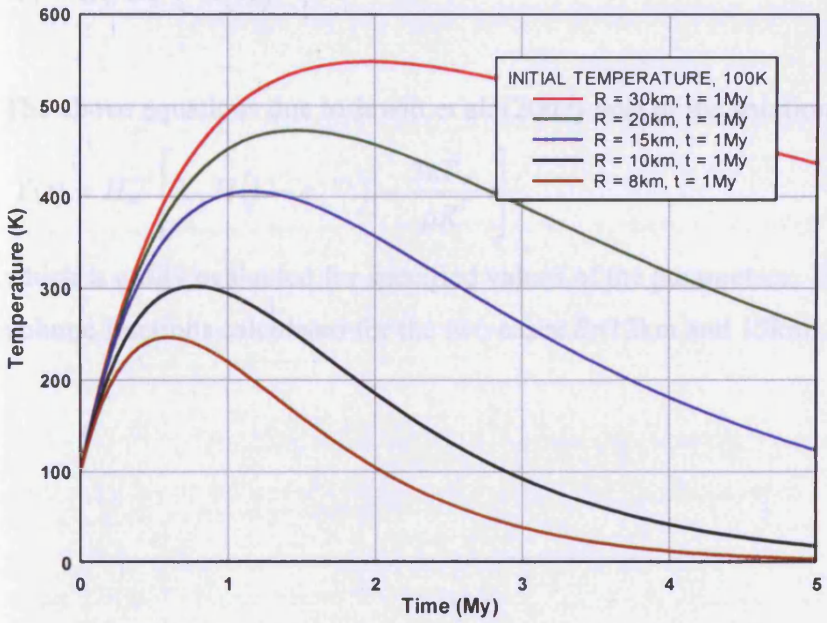

Figure 39: Calculation of the average internal temperature of a comet accumulated 1My after incorporation of ^{26}Al as a function of the subsequent time. Temperatures above 273 are artifacts of the idealised model. The temperature would flatten and subsequently decline after 273K is reached.

Fig. 39 shows the computed temperature by numerically solving equation (7.5) with T_o = 60, 100K. For T_o = 100K, comets with radii R>10km reach 273K, and for T_o = 60K comets with radii R>15km do likewise at times $t = t_l$ <0.5My. The subsequent thermal evolution T > 273K, $t > t_l$ as calculated according to (7.5) is of course unrealistic. Once the temperature T_m = 273K is reached further heat released from radioactive decay is absorbed by the melting ice and T does not continue to rise. The energy balance equation at later times is given by

$$H_m \frac{dY}{dt} = X_1 H\tau^{-1} e^{-t/\tau} - \frac{3\kappa T_m}{\rho R^2} \qquad (7.6)$$

where Y refers to the volume fraction of the comet melted at time t and X_l is the remaining fraction of ^{26}Al when the melting temperature is first reached

$$X_1 = X_0 \exp\left(-t_1/\tau\right) \qquad (7.7)$$

The above equations due to Jewitt et al. (2007) lead to the solution

$$Y(t) = H_m^{-1}\left[X_1 H\left(1 - e^{-t/\tau}\right) - \frac{3\kappa T_m}{\rho R^2} t\right] \qquad (7.8)$$

which is easily evaluated for specified values of the parameters. Fig. 40 shows the volume fractions calculated for the two cases R=12km and 15km.

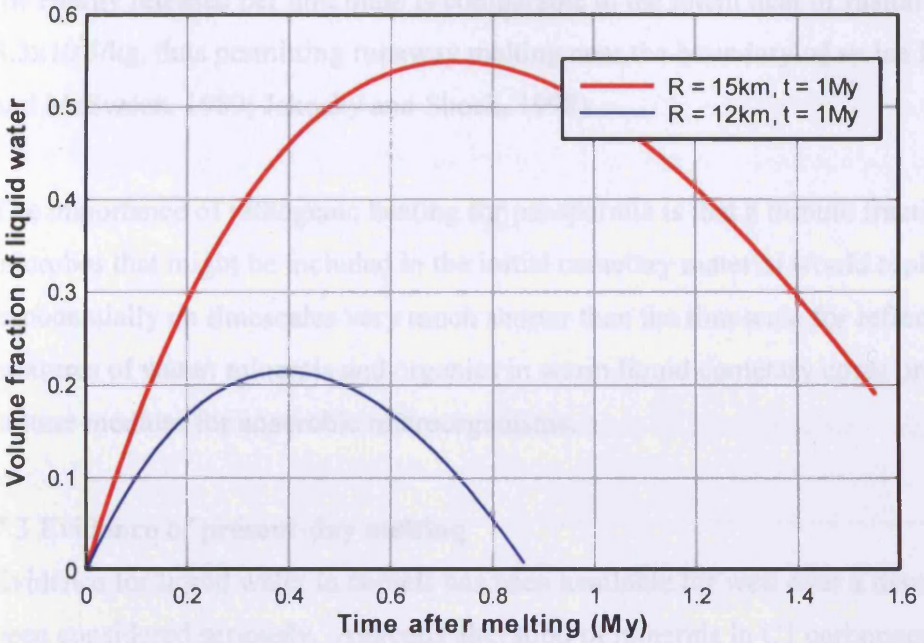

Figure 40: Volume fractions of water sustainable after melting first occurs

It is seen here that for smaller comets, even when they have radiogenically produced liquid cores, their volume fractions and durations are less than for larger comets. However, for a plausible set of parameters we see that primordial water in comets is possible even for comets as small as 12km. These results are generally in agreement with the trends shown in calculations by other authors (Jewitt et al., 2007). However, uncertainties of the precise limiting comet size for liquid formation persist and are attributable to uncertainties in relevant thermal constants and/or detailed physical processes involved in the transport of energy through the comet.

Once a liquid core is established heat sources from exothermic recombination of radicals and organic chemicals would produce more melting (Hoyle and Wickramasinghe, 1985). Heat production will also follow from the hydration of rock particles. For a serpentine producing reaction

$$Mg_2SiO_4 + MgSiO_3 + 2H_2O \leftrightarrow Mg_3Si_2O_5(OH)_4$$

the energy released per unit mass is comparable to the latent heat of fusion of ice, 3.3×10^5J/kg, thus permitting runaway melting near the boundary of an ice layer (Grimm and McSween, 1989; Jakosky and Shock, 1998).

The importance of radiogenic heating for panspermia is that a minute fraction of viable microbes that might be included in the initial cometary material would replicate exponentially on timescales very much shorter than the timescale for refreezing. The mixtures of water, minerals and organics in warm liquid cometary cores provide an ideal culture medium for anaerobic microorganisms.

7.3 Evidence of present-day melting

Evidence for liquid water in comets has been available for well over a decade but has not been considered seriously. Aqueous alteration of minerals in C1 carbonaceous chondrites inferred from geochemical and textural analyses provides compelling evidence for liquid water in their parent bodies (McSween, 1979). If comets are accepted as being parent bodies of a large class of carbonaceous chondrites (Hoover, 2005) liquid water in comets needs no further proof. Cometary dust (interplanetary dust particles) collected in the atmosphere has also exhibited aqueous alteration in hydrated states. They include components of clays, serpentines and carbonates sharing many mineralogic similarities with chrondritic material (Brownlee, 1978).

The first space probes to a comet in 1986 explored comet Halley at close range and made discoveries that were at odds with the hard-frozen icy conglomerate model. As predicted by Hoyle and Wickramasinghe (1986) the comet's surface turned out to be exceedingly black, with albedos ~3%, blacker than soot as to be hardly visible. Mass spectroscopy with Giotto instruments confirmed a chondritic composition of comet dust.

Infrared maps of comet Halley by Vega 1 showed temperatures in the range $T \approx 320$-400K at 0.8AU, considerably higher than the sublimation temperature of water ice in space ~200K. More recently-studied comets have led to similar conclusions on the whole. Comet 19/P Borrelly observed by *Deep Space 1* in 2001 at 1.4AU showed a very

dark surface with an average albedo ~3%, but with local spots even darker with albedos of less than 0.008 – darker than carbon black. Again surface temperatures were found to be in the range 300–340 K, with no traces of water. The surface temperatures 300-340 K at 1.4 AU are appropriate to solar heating with little thermal conduction. Comet 81/P Wild 2 observed by *Stardust* also showed similar low albedos, as did comet Tempel 1.

The observation of comets showing the presence of insulating crusts that resist high sub-solar temperatures prompted the model that is now described. Our objective will be to discover whether liquid water can be produced by solar heating at some depth below the surface crust.

We first consider a non-rotating stationary comet under sub-solar insolation with a view to solving the heat conduction equation

$$\frac{\partial T}{\partial t} = \kappa \nabla^2 T \qquad (7.9)$$

which in a one-dimensional infinite plane approximation simplifies to

$$\frac{\partial T}{\partial t} = \kappa \frac{\partial^2 T}{\partial z^2} \qquad (7.10)$$

We envisage a layered one-dimensional structure to emerge over a depth of ~1m of comet material due to outgassing near perihelion passage. Over this depth porous organic lag material would accumulate following percolation/sublimation of volatiles, but the outermost 1-2 cm would inevitably comprise a sun-burnt insulating crust that can frequently crack and reseal under the pressure ~10mb of escaping water vapour and volatiles. Organic volatiles reaching the surface would continually re-seal and strengthen this 'mobile' outer crust. Below a certain depth of organic material we envisage the possibility of liquid water being maintained through solar heating and with the saturation vapour pressure ~6mb supported by overlying crust.

Consider a three-layer structure with burnt insulating material at the top from $z = 0$ to $z = d_1$ with thermal conductivity $\kappa_2 = 0.17$ W/(mK) (corresponding to bitumen), a layer with $d_1<z<d_2$ possessing conductivity $\kappa_1 = 1.7$ W/(mK) (organic-ice mix). The possibility of liquid water is considered for a depth $z>d_2$.

The energy balance is controlled by the receipt of solar radiation at r AU

$$F_0 = \frac{1.4}{(r/AU)^2} \quad kW/m^2 \tag{7.11}$$

on the comet's surface, and the thermal re-emission

$$\sigma \varepsilon_{IR} T^4 \tag{7.12}$$

which yields

$$\sigma \varepsilon_{IR} T^4 = \frac{(1-A)F_0}{(r/AU)^2} - \Phi_{down} \tag{7.13}$$

where

$$\Phi_{down} = \kappa \frac{dT}{dz} \tag{7.14}$$

is the net downward flux of radiation during the day and A is the albedo, A being taken to be 0.03.

If water is mixing and convecting in a steady state of heat flow the solution satisfies

$$\Phi_{down} = \kappa_1 (T_0 - T_i)/d_1 = \kappa_2 (T_i - 273) \tag{7.15}$$

where T_0 is the maximum outer temperature of the comet, T_i is the temperature between the outermost burnt layer and the organic crust, and 273 K is the interface temperature between the organic crust and the water layer.

The outer temperature T_0 is calculated from equations (7.13) and (7.15), and a schematic temperature resulting from such a calculation is set out in Fig. 41.

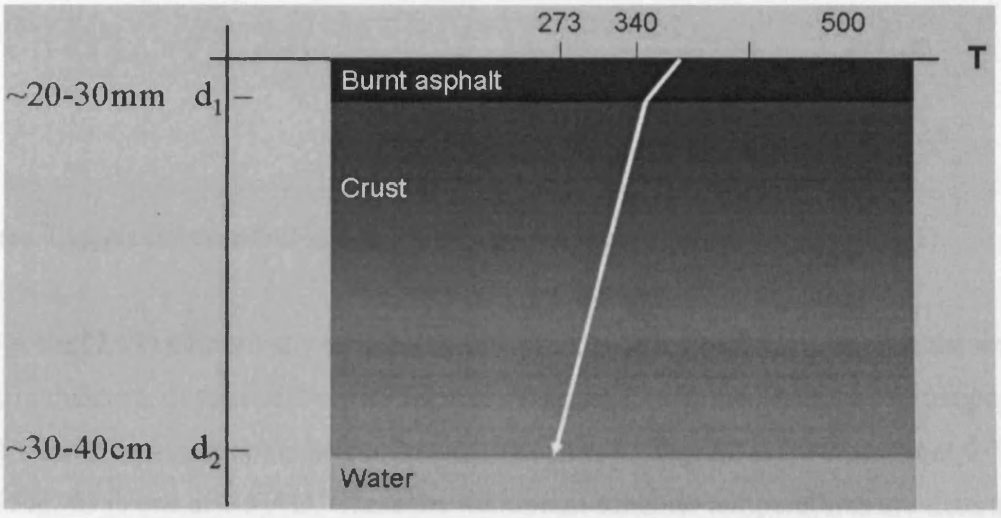

Figure 41: A schematic temperature profile of a comet

We now consider a hypothetical layered structure as described above, but with the outer surface exposed to diurnal variations as it would be for a tumbling comet. In the case of comet Halley the tumbling period is 90 hr. For a comet rotating with period τ, the temperature at a depth x below an area of thin insulating crust is approximated by a harmonic function. We use an infinite half-plane model to solve the heat conduction equation

$$\frac{\partial T}{\partial x} = \alpha \frac{\partial^2 T}{\partial x^2} \qquad (7.16)$$

where $\alpha = \kappa/C\rho$, κ being the thermal conductivity, C the thermal capacity and ρ the density. With values appropriate to the organic comet material $C = 0.8$ J/cm^{3}K, $\kappa = 1.7$ W/mK we have $\alpha = 0.003$m^2/h for use in (7.9) and a thermal skin depth ~30cm.

For an infinite half-plane maintained at the surface $x = 0$ with an oscillatory (sine-wave) temperature variation of amplitude T_{ampl} and period τ about a mean temperature T_{mean}, (determined by long-term solar insolation) the analytical solution of (7.9) is

$$T(x,t) = T_{mean} + T_{ampl} \cos\left(\sqrt{\frac{\pi}{\alpha\tau}} - 2\pi\,\frac{t}{\tau}\right) e^{-\sqrt{\frac{\pi}{\alpha\tau}}\,x} + \frac{2\,T_{initial}}{\sqrt{\pi}} \int_0^{x/2\sqrt{\alpha t}} e^{-\xi^2}\,d\xi \qquad (7.17)$$

where $T_{initial}$ is the constant initial temperature of the medium (Carslaw, 1921).

We solve (7.17) numerically with $\alpha = 0.003$ m^2/h as an appropriate value for the organic matrix underneath the burnt crust. Figures 42 and 43 show the variations of temperature with time at various depths below the insulating crust. Fig. 42 is for a comet at 0.7 AU and Fig. 43 is one at 1.5 AU, where the maximum subsolar temperatures are determined by midday solar heating assuming an emissivity $\varepsilon = 1$.

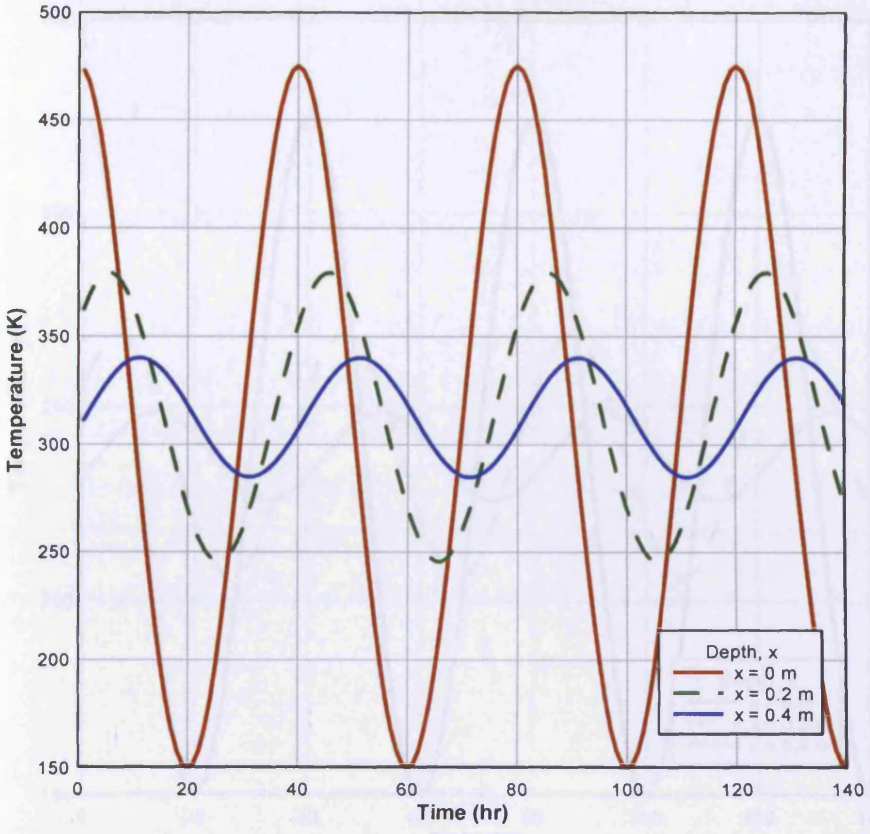

Figure 42: Variations of temperature with time at depth, x beneath an insulating crust of comet with emissivity $\varepsilon = 1$ at 0.7AU rotating with period 40hr

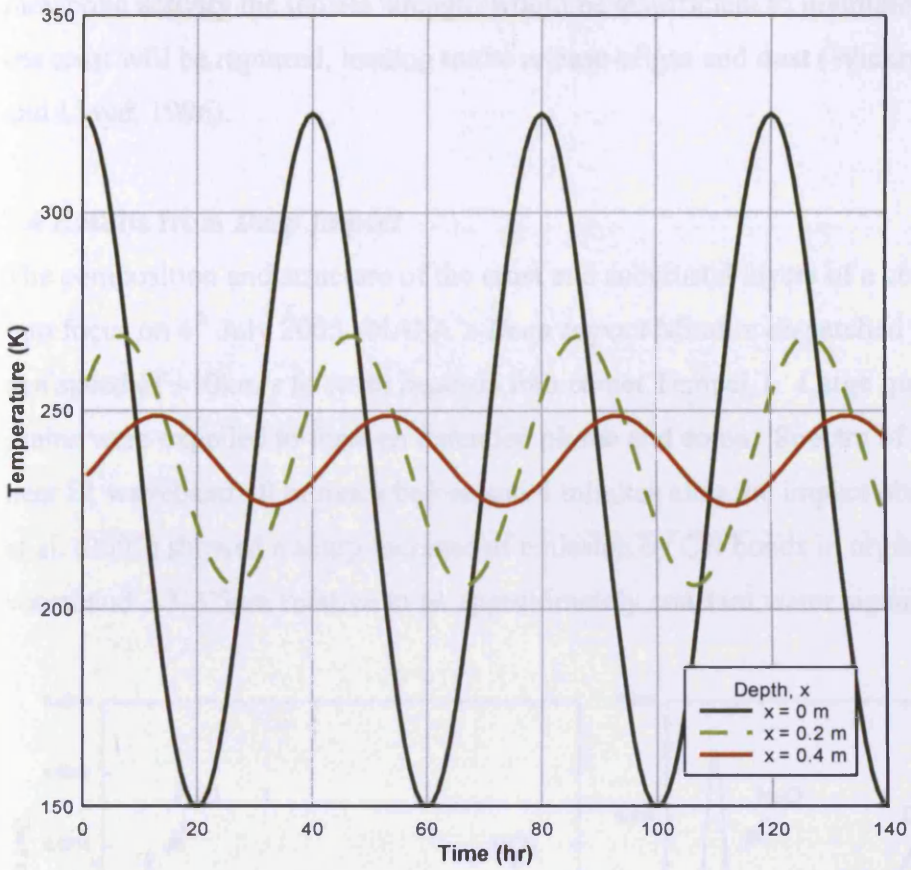

Figure 43: Variations of temperature with time at depth, x beneath an insulating crust of a comet with emissivity $\varepsilon = 1$ at 1.5 AU rotating with period 40hr

In Fig. 42 we note that liquid water can persist below 0.2m (e.g. comet Halley); in Fig. 43 (e.g. comet Tempel 1) no liquid water is possible. According to these calculations the generation of transient subsurface liquid water domains requires the temperatures at some depth to remain above a notional melting temperature (T=273K assumed, but could be lower, even 250K for organic-water-ice mixtures) throughout a diurnal cycle. For perihelion distances < 1AU this could be feasible at depths ~ 0.3-0.5m, subsurface pools persisting for days or weeks near perihelion. This provides ample time for a vast amplification for a population of dormant bacteria that may have been present (c.f. Eq. 7.4, with typical doubling times of hours). The liquid pools themselves would be maintained by the tensile strength of the overlying layer which would be at least 100 times the water vapour pressure ~ 6mb. If, however, gas pressure builds up due to

metabolic activity the tensile strength would be insufficient to maintain equilibrium and the crust will be ruptured, leading to the release of gas and dust (Wickramasinghe, Hoyle and Lloyd, 1996).

7.4 Results from *Deep Impact*

The composition and structure of the crust and subcrustal layers of a comet came sharply into focus on 4th July 2005. NASA's *Deep Impact* Mission dispatched a 370kg projectile at a speed of ~10km/s to crash head-on into comet Tempel 1. Large quantities of gas and grains were expelled to form an extended plume and coma. Spectra of the coma in the near IR waveband 10 minutes before and 4 minutes after the impact obtained by A'Hearn et al. (2005) showed a sharp increase of emission by CH bonds in organic dust over the waveband 3.3-3.5μm relative to an approximately constant water signal (Fig. 44).

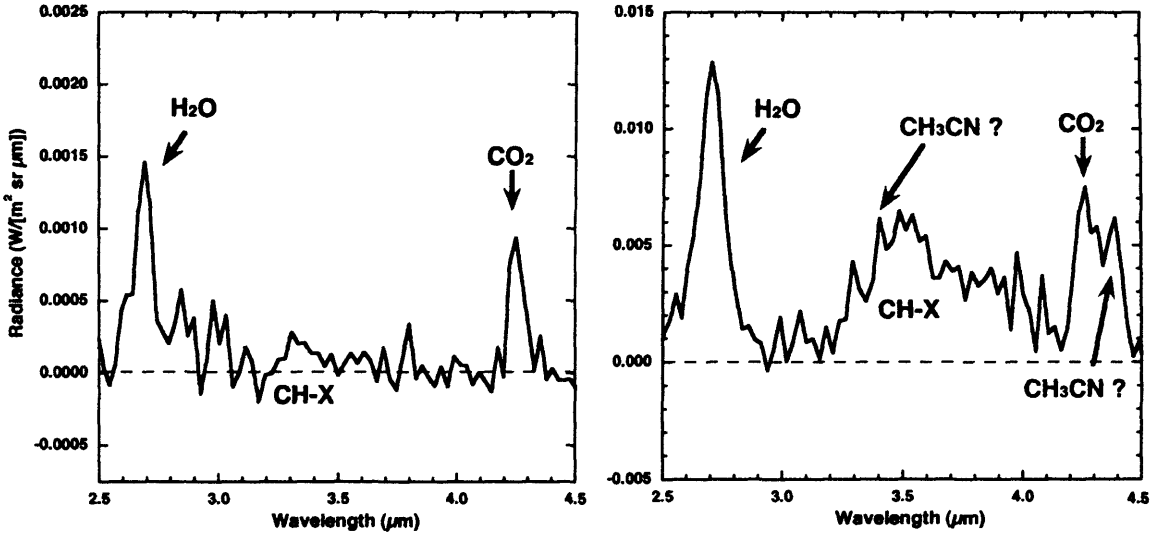

Figure 44: Spectra of coma of Tempel 1. Ten minutes before (left panel) and four minutes after the impact (right panel) on July 4th 2005

The excess radiation over this waveband in the post-impact plume that cannot be modelled by inorganic coma gases are best explained on the basis of degraded biologic-type organic material. We considered the type of organic dust discussed by Hoyle and Wickramasinghe for explaining the mean 3.3-3.5 μm emission profile for comet Halley

and other comets (organic/biologic and asphalt-like material presumed to result from its degradation). Fig. 45 shows the normalised emissivity calculated for such a model compared with the observations of the post-impact plume of Tempel 1 on 4th July 2005.

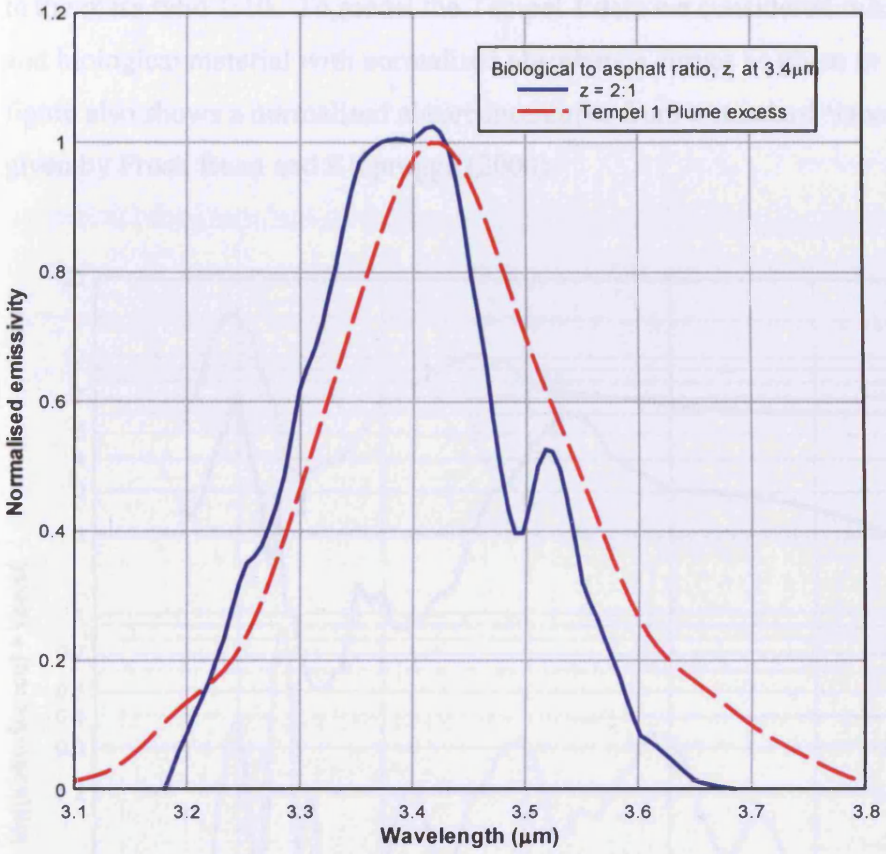

Figure 45: Normalised emissivity near 3.4 μm for a mix of 'normal' cometary dust matching biological material with asphalt. For comparison is plotted the 'unexplained' component of emission from the plume following impact on 4th July 2005.

We see that with a 2:1 contribution of biological material to asphalt in the emissivity at 3.4 μm an approximate match with the data is obtained. This is satisfactory considering the fact that asphalt is likely to be an over-simplified representation of degraded biomaterial.

Observations of Tempel 1 some 20 hours following impact using the Spitzer Telescope yielded 5-37 μm spectra generally similar to the spectra of comet Hale-Bopp taken by ISO (Infrared Space Observatory). The Hale-Bopp data was interpreted by Hoyle and Wickramasinghe (1999) on the basis of a model involving olivine and biological material in the mass ratio 1:10. To model the Tempel 1 data we considered mixtures of olivine and biological material with normalised absorbance curves as given in Fig. 46. This figure also shows a normalised absorbance curve from a standard 'laboratory' clay as given by Frost, Ruan and Kloprogge (2000).

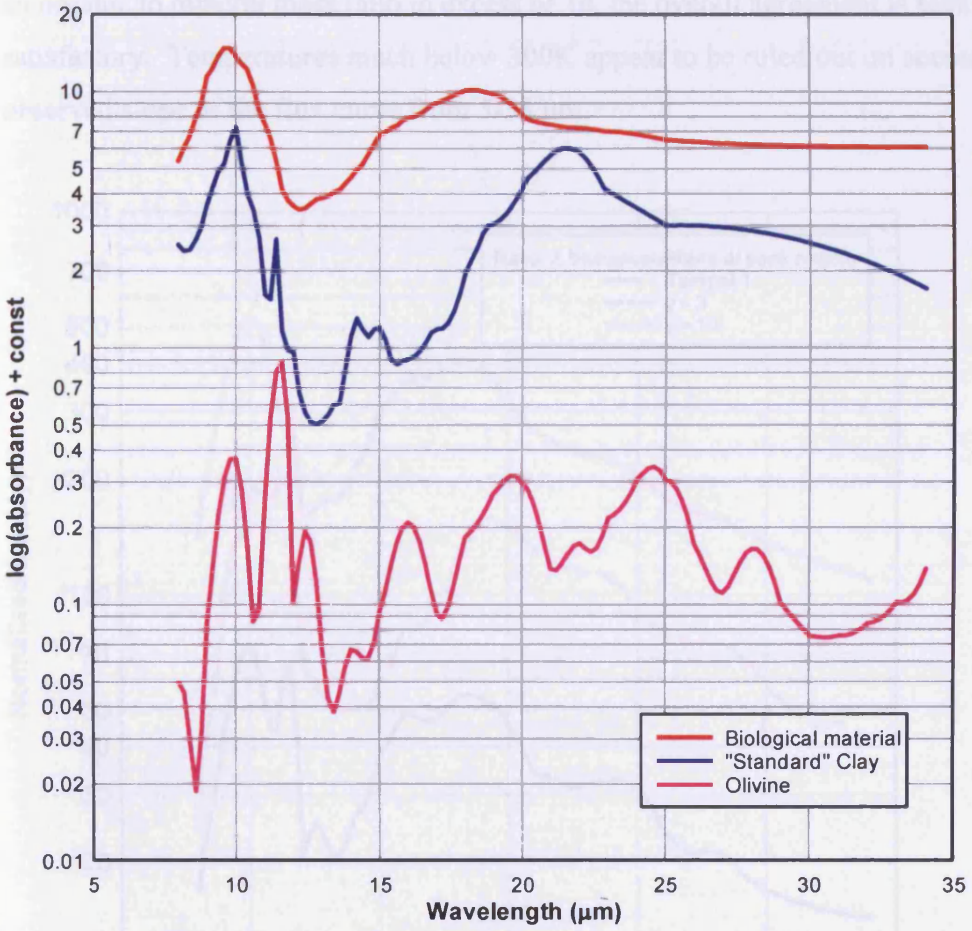

Figure 46: Absorbance data used for the calculations

The absorbance data for olivine and biomaterial are taken from compilations by Hoyle and Wickramasinghe (1999). The two materials were conceptually mixed with opacity contributions at their peak maxima in the ratio organic: olivine = z:1. Since for olivine/clay the maximum mass absorption coefficient near the 9 μm peak is over 5 times that of the less well-ordered organics, the corresponding mass ratios are near 5z:1.

In Fig. 47 we plot the normalised flux curves for emission from biological/olivine mixtures for grain temperatures T = 350K with z = 10 and 3. The dashed curve is the normalised flux obtained from Tempel 1 (Lisse et al., 2006). For z = 3 corresponding to an organic to mineral mass ratio in excess of 10, the overall agreement is seen to be satisfactory. Temperatures much below 300K appear to be ruled out on account of the observed slope of the flux curve from 5-33 μm.

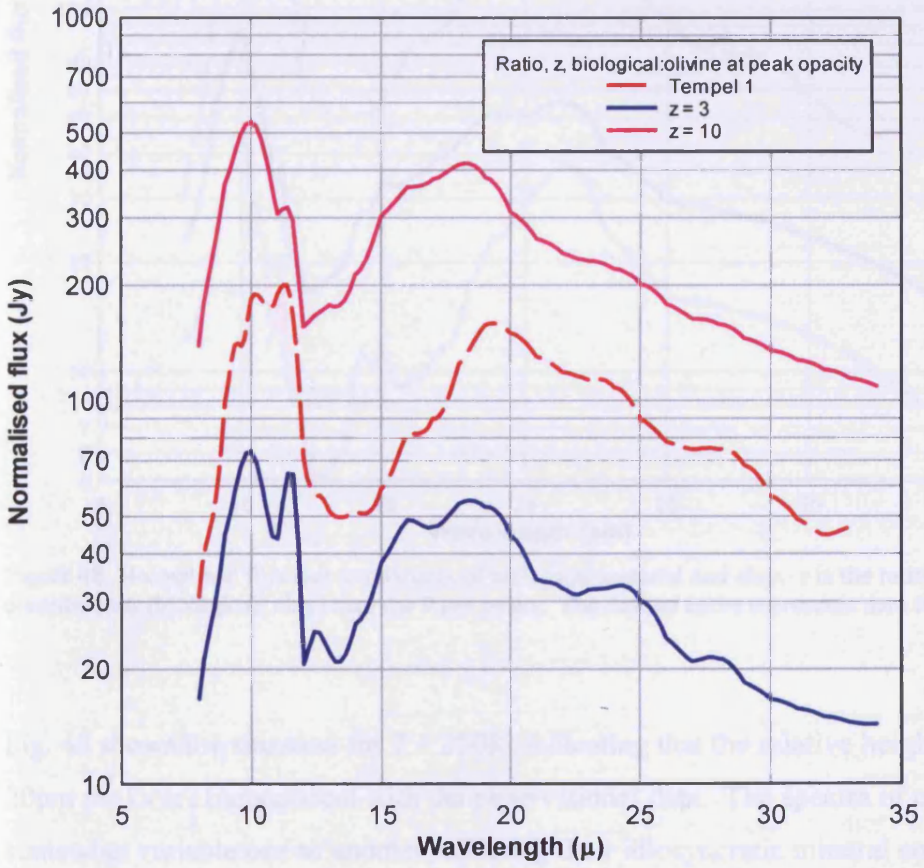

Figure 47: Normalised flux due to mixtures of biological material and olivine. z is the ratio of opacity contributions (biological: olivine) near the 9 μm peaks. The dashed curve represents data for Tempel 1.

Figure 48 displays computed flux curves for mixtures of clay and biological grains, again heated to 350K. Very similar relative abundance conclusions can be drawn in this instance, with mass ratios of biological to clay again well in excess of 10:1. The temperature 300 – 350K appears to be necessary to match the underlying continuum of the Tempel 1 dust spectrum.

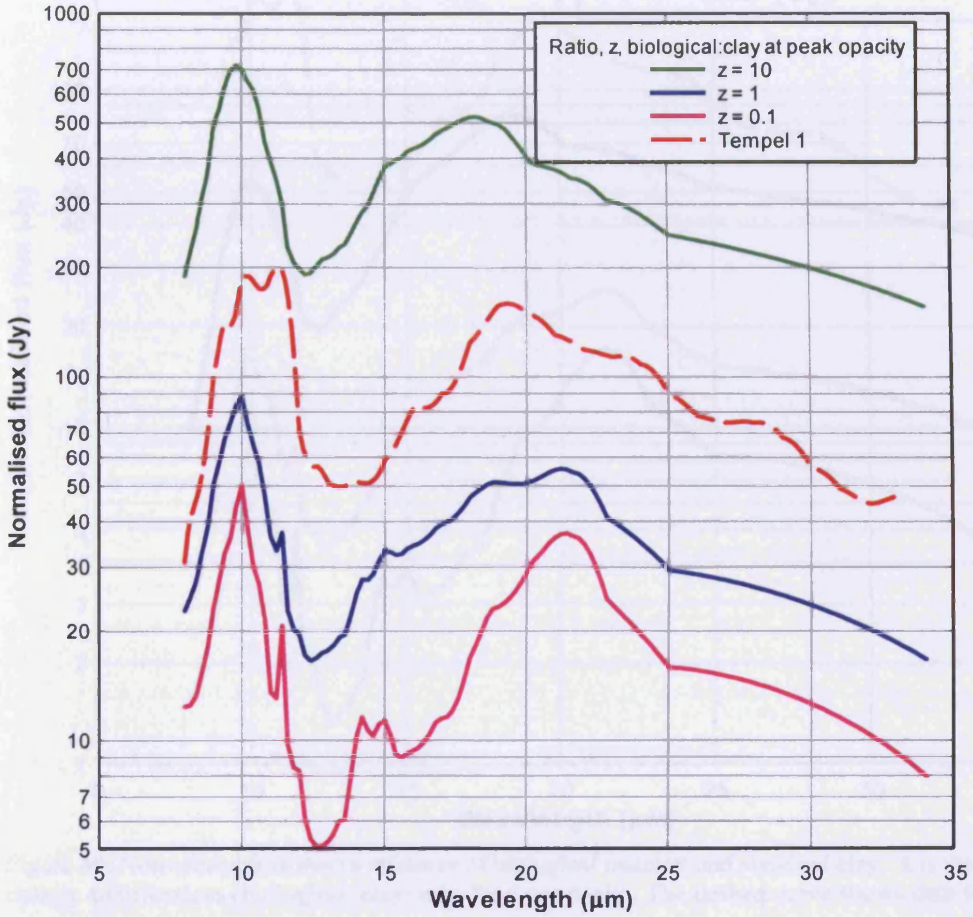

Figure 48: Normalised flux due to mixtures of biological material and clay. z is the ratio of opacity contributions (biological: clay) near the 9 μm peaks. The dashed curve represents data for Tempel 1.

Fig. 49 shows the situation for $T = 250$K, indicating that the relative heights of the 10 and 20μm peaks are inconsistent with the observational data. The spectra of clays tend to be somewhat variable one to another reflecting their idiosyncratic mineral configurations. However, fine structure in the 8 – 11μm absorption band centred near 9, 10 and 11μm

can be in general be regarded as signifying a clay, and these indeed have been found in the higher resolution spectra of Tempel 1 following the *Deep Impact* event.

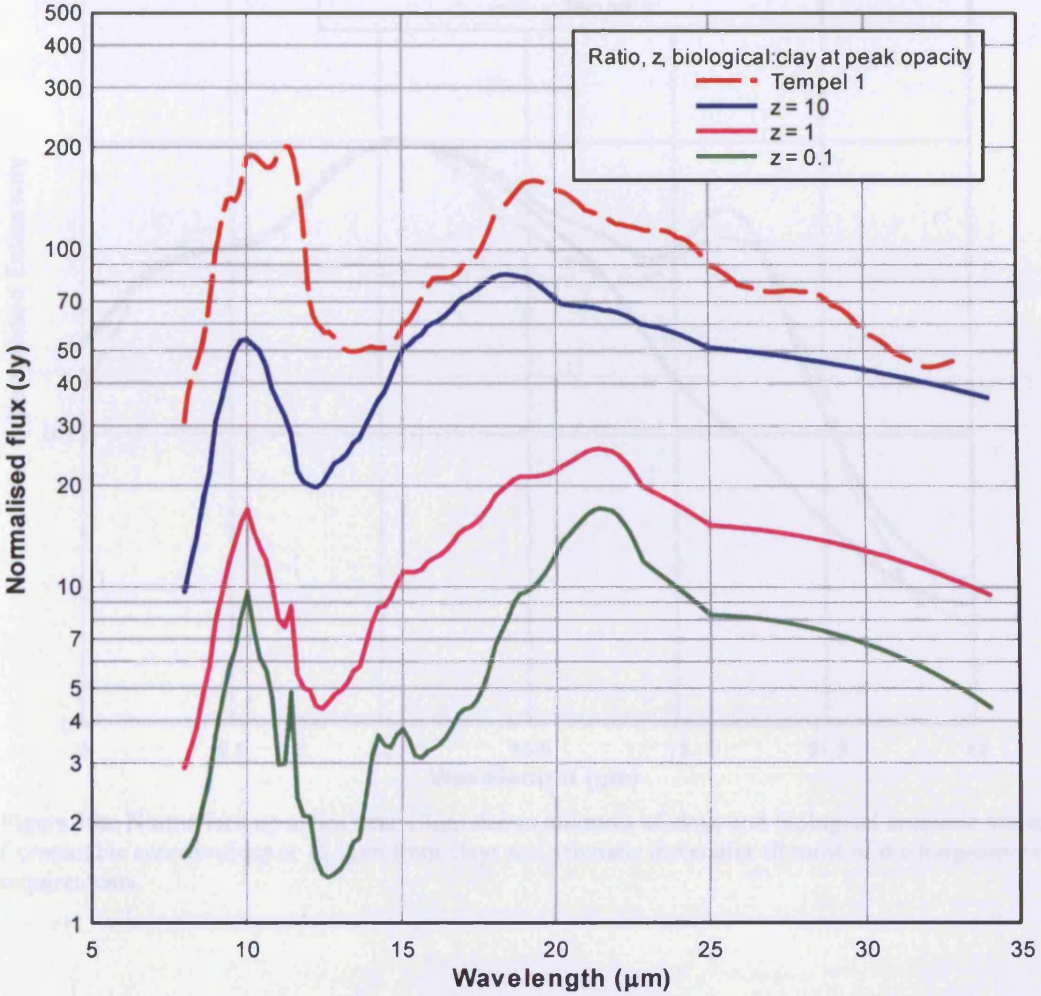

Figure 49: Normalised flux due to mixtures of biological material and standard clay. z is the ratio of opacity contributions (biological: clay) near the 9 μm peaks. The dashed curve shows data for Tempel 1.

Over the 8 - 13 μm wavelength interval we combined the standard clay spectrum given by Frost and Kloprogge with three other clay spectra, yielding the normalised emissivity plotted in Fig. 50a. The average emissivity spectrum (post-impact) of Tempel 1, shows good agreement with clay at 9 and 10 μm, but a significant excess centred near 11.2 μm (Lisse et al., 2006). This 'missing' flux has been attributed to PAH's although individual compact PAH's tend to possess a 11.2 μm feature that is too narrow to fit the bill.

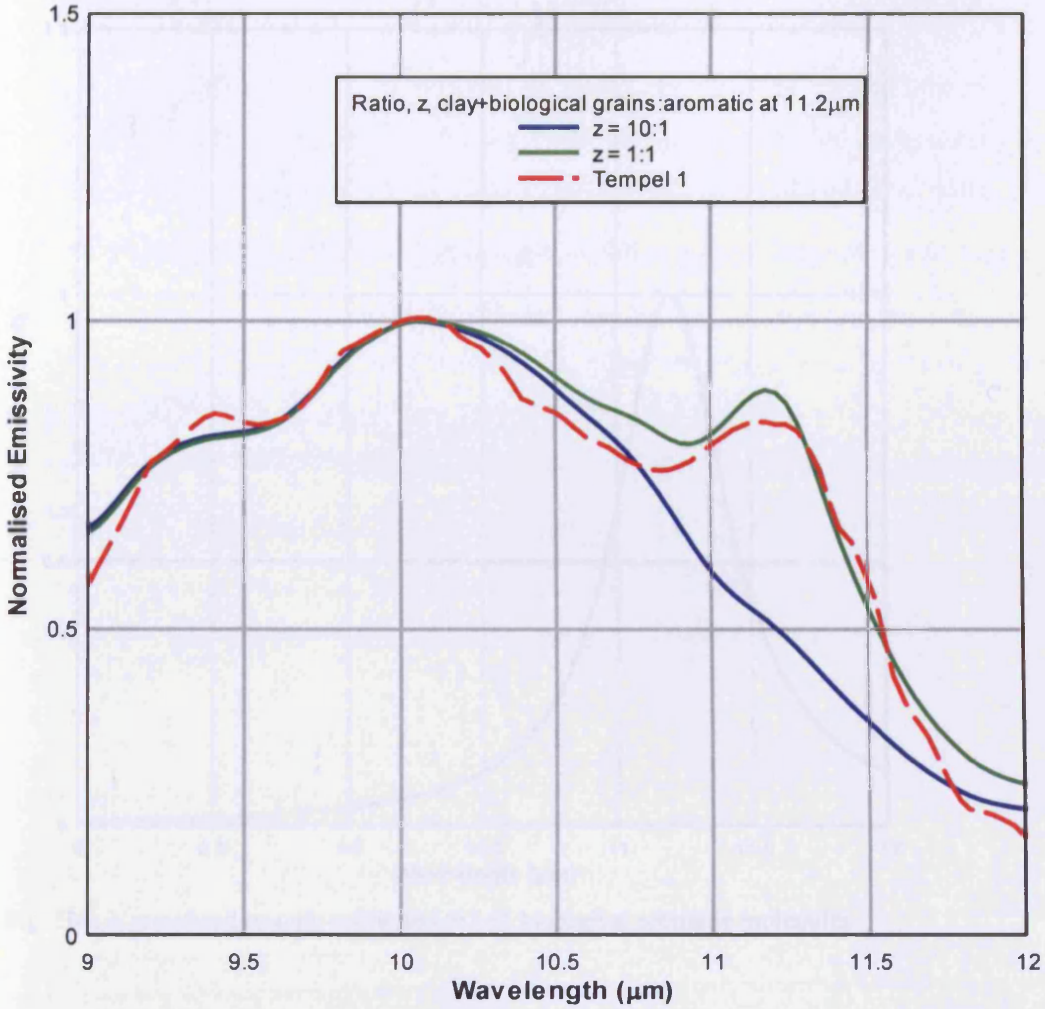

Figure 50a: Normalised opacities near 10μm due to mixtures of clays and biological aromatic molecules. Comparable contributions at 11.2μm from clays and aromatic molecules fit most of the long-wave opacity requirements.

Hoyle and Wickramasinghe (1991) had argued that an ensemble of biological aromatic molecules might explain the UIB's (unidentified infrared bands) in interstellar spectra, and their set of 115 biological aromatics do indeed provide an 11.2μm band with a half width at maximum intensity of ~0.3 μm. Such as absorption can fit a Lorentzian profile such as calculated in Fig. 50b. Emission in such a 11.2μm band contributing an equal flux to that from clay at the band centre adds up to the curve shown in Fig. 50a, exhibiting satisfactory overall agreement with the observations.

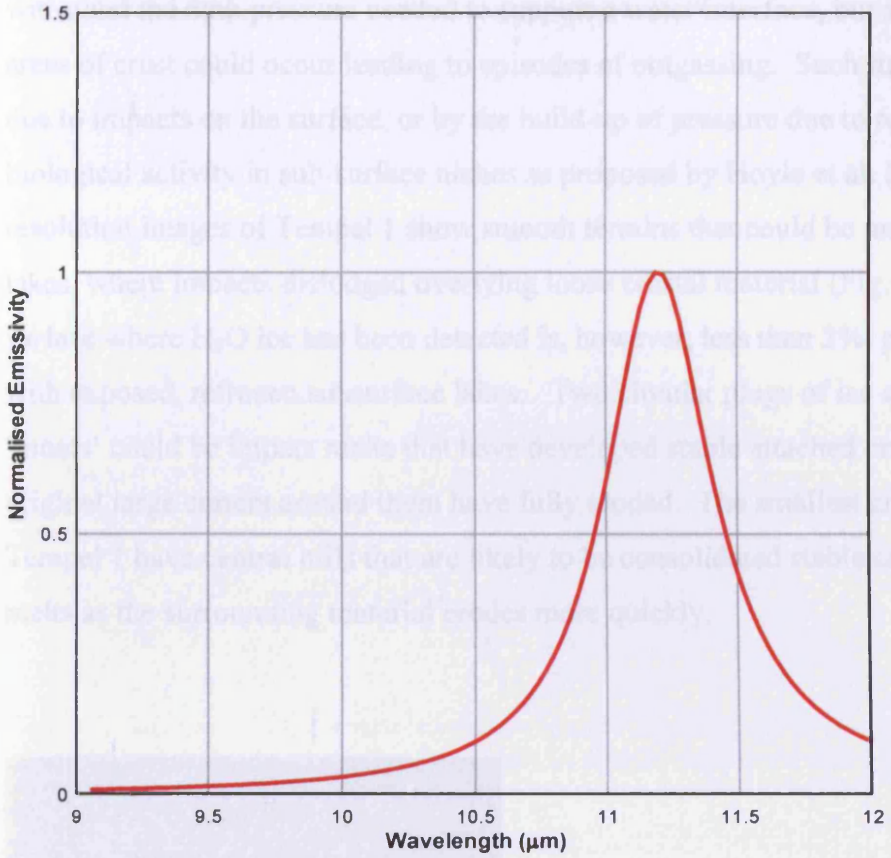

Fig. 50b: Normalised opacity attributed to 115 biological aromatic molecules

We thus confirm the conclusions already reached by Lisse et al. (2006) that clay minerals, complex organics and PAH-type material are present in the post-impact ejecta from Tempel 1. Earlier claims in the last decade of similar materials in IDPs (interstellar dust particles) and in C1 carbonaceous chondrites cannot now be ignored. Furthermore, since clay minerals are thought to form only in contact with liquid water, water in comets now appears a virtual certainty. The question of comets serving as microbial habitats and amplifiers needs now to be urgently addressed.

Transient sub-surface pools with organic nutrients and viable microbes imply that continuing biological activity could occur in comets. The pools in our model are maintained a few tens of centimetres below a sealed outer crust that is continually regenerated due to condensation of diffusing organic materials. Such a crust can easily

withstand the 6mb pressure needed to support a water interface, but sporadic rupturing of areas of crust could occur leading to episodes of outgassing. Such rupturing could occur due to impacts on the surface, or by the build-up of pressure due to resumption of biological activity in sub-surface niches as proposed by Hoyle et al. (1998). High resolution images of Tempel 1 show smooth terrains that could be understood as refrozen lakes, where impacts dislodged overlying loose crustal material (Fig. 51). The fraction of surface where H_2O ice has been detected is, however, less than 3%, possibly connected with exposed, refrozen subsurface lakes. Two circular plugs of ice surrounded by 'moats' could be impact melts that have developed stable attached crusts, while the original large craters around them have fully eroded. The smallest craters seen on Tempel 1 have central hills that are likely to be consolidated stable crusts left by impact melts as the surrounding material erodes more quickly.

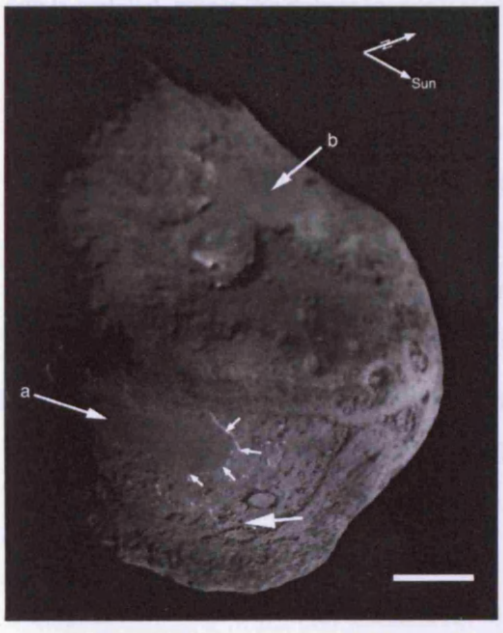

Figure 51: High resolution image of Tempel 1

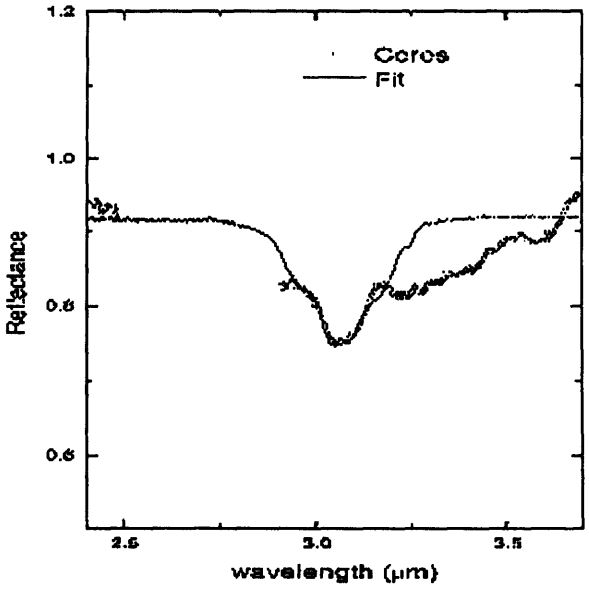

Figure 52: Spectrum of 1 Ceres showing the 3.06 absorption band due to crystalline water ice. The thin line is a model, where the data at longer wavelengths requires another absorber (from Vernazza et al., 2005)

Comets are not the only small bodies in the solar system that show evidence of frozen water surfaces. The main belt asteroid Ceres, which has a mean diameter of 952km, eccentricity e=0.08 and semimajor axis 2.77AU, has recently revealed a water ice surface as indicated in the spectrum shown in Fig. 52 (Vernazza et al., 2005). It is argued that the water-ice surface has been recently emplaced because sublimation life-time at 2.8AU is relatively short. Here then is another instance of a recently-exposed subsurface lake as in a comet.

7.5 Concluding remarks

In this thesis the ancient theory of panspermia has been re-examined with regard to its possible link to comets. Taking account of recent space-probe studies of comets dynamical calculations were carried out exploring the interaction of solar-system comets with the external interstellar environment. It was shown in this chapter that comets could serve as carriers and amplifiers of microorganisms, amplification occurring within radioactively melted interiors. In this way the dispersal and seeding of life within a

planetary system could occur. Comets impacting a life-bearing Earth-like planet could also expel entire ecologies of evolved microbial life into interplanetary space and thence make relatively short journeys to reach new planetary systems. The well-attested radiation resistance of microorganisms is shown to be adequate to make such transits with a significant viable fraction being preserved.

The Oort cloud of comets that surrounds our solar system comes to be perturbed on a time scale of 20-40My through encounters with molecular clouds in which new stars and planets form. We show in Chapter 4 that such encounters lead to periodic surges of comets gravitationally deflected into the inner regions of the solar system, some to collide with Earth. The cratering record on the Earth bears out such a periodicity, and collisions with comets are the most likely explanation. An unshocked fraction of the material (in the form of dust) excavated from craters reaches escape speed (Chapter 6) and is ejected by solar radiation pressure from the entire solar system. Such material must include a fraction of viable microbes, and their expulsion at ~30km/s enables them to reach nascent planetary systems in an approaching nebula on timescales as short as ~ 1My. The next step in the logic is to suppose that extrasolar planetary systems are no different from our solar system in having Oort-type clouds of comets. It is easy to envisage that a few viable bacteria from Earth ejecta can enter exosolar comets at the time of their aggregation, and the arguments about radiogenic heating and exponential replication discussed in this chapter would apply. Such life, amplified and viable, then has a chance of seeding an embryonic Earth-like planet. This process must then continue all through the Galaxy. As long as there are at least 1.1 exoplanetary systems in every perturbing molecular cloud, microbial life and the products of its evolution would propagate throughout the Galaxy.

The ongoing-panspermia model developed in this thesis presents several challenges to conventional biological thought. Darwinian evolution, survival of the fittest, would proceed not in a closed system, but in an open system permitting, as well as depending upon, periodic injections of new genetic material from space. If the same genotypes are

periodically re-introduced to the planet from a frozen and non-evolving reservoir within comets, conventional views about phylogenetics may need to be revised.

In summary the arguments presented in this thesis support the view that comets are responsible not only for the origin of life on Earth (and on similar exosolar planets) but for its subsequent evolution as well. Comets are the carriers, amplifiers and distributors of life. Our cosmic ancestry is firmly linked with comets.

Appendix A

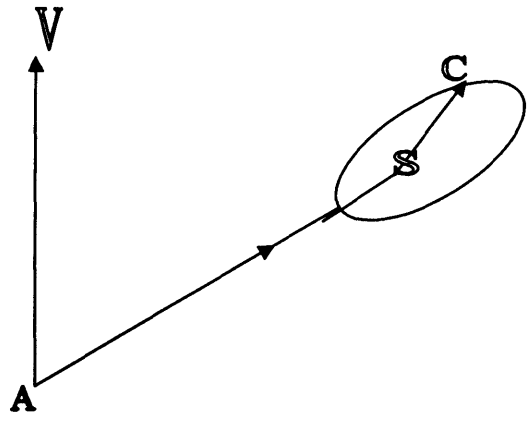

Figure A: Schematic sketch of GMC/solar system geometry during encounter

Consider a molecular cloud at A moving with velocity vector **V**.

Let S be the Sun located at position vector AS = **R** relative to A, and let SC = **r** be the position vector of the comet relative to the Sun.

The instantaneous acceleration of S relative to the molecular cloud at A is

$$\frac{GM}{R^3}\mathbf{R}$$

and the instantaneous acceleration of C relative to molecular cloud at A is

$$\frac{GM}{R^3}(\mathbf{R}+\mathbf{r})$$

Therefore the instantaneous acceleration of C relative to S is

$$\frac{GM}{R^3}\mathbf{r}$$

For each element of trajectory Δx along the velocity vector **V**, the impulsive velocity delivered to the comet C is thus

$$\frac{\Delta x}{V}\frac{GM}{R^3}\mathbf{r}$$

which is always a vector in the direction of the radial coordinate of C in its orbit around the Sun. The two remaining orthogonal velocity components conveniently vanish. This result simplifies the application of the Archie Roy impulse equations which are used in Chapter 4.

Bibliography

A'Hearn, M.F. et al., 2005. Deep Impact: Excavating Comet Tempel 1. *Science* , **310**, pp. 258-264.

Abraham, M. and Becker, R., 1950. *The Classical Theory of Electricity and Magnetism.* 2nd ed. London: Blackie.

Allen, C.W., 2000. *Astrophysical Quantities.* 4th ed. New York: Springer.

Allen, D.A. and Wickramasinghe, D.T., 1981. Diffuse interstellar absorption bands between 2.9 and 4.0 μm. *Nature,* **294**, pp. 239-240.

Alvarez, L. W., Alvarez, W., Asaro, F. and Michel, H. V., 1980. Extraterrestrial Cause for the Cretaceous-Tertiary Extinction. *Science* **208**, pp. 1095-1108.

Arrhenius, S., 1903. Die Verbreitung des Lebens im Weltenraum. *Die Umschau,* **7**, pp. 481-485.

Arrhenius, S., 1908. *Worlds in the Making.* London: Harper.

Bailey, M. E., 1990. *In:* D. Lynden-Bell and G. Gilmore, eds. Baryonic Dark Matter. Kluwer, Dordrecht, pp. 7

Bailey, M. E. and Emel'yanenko, V. V., 1998. *In:* M. M.Grady et al., eds. *Meteorites: Flux with Time and Impact Effects.* London: Geol. Soc. London, pp. 11.

Bailey, M. E., Clube, S. V. M. and Napier, W. M., 1990. *The Origin of Comets.* Oxford: Pergamon.

Becquerel, P., 1924. La Vie Terrestre provient-elle d'un Autre Monde? *Bull.Soc.Astron.*, **38**, pp. 393-417.

Bockelee-Morvan, D. et al., 1998. Deuterated Water in Comet C/1996 B2 (Hyakutake) and Its Implications for the Origin of Comets. *Icarus*, **133**, pp. 147-162.

Bohren, C. F., Wickramasinghe, N. C., 1977. On the computation of optical properties of heterogeneous grains. *Astrophys. and Space Sci.*, **50**, pp. 461-472.

Brandt, J. C. and Chapman, R. D., 2004. *Introduction to Comets.* 2nd ed. Cambridge: Cambridge Univ. Press.

Brooke, T.Y., Tokunaga, A.T. and Knacke, R.F., 1991. Detection of the 3.4 micron emission feature in Comets P/Brorsen-Metcalf and Okazaki-Levy-Rudenko (1989r) and an observational summary. *Astron. J.*, **101**, pp. 268-278.

Brownlee, D.E., 1978. *In:* T. Gehrels, ed. *Protostars and Planets.* Tuscon: Univ. of Arizona Press, pp.134

Burbidge, E. M., Burbidge, G. R., Fowler, W. A., and Hoyle, F., 1957. Synthesis of the Elements in Stars. *Rev. Mod. Phys.*, **29**, pp. 547-650.

Burchell, M.J., Mann J.R. and Bunch, A.W., 2004. Survival of bacteria and spores under extreme shock pressures. *MNRAS,* **352,** pp. 1273-1278.

Butler, R.P. et al., 2006. Catalog of Nearby Exoplanets. *The Astrophys. Journal*, **646**(1), pp. 505-522.

Byl J., 1986. The effect of the Galaxy on cometary orbits. *Earth, Moon, and Planets*, **36**, 263-273.

Cano, R.J. and Borucki, M., 1995. Revival and identification of bacterial spores in 25- to 40-million-year-old Dominican amber. *Science*, **268**, pp. 1060-1064.

Carslaw, H.S., 1921. *The Conduction of Heat.* London: Macmillan and Co.

Cataldo, F., Keheyan, Y. and Heymann, D., 2004. Complex Organic Matter in Space: About the Chemical Composition of Carriers of the Unidentified Infrared Bands (UIBs) and Protoplanetary Emission Spectra Recorded from Certain Astrophysical Objects. *Origins of Life and Evol. Of Biospheres,* **34,** 13-24.

Chambers, J. E. and Migliorini, F., 1997. Mercury - A New Software Package for Orbital Integrations. *Bulletin of the American Astronomical Society*, **29**, 1024.

Christensen, E.A., 1964. Radiation resistance of Enterococci dried in air. *Acta Path. et Microbiol. Scandinavia*, **61**, pp. 483-486.

Claus, G., Nagy, B. and Europa, D.L., 1963. Further observations on the properties of the "organized elements" in carbonaceous chondrites. *Ann. NY Acad. Sci.*, **108**, pp. 580-605.

Cleaves, H.J. and Chalmers, J.H., 2004. Extremophiles may be irrelevant to the origin of life. *Astrobiology,* **4**(1), pp. 1-9.

Clube, S. V. M. and Napier, W. M., 1986. *The galaxy and the solar system.* Tucson: University of Arizona Press, pp. 260-285.

Clube, S. V. M. and Napier, W. M., 1996. Galactic dark matter and terrestrial periodicities. *QJRAS*, **37**, pp. 617-642.

Cowan, D and Grady, M., 2000. In search of a second evolutionary experiment. *Microbiol. Today*, **27**, pp. 174-177.

Crick, F. H. C., 1968. The Origin of the Genetic Code. *J. Mol. Biol.*, **38**, pp. 367-379.

Crick, F. H. C. and Orgel, L. E., 1973. Directed panspermia. *Icarus*, **19**, pp. 341-346.

Crovisier, J. et al., 1997. The Spectrum of Comet Hale-Bopp (C/1995 O1) Observed with the Infrared Space Observatory at 2.9 Astronomical Units from the Sun. *Science*, **275**, pp. 1904-1907.

Darbon, S., Perrin, J.-M. and Sivan, J.-P, 1998. Extended red emission (ERE) detected in the 30 Doradus nebula. *Astron. and Astrophys.*, **333**, pp. 264-268.

Debye, P., 1909. Der Lichtdruck auf Kugeln von beliebigem Material. *Ann. Physik*, **30**, pp.57-136.

Desvoivres E., Klinger J., Levasseur-Regourd A. C. and Jones G. H., 2000. Modeling the Dynamics of Cometary Fragments: Application to Comet C/1996 B2 Hyakutake. *Icarus*, **144**, pp. 172-181.

Diehl, R., et al., 1997. Galactic Gamma-Ray Line Emission from Radioactive Isotopes. *In* C.D. Dermer et al., eds. *AIP Conference Proceedings*, **410**, pp. 218-248.

Elst, E. W. et al., 1996. Comet P/1996 N2 (Elst-Pizarro). *IAU Circ.*, **6456**, 1.

Emel'yanenko, V. V., 2007. *Private Communication.*

Emel'yanenko, V. V. and Bailey M. E., 1998. Capture of Halley-type comets from the near-parabolic flux. *MNRAS*, **298**(1), pp. 212-222.

Emel'yanenko, V. V., Asher, D. J. and Bailey M. E., 2005. Centaurs from the Oort cloud and the origin of Jupiter-family comets. *MNRAS*, **361**(4), pp. 1345-1351.

Falco, E.E. et al., 1999. Dust and Extinction Curves in Galaxies with $z>0$: The Interstellar Medium of Gravitational Lens Galaxies *Astrophys. J*, **523**, pp. 617-632.

Fernández, J.A., 1980. On the existence of a comet belt beyond Neptune. *MNRAS,* **192,** pp. 481-491.

Fernández, J.A., 2005. *Comets - Nature, Dynamics, Origin and their Cosmological Relevance*. Dordrecht: Springer.

Fernández, J. A. and Ip, W.-H., 1987. Time-dependent injection of Oort cloud comets into Earth-crossing orbits. *Icarus*, **71**, pp. 46-56.

Fernández, J.A., Gallardo, T. and Brunini, A., 2004. The scattered disk population as a source of Oort cloud comets: evaluation of its current and past role in populating the Oort cloud. *Icarus,* **172**(2), pp. 372-381.

Fernández, Y. R., Jewitt, D. C., and Sheppard, S. S. 2001. Low Albedos Among Extinct Comet Candidates. *Astrophys. J.*, **553**, pp. L197-L200.

Fernández, Y.R., Jewitt D.C. and Sheppard S. S., 2002. Thermal Properties of Centaurs Asbolus and Chiron. *Astronom. J.*, **123**, pp. 1050-1055.

Festou, M.C., Rickman, H. and West, R.M., 1993. Comets. I - Concepts and observations. *Ann. Rev. Astron. Astrophys.*, **4**, pp. 363-447.

Forterre, P. and Phillipe, H., 1999. Where is the root or the universal tree of life? *Bioessays,* **21**, pp. 871-879.

Fouchard, M., 2004. New fast models of the Galactic tide. *MNRAS,* **349**(1), pp. 347-356.

Franck, S., Cuntz, M., von Bloh, W., and Bounama, C., 2003. The habitable zone of Earth-mass planets around 47 UMa: results for land and water worlds. *Int. J. Astrobiology*, **2**(1), pp. 35-39.

Franck, S. et al., 2000. Determination of habitable zones in extrasolar planetary systems: Where are Gaia's sisters? *Journal of Geophysical Research,* **105**, pp. 1651-1658.

Franck, S., von Bloh, W., and Bounama, C., 2007. Maximum number of habitable planets at the time of Earth's origin: new hints for panspermia and the mediocrity principle. *Int. J. Astrobiology* , in press.

Frost, R.L., Ruan, H. and Kloprogge, J.T., 2000. Application of infrared emission spectroscopy to the study of natural and synthetic materials. *The Internet Journal of Vibrational Spectroscopy,* **4**, pp. 1-12.

Furton, D.G. and Witt, A.N., 1992. Extended red emission from dust in planetary nebulae. *Astrophys. J.,* **386**, pp. 587-603.

Gold, T., 1992. The Deep, Hot Biosphere. *Proc.Natl.Acad.Sci.*,**89,** pp. 6045-6049.

Gordon, K.D. et al., 2003. A Quantitative Comparison of the Small Magellanic Cloud, Large Magellanic Cloud, and Milky Way Ultraviolet to Near-Infrared Extinction Curves. *Astrophys. J.*, **594**, pp. 279-293.

Greenblatt, C.L. et al., 1999. Diversity of Microorganisms Isolated from Amber. *Microbial Ecology*, **38**, pp. 58-68.

Grimm, R.E. and Mc Sween, H.Y., 1989. Water and the thermal evolution of carbonaceous chondrite parent bodies. *Icarus*, **82**, pp. 244-280.

Guillois, O. et al., 1999. *Solid Interstellar Matter: The ISO Revolution.* Les Houches, No.11, EDP Sciences, Les Ulis.

Haldane, J.B.S., 1929. *The Origin of Life*. London: Chatto and Windys.

Hamilton, V. E., 2005. A Source Region for Martian Meteorite ALH 84001: Eos Chasma, Mars. *Proc. 68th Annual Meeting of the Meteoritical Society*, 12-16 September 2005 Gatlinburg, Tennessee, **40**, pp. 5128.

Harris, M. J., Wickramasinghe, N.C., Lloyd, D. et al., 2002. Detection of living cells in stratospheric samples. *Proc. SPIE*, **4495**, pp. 192-198.

Herschel, W., 1785. On the Construction of the Heavens. *Phil. Trans.*, **75**, pp. 213-266.
Holmberg, J. and Flynn, C., 2004. The local surface density of disc matter mapped by *Hipparcos.* MNRAS, **352**(2), pp. 440-446.

Hoover, R. B., 1997. Meteorites, microfossils, and exobiology. *Proceedings of SPIE*, **3111**, pp. 115-136.

Hoover, R. B., 2005, *In*: R.B. Hoover, A.Y. Rozanov and R.R. Paepe, eds. *Perspectives in Astrobiology*. Amsterdam: IOS Press, **366**, pp. 43.

Hoover, R.B, et al., 1986. Diatoms on earth, comets, europa and in interstellar space. *Earth, Moon and Planets,* **35**, pp. 19-45.

Horneck, G., 1993. Responses of *Bacillus subtilis* spores to space environment: Results from experiments in space. *Origins of Life and Evol. of Biospheres,* **23**, pp. 37-52.

Horneck, G. et al., 1995. Biological responses to space: results of the experiment "Exobiological Unit" of ERA on EURECA I. *Adv. Space Res.*, **16**(8), pp. 105-118.

Horneck, G., Mileikowsky, C., Melosh, H. J. et al., 2002. Viable transfer of microorganisms in the solar system and beyond. *In*: G. Horneck, C. Baumstark-Khan, eds. *Astrobiology. The quest for the conditions of life.* Berlin: Springer.

Hoyle, F., 1978. *The Cosmogony of the Solar System.* Cardiff: Univ. College Cardiff Press.

Hoyle, F. and Wickramasinghe, N.C., 1977. Identification of the λ2200A interstellar absorption feature. *Nature*, **270**, pp. 323-324.

Hoyle, F. and Wickramasinghe, N.C., 1978a. Comets, ice ages, and ecological catastrophes. *Astrophys.Sp.Sci.*, **53**, pp. 523-526.

Hoyle, F. and Wickramasinghe, N.C., 1978b. *Lifecloud: the origin of life in the galaxy.* London: J.M. Dent.

Hoyle, F. and Wickramasinghe, N.C., 1979. On the nature of interstellar grains. *Astrophys.Sp.Sci.*, **66**, pp. 77-90.

Hoyle, F. and Wickramasinghe, N.C., 1981. *In:* C. Ponnamperuma, ed. *Comets and the Origin of Life*. Dordrecht: D. Reidel, pp. 227.

Hoyle, F. and Wickramasinghe, N.C., 1982. Proofs that Life is Cosmic. Colombo: Govt. Press, Sri Lanka

Hoyle, F. and Wickramasinghe, N.C., 1985. *Living Comets*. Cardiff: Univ. College, Cardiff Press.

Hoyle, F. and Wickramasinghe, N.C., 1986. Some predictions on the nature of Comet Halley. *Earth, Moon and Planets*, **36**, pp. 289-293.

Hoyle, F. and Wickramasinghe, N.C., 1989. A unified model for the 3.28-micron emission and the 2200 A interstellar extinction feature. *Astrophys.Sp.Sci.*, **154**, pp. 143-147.

Hoyle, F. and Wickramasinghe, N.C., 1991. *The Theory of Cosmic Grains*. Dordrecht: Kluwer Academic Press.

Hoyle, F. and Wickramasinghe, N.C., 2000. *Astronomical Origins of Life: Steps towards Panspermia*. Kluwer Academic Press.

Hoyle, F. et al., 1982. Infrared spectroscopy over the 2.9-3.9 microns waveband in biochemistry and astronomy. *Astrophys.Sp.Sci,* **83**, pp. 405-409.

Hsieh, H. H. and Jewitt, D.C., 2006. A Population of Comets in the Main Asteroid Belt. *Science* **312,** pp. 561-563.

Hsieh, H. H., Jewitt, D.C and Fernández, Y.R, 2004. The Strange Case of 133P/Elst-Pizarro: A. Comet Among the Asteroids. *Astronomical J.*, **127**, pp. 2997-3017.

Hughes, D. W., 1996. The Size, Mass and Evolution of the Solar System Dust Cloud. *QJRAS*, **37**, pp. 593-604.

Hughes, D. W., 2001. The magnitude distribution, perihelion distribution and flux of long-period comets. *MNRAS*, **326**, pp. 515-523.

Hughes, D. W., 2003. The approximate ratios between the diameters of terrestrial impact craters and the causative incident asteroids. *MNRAS*, **338**, pp. 999-1003.

Ibadinov, Kh. I., 1989. Laboratory Investigation of the Sublimation of Comet Nucleus Model. *Adv. Spa. Res.*, **9**, pp. 97-112.

Ibadinov, Kh. I., 1993. *In:* J. Stohl. and I. P. Williams, eds. *Meteoroids and their Parent Bodies.* Bratislava: Astr. Inst. Slovak Acad. Sci., 373.

Ibadinov, Kh. I., Rahmonov, A. A. and Bjasso, A. Sh., 1991. Laboratory Simulation of Cometary Structures. *In:* in R.L. Newburn, M. Neugebauer and J. Rahe, eds. *Comets in the Post-Halley Era.* Dordrecht: Kluwer, pp. 299-311.

Igenbergs, E. et al., 1991. The Munich Dust Counter cosmic dust experiment - Results of the first year of operation. *IAF, International Astronautical Congress, 42nd*, 5-11 October 1991 Montreal. pp.13.

Jakosky, B.M. and Shock, E.L., 1998. The biological potential of Mars, the early Earth, and Europa. *J. Geophys.Res*, **103**, pp. 19359-19364.

Jeffers, S. V., Manley, S. P., Bailey, M. E. and Asher D. J., 2001. Near-Earth object velocity distributions and consequences for the Chicxulub impactor. *MNRAS*, **327**, pp. 126-132.

Jewitt, D.C., 2005. A First Look at the Damocloids. *The Astronomical Journal*, **129**, pp. 530-538.

Jewitt, D.C. and Luu, J., 1993. Discovery of the candidate Kuiper belt object 1992 QB_1. *Nature*, **362**, pp. 730-732.

Jewitt, D.C., Chizmadia, L., Grimm, R. and Prialnik, D., 2007. *In:* V, B. Reipurth, D. Jewitt, and K. Keil, eds. *Protostars and Planets.* Tuscon: Univ. of Arizona Press. pp.863.

Jones, B.W., 2003. *Introduction to Astrobiology.* Cambridge: Cambridge Univ. Press.

Junge, K., Eicken, H. and Deming, J. W., 2004. Bacterial Activity at -2 to -20°C in Arctic Wintertime Sea Ice. *Appl. Environ. Microbiol.* **70,** pp. 550-557.

Karl, D.M. et al., 1999. Microorganisms in the Accreted Ice of Lake Vostok, Antarctica. *Science,* **286**, pp. 2144-2147.

Kelvin, Lord (William Thompson), 1871. On the Origin of Life. *Report of the Forty-First Meeting of the British Association for the Advancement of Science,* August 1871 Edinburgh. pp. lxxxiv-cv.

Koornneef, J., 1982. The gas to dust ratio and the near-infrared extinction law in the Large Magellanic Cloud. *Astron. and Astrophys.*, **107**, pp. 247-251.

Krueger, F.R. and Kissel, J., 2000. Erste direkte chemische analyse interstellarer staubteikhen. *Stern und Weltraum,* **39**, pp. 326-329.

Krueger, F.R. Werther, W., Kissel, J. and Schmid, E.R., 2004. Assignment of quinone derivatives as the main compound class composing 'interstellar' grains based on both polarity ions detected by the 'Cometary and Interstellar Dust Analyser' (CIDA) onboard the spacecraft STARDUST. *Rapid Comm. Mass Spectros.,* **18**, pp. 103-111.

Kührt, E. K. and Keller, H. U., 1996. On the Importance of Dust in Cometary Nuclei. *Earth, Moon, and Planets*, **72**, pp. 79-89.

Lambert, L.H. et al., 1998. Staphylococcus succinus sp. nov., isolated from Dominican amber. *Int. J. Syst. Bact.,* **48**, pp. 511-518.

Leitch, E. M. and Vasisht, G., 1998. Mass Extinctions and The Sun's Encounters with Spiral Arms. *New Astron.,* **3,** pp. 51-56.

Levison, H. F. et al., 2002. The Mass Disruption of Oort Cloud Comets. *Science*, **296**, pp. 2212-2215.

Levison, H. F. and Duncan, M. J., 1997. From the Kuiper Belt to Jupiter-Family Comets: The Spatial Distribution of Ecliptic Comets. *Icarus,* **127**, pp. 13-32.

Lewis, N.F., 1971. Studies on a radio-resistant coccus isolated from Bombay duck (Harpodon nehereus). *J. Gen. Microbiol,* **66**, pp. 29-35.

Lindahl, T., 1993. Instability and decay of the primary structure of DNA. *Nature,* **362,** pp. 709-715.

Lisse, C.M., van Cleve, J., Adams, A.C. et al., 2006. Spitzer Spectral Observations of the Deep Impact Ejecta. *Science*, **313**, pp. 635 – 640.

Love, S. G. and Brownlee, D. E., 1993. A Direct Measurement of the Terrestrial Mass Accretion Rate of Cosmic Dust. *Science*, **262**, pp. 550-553.

MacPherson, G.J., Davis, A.M. and Zinner, E.K., 1995. The distribution of aluminum-26 in the early Solar System - A reappraisal. *Meteoritics,* **30,** pp. 365-386.

Marcy, G.W. and Butler, R.P., 1996. A Planetary Companion to 70 Virginis. *Ap. J.,* **464,** pp. L147-L151.

Matese, J. J., Whitman, P. G., Innanen, K. A. and Valtonen, M. J., 1995. Periodic modulation of the Oort cloud comet flux by the adiabatically changing Galactic tide. *Icarus,* **116,** pp. 255-258.

Mattila, K., 1979. Optical extinction and surface brightness observations of the dark nebulae LYNDS 134 and LYNDS 1778/1780. *Astron & Astrophys.,* **78**, pp. 253-263.

Mayor, M. and Queloz, D., 1995. A Jupiter-Mass Companion to a Solar-Type Star. *Nature*, **378,** pp. 355-359.

McCaughrean, M.J. and O'Dell, C.R., 1996. Direct Imaging of Circumstellar Disks in the Orion Nebula. *The Astronomical Journal*, **111,** pp. 1977-1987.

McCrea, W. H., 1975. Ice ages and the Galaxy. *Nature*, 255, pp. 607-609.

McIntosh, B. A. and Hajduk A., 1983. Comet Halley meteor stream - A new model. *MNRAS*, **205,** pp. 931-943.

McKay, D.S. et al., 1996. Search for Past Life on Mars: Possible Relic Biogenic Activity in Martian Meteorite ALH84001. *Science,* **273**, pp. 924-930.

McSween, H.Y., 1979. Alteration in CM carbonaceous chondrites inferred from modal and chemical variations in matrix. *Geochim Cosmochim.Acta,* **43**, pp. 1761-1765.

Melosh, H. J., 1989. *Impact Cratering: A Geologic Process.* New York: OUP.

Melosh, H.J., 1988. The rocky road to panspermia. *Nature,* **332**, pp. 687-688.

Merk, R. and Prialnik, D., 2003. Early Thermal and Structural Evolution of Small Bodies in the Trans-Neptunian Zone. *Earth, Moon and Planets*, **92**, pp. 359-374.

Mie, G., 1908. Beitrage zur optik truber medien, speziell kolliodaler metallo sungen. *Ann. Physik*, **25**, pp. 377-442.

Mileikowsky, C., et al., 2000. Natural Transfer of Viable Microbes in Space: 1. From Mars to Earth and Earth to Mars. *Icarus,* **145**, pp. 391-427.

Miller, S.L. and Urey, H.C., 1959. Organic Compound Synthesis on the Primitive Earth. *Science,***130**, pp. 245-251.

Mojzsis, S.J. et al., 1996. Evidence for life on Earth before 3,800 million years ago. *Nature* **384**, pp. 55-59.

Mojzsis, S.J. et al., 2001. Oxygen-isotope evidence from ancient zircons for liquid water at the Earth's surface 4,300 Myr ago. *Nature*, **409**, pp. 178-181.

Morbidelli A. et al., 2002. From Magnitudes to Diameters: The Albedo Distribution of Near Earth Objects and the Earth Collision Hazard. *Icarus,* **158,** pp. 329-342.

Morgan, D.H. and Nandy, K., 1982. Infrared interstellar extinction in the LMC. *MNRAS*, **199**, pp. 979-986.

Mostefaoui, S., Lugmair, G.W., Hoppe, P. and Goresy, A. El., 2004. Evidence for live ^{60}Fe in meteorites. *New Astronomoy Reviews*, **48**, pp. 155-159.

Motta, V. et al., 2002. Detection of the 2175A Extinction Feature at $z = 0.83$. *Astrophys. J.,* **574**, pp. 719-725.

Nadeau, D. et al., 1991. Infrared and visible photometry of the gravitational lens systems 2237 + 030. *Astrophys. J.*, **376**, pp. 430-438.

Nandy, K., Morgan, D.H. and Houziaux, L., 1984. Infrared extinction in the Small Magellanic Cloud. *MNRAS*, **211**, 895-900.

Napier, W.M., 2004. A mechanism for interstellar panspermia. *MNRAS*, **348,** pp. 46-51.

Napier, W.M., 2006. Evidence for cometary bombardment episodes. *MNRAS*, **36**(3), pp. 977-982.

Napier, W.M., 2007. *Int. J. Astrobiology,* in press.

Napier, W. M. and Clube, S. V. M., 1979. A theory of terrestrial catastrophism. *Nature*, **282**, pp. 455-459.

Napier, W. M. and Staniucha, M., 1982. Interstellar planetesimals. I - Dissipation of a primordial cloud of comets by tidal encounters with massive nebulae. *MNRAS,* **198**, pp. 723-735.

Narlikar, J. V. N. et al., 2003. A Balloon Experiment to detect Microorganisms in the Outer Space. *Astrophys.Sp.Sci.* **285**(2), pp. 555-562.

Nelson, R. M., Soderblom, L. A. and Hapke, B. W., 2004. Are the circular, dark features on Comet Borrelly's surface albedo variations or pits? *Icarus*, **167,** pp. 37-44.

Neslusan, L., 2007. The fading problem and the population of the Oort cloud. *Astron. and Astrophys.*, **461**, pp. 741-750.

Neukum, G. and Ivanov, B. A., 1994. *In:* T. Gehrels, ed. *Hazards due to Comets and Asteroids.* Tucson: Univ. of Arizona.

Nicholson, W.L. et al., 2000. Resistance of Bacillus Endospores to Extreme Terrestrial and Extraterrestrial Environments. *Mol. Biol. Rev.* **64,** pp. 548-572.

Nisbet, E.G. and Sleep, N.H., 2001. The habitat and nature of early life. *Nature* **409,** pp. 1083-1091.

Nurmi P., Valtonen M. and Zheng J. Q., 2001. Periodic variation of Oort Cloud flux and cometary impacts on the Earth and Jupiter *MNRAS*, **327**, pp. 1367-1376.

O'Keefe J. D. and Ahrens T. J., 1993. Planetary cratering mechanics. *J. Geophys. Res.,* **98**, pp. 17011-17028.

Olsen, G.J. and Woese, C..R., 1997. Archaeal Genomics: An Overview. *Cell*, **89**, 991-994.

Oort J. H., 1950. The structure of the cloud of comets surrounding the Solar System and a hypothesis concerning its origin. *Bull. Astron. Inst. Neth.*, **11**, pp. 91-110.

Oparin, A.I., 1953. *The Origin of Life*, transl by S. Margulis. New York: Dover.

Overmann, J. and van Gemerden, H., 2000. Microbial interactions involving sulfur bacteria: implications for the ecology and evolution of bacterial communities. *FEMS Microbiol. Rev.*, **24,** pp. 591-599.

Pasteur, L.C.R., 1857. Mémoire sur la fermentation appelée lactique. *Acad. Sci.*, **45**, pp. 913-916.

Perrin, J.-M., Darbon, S. and Sivan, J.-P., 1995. Observation of extended red emission (ERE) in the halo of M82. *Astron. and Astrophys.*, **304**, pp. L21-L24.

Pflug, H.D., 1984. *In:* N.C. Wickramasinghe, ed. *Fundamental Studies and the Future of Science*, Cardiff: Univ. College Cardiff Press.

Rickman, H. et al., 2001. *In:* M.Y. Marov and H. Rickman, eds. *Astrophys. Space Sci. Librabry Vol. 261, Collisional Processes in the Solar System.* Dordrecht: Kluwer, pp.131.
Rietmeijer, F. J. M., 2002. *In*: E. Murad and I.P. Williams, eds. *Meteors in the Earth's Atmosphere.* Cambridge: Cambridge Univ. Press, pp. 215.

Rivkina, E.M., Friedmann, E.I., McKay, C.P. and Gilichinsky, D.A., 2000. Metabolic Activity of Permafrost Bacteria below the Freezing Point. *App. Environ. Microbiol,* **66**(8), pp. 3230-3233.

Robert, F. et al., 2000. The Solar System d/h Ratio: Observations and Theories. *Sp. Sc. Rev.*, **92**, pp. 201-224.

Roy, A.E., 1978. *Orbital Motion.* Bristol: Adam Hilger Ltd., pp.309.

Salpeter, E.E. and Wickramasinghe, N.C., 1969. Alignment of Interstellar Grains by Cosmic Rays. *Nature*, **222**, pp. 442-444.

Sandford, S.A. et al., 2006. Organics Captured from Comet 81P/Wild 2 by the Stardust Spacecraft. *Science*, **314**, pp. 1720-1724.

Sapar, A. and Kuusik, I., 1978. Mean interstellar extinction curve from space observations. *Publ.Tartu.Astrophys.Obs.*, **46**, pp. 71-84.

Secker, J., Wesson, P.S. and Lepock, J.R., 1994. Damage due to ultraviolet and ionizing radiation during the ejection of shielded micro-organisms from the vicinity of $1M_{\Theta}$ main sequence and red. *Astrophys.Sp.Sci.* **219**, pp. 1-28.

Sekanina Z., 1984. Disappearance and disintegration of comets. *Icarus.*, **58**, pp. 81-100.

Sivan, J.P. and Perrin, J.M., 1993. Scattering and luminescence in the Bubble Nebula. *Astrophys.J.*, **404**, pp. 258-263.

Sommer, A. P., Miyake, N., Wickramasinghe, N. C., Narlikar, J. V. and Al-Mufti, S., 2004. Functions and Possible Provenance of Primordial Proteins. *Journal of Proteome Research,* **3**(6), pp. 1296-1299.

Southworth, R. B. and Hawkins, G. S., 1963. Statistics of meteor streams. *Smithsonian Contributions to Astrophysics,* **7**, pp. 261-285.

Spitzer, L., 1978. *Physical Processes in the Interstellar Medium.* New York:Wiley & Sons.

Stebbins, J., Huffer, C.H. and Whitford, A.E., 1939. Space reddening in the galaxy. *Astrophys. J.*, **90**, pp.209-232.

Steel D. I., 1993. Collisions in the solar system. V - Terrestrial impact probabilities for parabolic comets. *MNRAS*, **264**, pp. 813-817.

Stetter, K. O. et al., 1990. Hyperthermophilic microorganisms. *FEMS Microbiol. Rev.* **75**, pp. 117-124.

Stothers, R.B., 2006. The period dichotomy in terrestrial impact crater ages. *MNRAS*, **365**, 178-180.

Svensmark, H., 2007. Cosmoclimatology: a new theory emerges. *A&G*, **48**, pp. 1.18-1.24.

Szomouru, A. and Guhathakurta, P., 1998. Optical Spectroscopy of Galactic Cirrus Clouds: Extended Red Emission in the Diffuse Interstellar Medium. *Astrophys.J.,* **494**, L93-L97.

Taft, E.A. and Phillipp, H.R., 1965. Optical Properties of Graphite. *Phys.Rev.* **138**, pp. A197-A202.

Tegler S.C. and Romanishin, W., 2000. Extremely red Kuiper-belt objects in near-circular orbits beyond 40 AU. *Nature*, **407**, pp. 979-981.

Tepfer, D. and Leach, S., 2006. Plant Seeds as Model Vectors for the Transfer of Life Through Space. *Astrophys. and Space Sci.*, **306**, pp. 69-75.

Underwood, D.R., Jones, B.W. and Sleep, P.N., 2003. The evolution of habitable zones during stellar lifetimes and its implications on the search for extraterrestrial life. *Int. J. Astrobiol.*, **2**, pp. 289-299.

UNSCEAR, 2000. Sources and Effects of Ionizing Radiation. *United Nations Scientific Committee on the Effects of Atomic Radiation UNSCEAR 2000 Report to the General Assembly, with Scientific Annexes*, United Nations, 2000.

Vernazza, P. et al., 2005. Analysis of near-IR spectra of 1 Ceres and 4 Vesta, targets of the Dawn mission. *Astron.Astrophys.*, **436**, pp. 1113-1121.

von Bloh, W., Bounama, C., Cuntz, M. and Franck, S., 2007. The habitability of super-Earths in Gliese 581. *Astron Astrophys in press.*

von Helmholtz, H., 1874. *In:* W. Thomson and P.G. Tait, eds. *Handbuch de Theortetische Physik*, **1**(2), Brancscheig.

Vreeland, R.H., Rosenzweig, W.D. and Powers, D., 2000. Isolation of a 250 million-year-old halotolerant bacterium from a primary salt crystal. *Nature*, **407**, pp. 897-900.

Wallis, M.K., 1980. Radiogenic melting of primordial comet interiors. *Nature* **284**, pp. 431-433.

Wallis M. K. and Al-Mufti S., 1996. Processing of cometary grains at the nucleus surface *Earth, Moon, and Planets*, **72**, pp. 91-97.

Wallis, M.K. and Wickramasinghe, N.C., 1985. Halley's comet - Its size and decay rate. *MNRAS.*, **216**, pp. 453-458.

Wallis, M.K. and Wickramasinghe, N.C.,1995. Role of major terrestrial cratering events in dispersing life in the solar system. *Earth Planet Sci. Lett.*, **130**, pp. 69-73.

Wallis, M.K. and Wickramasinghe, N.C., 2004. Interstellar transfer of planetary microbiota. *MNRAS.*, **348**, pp. 52-61.

Weingartner, J.C. and Draine, B.T., 2001. Dust Grain–Size Distributions and Extinction in the Milky Way, Large Magellanic Cloud, and Small Magellanic Cloud. *The Astrophysical Journal*, **548**, pp. 296-309.

Weiss, B. P. et al., 2000. A Low Temperature Transfer of ALH84001 from Mars to Earth. *Science*, **290**, pp. 791-795.

Weissman P. R. and Lowry S. C., 2001. The Size Distribution of Cometary Nuclei. *Bull. Am. Astron. Soc.*, **33**, pp. 1094.

Wickramasinghe, D.T. and Allen, D.A., 1986. Discovery of organic grains in comet Halley. *Nature,* **323**, pp. 44-46.

Wickramasinghe, D.T., Hoyle, F., Wickramasinghe, N.C. and Al-Mufti, S., 1986. A model of the 2-4 micron spectrum of Comet Halley. *Earth, Moon and Planets,* **36,** pp. 295-299.

Wickramasinghe, N.C., 1967. *Interstellar Grains.* London: Chapman and Hall.

Wickramasinghe, N.C., 1973. *Light Scattering Functions for Small Particles.* New York: Wiley.

Wickramasinghe N. C., 1974. Formaldehyde polymers in interstellar space. *Nature*, **252**, pp. 462-463.

Wickramasinghe, N .C., 1993. *In:* A. Mampaso, M. Prieto and F. Sanchez, eds. *Infrared Astronomy.* Cambridge: Cambridge University Press, pp.303.

Wickramasinghe, N.C., 2004. The Universe: a cryogenic habitat for microbial life. *Cryobiology,* **48**, pp. 113-115.

Wickramasinghe N. C. and Hoyle F., 1998. The Astonishing Redness of Kuiper-Belt Objects. *Astrophys. and Space Sci.*, **259,** pp. 205-208.

Wickramasinghe N. C. and Hoyle F., 1999. Infrared Radiation From Comet Hale-Bopp. *Astrophys. and Space Sci.*, **268,** pp. 379-382.

Wickramasinghe N. C., Hoyle F. and Al-Jubory, T., 1989. Aromatic hydrocarbons in very small interstellar grains. *Astrophys. and Space Sci.*, **158,** pp. 135-140.

Wickramasinghe, N.C., Hoyle, F. and Lloyd, D., 1996. Eruptions of comet Hale-Bopp at 6.5 AU. *Astrophys. Sp. Sci.,* **240,** pp. 161-165.

Wickramasinghe, N.C., Lloyd, D. and Wickramasinghe, J.T., 2002. Evidence of photoluminescence of biomaterial in space. *Proc. SPIE*, **4495**, pp. 255-260.

Wickramasinghe, N.C., Wainwright, M., Narlikar, J.V. et al., 2003. Progress towards the vindication of panspermia. *Astrophys. and Space Sci.*, **283,** pp. 403-413.

Wilner, D.J. et al., 2005. Toward Planetesimals in the Disk around TW Hydrae: 3.5 Centimeter Dust Emission. *The Astrophysical Journal,* **626**(2), pp. L109-L112.

Woese, C. and Fox, G., 1977. Phylogenetic Structure of the Prokaryotic Domain: The Primary Kingdoms. *Proc. Natl Acad. Sci.USA,* **74**(11), pp. 5088-5090.

Yabushita, S., 1993. Thermal Evolution of Cometary Nuclei by Radioactive Heating and Possible Formation of Organic Chemicals. *MNRAS*, **260**, pp. 819-825.

Yabushita, S., 2004. A spectral analysis of the periodicity hypothesis in cratering records. *MNRAS*, **355**, pp. 51-56.

Zook, H. A. and Berg, O. E., 1975. A source for hyperbolic cosmic dust particles. *Planetary and Space Sci.*, **23**, pp. 183-203.

Published Papers:

Wickramasinghe, N.C., Lloyd, D. and Wickramasinghe, J.T., 2002. Evidence of photoluminescence of biomaterial in space. *Proc. SPIE*, **4495**, pp. 255-260.

Wickramasinghe, N. C. and Wickramasinghe, J. T., 2003. Radiation pressure on bacterial grain clumps in the solar vicinity and their survival between interstellar transits. *Astrophys. Sp. Sci.*, **286**, pp. 453-459.

Napier, W. M., Wickramasinghe, J. T. and Wickramasinghe, N. C., 2004. Extreme albedo comets and the impact hazard, *MNRAS*, **355**, pp. 191-195.

Wickramasinghe J. T., Wickramasinghe N. C. and Napier, W. M., 2004. Sedna's missing moon. *The Observatory,* **124**, pp. 300-313.

Wickramasinghe N. C., Wickramasinghe J. T. and Mediavilla, E., 2005. The interpretation of a 2175A absorption feature in the gravitational lens galaxy SBS0909+532 at z=0.83. *Astrophys. Sp. Sci.*, **298**, pp. 453-460.

Wickramasinghe, J. T. and Wickramasinghe, N. C., 2006. A Cosmic Prevalence of Nanobacteria? *Astrophys. Sp. Sci.*, **305**, pp. 411-413.